

Durham E-Theses

The measurement of the absolute viscosity of fluids exhibiting anomalous flow properties and a study of the phenomenon of thixotropy

Donald Rae

How to cite:

Rae, Donald (1952) The measurement of the absolute viscosity of fluids exhibiting anomalous flow properties and a study of the phenomenon of thixotropy. Doctoral thesis, Durham University.

Use policy

The full-text may be used and/or reproduced, and given to third parties in any format or medium, without prior permission or charge, for personal research or study, educational, or not-for-profit purposes provided that:

- a full bibliographic reference is made to the original source
- a <https://etheses.durham.ac.uk/id/eprint/9127/> is made to the metadata record in Durham E-Theses
- the full-text is not changed in any way

The full-text must not be sold in any format or medium without the formal permission of the copyright holders.

Please consult the [full Durham E-Theses policy](#) for further details.

THE MEASUREMENT OF THE
ABSOLUTE VISCOSITY OF FLUIDS
EXHIBITING ANOMALOUS FLOW
PROPERTIES AND A STUDY OF THE
PHENOMENON OF THIXOTROPY

being an account of the work carried out by

DONALD RAE, B.Sc.,

under the direction of S. THORNTON, B.Sc., Ph.D.,

between October 1948 and September 1951

in the Physics Department of the Durham Colleges

and submitted in candidature for the degree of

DOCTOR OF PHILOSOPHY

in the University of Durham.

August 1952.



A B S T R A C T

The theory of the measurement of the absolute viscosity (the ratio of shearing stress to rate of shear) of instantaneously thixotropic fluids from flow along a tube and from flow between concentric cylinders makes assumptions requiring critical examination. An instrument using flow along a tube is suitable only for instantaneously thixotropic fluids: an instrument using flow between concentric cylinders is also suitable for normally thixotropic fluids. The design of these instruments is particularly related both to the conditions necessary for the validity of the given theory and to the characteristics of the fluids used. The usually accepted treatment of the tube flow is in error if the fluid has a yield value. The fluids used, ball-mill dispersions of solid particles in liquid media, have static and dynamic yield values that are different, and this necessitates a special measuring procedure in both instruments. The relation between the rate of shear and the shearing stress determined by either instrument is the same within the limits of experimental error: this error is small so that the validity of the methods of measurement is demonstrated. The dynamic yield values of these fluids are independent of temperature, but the absolute viscosity at any given shearing stress (including the limiting viscosity for high rates of shear measured in another instrument of the concentric cylinder type) varies as the viscosity of the medium. At low shearing stresses the absolute viscosity can be represented as a function of shearing stress by a simple empirical equation. As the concentration of particles is reduced, the limiting viscosity approaches the viscosity of the medium more rapidly than predicted by Einstein's equation.

C O N T E N T S

CHAPTER I

INTRODUCTION.

	page
1. Viscosity.	1
2. Thixotropy.	3
3. The flow function.	5
4. Experimental method.	7

PART I

CHAPTER II

THE TUBE FLOW: THEORY AND ASSUMPTIONS.

1. Flow down a tube.	12
2. The sample fluid.	15
3. Assumptions which govern instrument design.	16
4. Assumption which governs measuring technique.	19

CHAPTER III

THE ROTARY FLOW: THEORY AND ASSUMPTIONS.

1. Flow between concentric cylinders.	22
2. The sample fluid.	24
3. Assumptions which govern instrument design.	25
4. Assumptions which govern measuring technique.	26

CHAPTER IV

METHODS FOR COMPARING THE RESULTS FROM THE INSTRUMENTS.

1. Direct comparison.	33
2. Derivation of q' -values from the W-f curve.	35
3. Derivation of W-values from the q' -f curve.	36
4. Method for incomplete curves.	37

CHAPTER V

THE TUBE INSTRUMENT: DESCRIPTION.

1. The essentials of the instrument.	39
2. The plunger-driving mechanism.	42
3. The reservoir and tube assembly.	45
4. The manometer lift.	50
5. The complete instrument.	52

CHAPTER VI

THE ROTARY INSTRUMENT: DESCRIPTION.

1. Essentials and initial adjustment.	56
2. The variable speed motor and drive.	60
3. The instrument proper.	62

CHAPTER VII

EXPERIMENTAL PROCEDURES.

1. Filling the instruments.	66
2. Procedure for comparative experiments.	70
3. Readings on the tube instrument.	72
4. Readings on the rotary instrument.	75

CHAPTER VIII

CALIBRATIONS OF THE INSTRUMENTS.

1. Tube instrument: methods.	78
2. Tube instrument: first method.	80
3. Tube instrument: second method.	87
4. Comparison of the two methods.	94
5. Rotary instrument: methods.	95
6. Rotary instrument: first method.	96
7. Rotary instrument: second method.	101

CHAPTER IX

FIRST COMPARATIVE EXPERIMENT - EXPERIMENT A.

1. The end correction in the rotary instrument.	103
2. Results from the rotary instrument.	105
3. Results from the tube instrument.	109
4. Comparison of the results.	112

CHAPTER X

SECOND COMPARATIVE EXPERIMENT - EXPERIMENT B.

1. Experiment B.	117
2. Results from the rotary instrument.	117
3. Results from the tube instrument.	121
4. Comparison of the results.	124
5. Discussion of the results.	126
6. Effect of change of temperature: Experiment C.	128

CHAPTER XI

THIRD COMPARATIVE EXPERIMENT - EXPERIMENT D.

1. Experiment D.	130
2. Results from the rotary instrument.	131
3. Results from the tube instrument.	133
4. Comparison of the results.	135

CHAPTER XII

CONCLUSION TO PART I.

1. Accuracy of the results.	138
2. The effects of the assumptions made.	140
3. Introduction to Part II.	142

PART II

CHAPTER XIII

A HIGH RATE OF SHEAR ROTARY INSTRUMENT.

1. The instrument.	144
2. Use and calibration of the instrument.	147
3. Approximate end corrections.	150

CHAPTER XIV

THE VARIATION OF THE FLOW FUNCTION WITH TEMPERATURE.

1. Introduction.	153
2. Experiment F.	155
3. Limiting viscosity.	159
4. Conclusion.	161

CHAPTER XV

AN EMPIRICAL EQUATION

1. Introduction.	162
2. The empirical equation applied to Experiment B.	163
3. The equation applied to the rotary instrument.	167
4. The equation applied to the tube instrument.	169
5. The empirical equation applied to Experiment D.	170
6. The equation and change of temperature.	172
7. Conclusion.	173

APPENDICES

APPENDIX I	THE PRODUCTION OF THE SAMPLES.	174
APPENDIX II	THE BALL-MILL.	177
APPENDIX III	CHANGE OF LIMITING VISCOSITY WITH CONCENTRATION.	181

FIGURES

I	on page	28	VII	on page	48	XII	on page	63
II		31	VIII		51	XIII		67
III		39	IX		53	XIV		68
IV		43	X		57	XV		88
V		45	XI		62	XVI		95
VI		46				XVII		179

GRAPHS

I	facing page	104	XIII	facing page	131
II		106	XIV		132
III		107	XV		133
IV		108	XVI		134
V		110	XVII		136
VI		114	XVIII		137
VII		115	XIX		148
VIII		118	XX		160
IX		119	XXI		164
X		120	XXII		165
XI		122	XXIII		168
XII		123	XXIV		182

CHAPTER I

INTRODUCTION.

1. Viscosity.

The law of viscous resistance in liquids was formulated by Newton, and may be stated as follows. Suppose that the space between two unit parallel planes at distance δx apart, one at rest and the other moving with velocity δv in its own plane, be filled with a liquid; then the tangential stress, f , on either plane is proportional to the velocity gradient $g = \delta v / \delta x$ in the liquid. Thus, in the limit:-

$$f = \eta g = \eta \frac{dv}{dx} \quad \dots 1.1$$

where η , the constant of proportionality, is the coefficient of viscosity. The fluidity, ϕ , is defined as the reciprocal of the viscosity.

For the purposes of this thesis, a substance which can undergo continuous shear without irreversible changes taking place in its flow properties is called a fluid. A substance which, under certain conditions,



behaves as a fluid will be said to be in its fluid state under those conditions. A fluid which obeys Newton's Law, equation 1.1, is called a normal fluid: a fluid which does not obey Newton's Law is said to exhibit anomalous flow properties, and will be called an anomalous fluid. The discussion will be restricted to those anomalous fluids where the displacement takes place only in the direction of the applied shearing stress, that is, anisotropy and elasticity are not considered.

If, in the case of an anomalous fluid, the shearing stress and the velocity gradient are known for a completely specified set of conditions at a point in a fluid, the ratio of f to g is called the absolute viscosity of the fluid under the conditions existing at that point in the fluid. The term absolute viscosity has been introduced in order to distinguish a measure of the actual ratio f/g from an arbitrary measure of viscosity called the apparent viscosity. If an anomalous fluid gives the same indication as does a normal fluid when subjected to measurement in a viscometer, the anomalous fluid is said to have an apparent viscosity which is numerically equal to the viscosity of the normal fluid. As the value of the

apparent viscosity depends on the type and dimensions of the viscometer used, and on the method of measurement, it has little significance; apparent viscosities will not therefore be considered. Where the term viscosity is used in this thesis, it will mean the ratio f/g , that is, the absolute viscosity.

2. Thixotropy.

If a substance is subjected to a continuous shearing stress which causes a time-dependent variation in its flow properties, and if, on the removal of this shearing stress, the substance after a time returns to its original state, then the substance is said to be a thixotropic fluid. This is the extreme case of an anomalous fluid as defined here. If a constant shearing stress is applied to such a fluid for a sufficiently long time the rate of shear approaches a constant value: this is the equilibrium rate of shear for the given shearing stress. The rate of shear has an initial value depending on the applied stress and the previous shear-history of the fluid, and, during the time of application of the given shearing stress, varies in a manner depending on the thixotropic

properties of the fluid, the applied stress, and its previous history. If the initial state of the fluid is an equilibrium rate of shear, then the previous shear-history has been eliminated and the thixotropic properties of the fluid can be examined by applying a new shearing stress and measuring the rate of shear as a function of time. A complete assessment of the thixotropic properties of a fluid can be obtained by measuring $\dot{\gamma}$ as a function of time for different initial equilibrium states and applied stresses.

In a similar way the rate of shear can be taken as the independent variable, and the change of shearing stress observed.

It may be noted here that an instrument which is used for the measurement of thixotropic properties must be capable of bringing the fluid to an equilibrium rate of shear. For this reason an instrument which makes use of flow along a tube is useless for general thixotropic measurements since the material entering the tube cannot be conditioned to an equilibrium rate of shear.

There is a special class of thixotropic fluids for which the tube instrument is suitable, and this case will be of particular interest here: if the changes of

rate of shear (or shearing stress) are immediate, or occur so quickly that the measuring instrument is incapable of responding to them, then the fluid is said to be an instantaneously thixotropic fluid.

3. The flow function.

The flow properties of an instantaneously thixotropic fluid can be described using only the fundamental quantities f and g in a relation of the form $F(f,g) = 0$, where F is an experimentally determined function; this will be called the flow function of the fluid. The absolute viscosity at any shearing stress (or rate of shear) can be obtained from this flow function.

In the case of normally thixotropic fluids, the time, t , and the initial conditions must also be included. If such a fluid has been brought to an equilibrium rate of shear, characterised by the equilibrium viscosity η_i , under the action of a constant shearing stress, the behaviour of the fluid under the action of a new constant shearing stress f applied for a time t can be represented by $F(f,g,t,\eta_i) = 0$; and the behaviour at a new constant

rate of shear g by $G(f, g, t, \eta_i) = 0$. For each value of the parameter η_i , F or G gives a surface, with coordinates f , g , and t , meeting the plane $t = 0$ in the straight line $f = \eta_i g$, and the plane $t = \infty$ in the curve $F_0(f, g) = 0$, where F_0 is the flow function for the equilibrium rates of shear. F and G are not the same, but are the flow functions under the conditions of constant applied shearing stress and constant applied rate of shear respectively. The absolute viscosity in each case can again be obtained from the flow functions, and it is specified at a given shearing stress (or rate of shear) and time.

If the flow function of an instantaneously thixotropic fluid is of the form:-

$$(f - f_0) - \eta_B g = 0, f \geq f_0; \quad g = 0, f < f_0$$

then the fluid is a 'Bingham' fluid, and the constant η_B is the 'Bingham' viscosity of the fluid. This viscosity, η_B , is not the same as the absolute viscosity, η : η_B is a constant of the fluid, but η depends on the applied shearing stress for a 'Bingham' fluid as well as for other anomalous fluids. The instantaneously thixotropic fluids examined here were found not to be 'Bingham' fluids.

4. Experimental method.

In the discussion above, it has been assumed that the whole of the fluid is subjected to the same shearing stress; in practice a sample of the fluid is made to flow in a certain pattern, where the shearing stress f (or the rate of shear g) is a known function of position, and the rate of shear (or the shearing stress) can be determined at a specified place. By varying the magnitude of f (or g) at this place, g (or f) can be determined as a function of f (or g) in the case of instantaneously thixotropic fluids, and as a function of the initial conditions and the time in the case of normally thixotropic fluids.

The flow function of a fluid is a property of the fluid alone: it does not depend on the method by which it is determined. If two distinct methods of measurement give the same flow function for a fluid, then it may be assumed that the flow function has been determined correctly by both methods. The prime concern here is to show that the two most widely used methods for the determination of viscosity can be made to yield the same flow function for a given fluid. The conditions for the validity of the theory of the

methods are examined critically, and it is shown that care must be taken to provide the necessary conditions in the instruments used and in the method of measurement.

In Part I, the theory is given for the determination of g as a function of f from the observable quantities involved in the production of two well-defined flow patterns. These patterns are (a) the flow along a cylindrical tube of circular cross-section, the observable quantities being the pressure difference over a length of the tube and the corresponding rate of flow along the tube; and (b) the flow between two coaxial cylindrical surfaces, one of which is at rest and the other rotating about the common axis, the observable quantities being the angular velocity of the moving cylinder and the corresponding couple exerted on the cylinders. In the former case, g can be found at the wall of the tube: in the latter case, g can be found at the surface of the inner cylinder.

The theory for the tube flow shows that its use is restricted to instantaneously thixotropic fluids. The use of the flow between concentric cylinders is not restricted in this way since it is possible in this

case to subject an element of the fluid to a known shearing stress for any length of time. In order to make the comparison outlined above, it is necessary therefore to use instantaneously thixotropic fluids. The extension of the use of the concentric cylinder flow to normally thixotropic fluids is not considered here: the theory of the method was given by Thornton (1948).

The comparison based on the two flow patterns is described in Part I and the results presented for a number of fluids. Particular attention has been paid to resolving any differences between the independently derived flow functions for the arbitrary fluids used rather than to a survey of the properties of instantaneously thixotropic fluids in general. The investigations which led to the reduction of originally large differences to within the limit of experimental error brought to light deficiencies in the accepted treatment of the tube flow; these deficiencies were found to account for the original disagreement. Some of the properties of the fluids used in Part I are presented in Part II: it is considered that these are typical instantaneously thixotropic fluids, so that the conclusions arrived at may well be of general

application to this class of fluid.

Two instruments were developed. The first, the Tube Instrument, uses the flow pattern (a), and the second, the Rotary Instrument, uses the flow pattern (b). The agreement between the flow functions obtained shows that the methods developed for using these instruments are satisfactory. Since the method for the rotary instrument can readily be extended to normally thixotropic fluids, satisfactory results can be expected for these fluids also, although no such measurements will be presented here.

Suitable instantaneously thixotropic samples for use in these experiments were produced by dispersing titanium dioxide particles in paraffin oil. The lack of time-dependence in the properties of these fluids was demonstrated in the rotary instrument, where it was seen that the application of a constant angular velocity resulted in a constant shearing stress at the inner cylinder at all times after its initial application.

The two instruments were constructed so that measurements in each could be made with comparable accuracy over the same range of shearing stress. The flow properties of the samples were controlled so that

a large range of viscosity could be measured accurately in this range of shearing stress.

PART I

CHAPTER II

THE TUBE FLOW: THEORY AND ASSUMPTIONS.

1. Flow down a tube.

The theory of the determination of g and f at the wall of a tube, g_R , f_R , in terms of the pressure difference, p , across a length D of the tube, and the total rate of flow, q , was first given by Rabinowitsch (1929) and may be put in the form:-

$$g_R = \frac{1}{\pi R^3} (3q + p \frac{dq}{dp}) \quad \dots 2.1$$

$$f_R = \frac{pR}{2D} \quad \dots 2.2$$

where R is the radius of the tube. The derivation of these formulae will be given here, special attention being paid to the assumptions made in their derivation.

Equation 2.2 is derived by considering the equilibrium of the forces acting on a thin cylinder, of radius r , length D , thickness dr , and whose axis is the axis of the tube. The tube is assumed to be a right circular cylinder. Equating the force on the end of the thin cylinder with the force on its curved surface

gives:-

$$p \, d(\pi r^2) = d(2\pi r D f) \quad \dots 2.3$$

where f is the shearing stress on the curved surface.

If it is assumed that p is the same for all r , equation 2.3 can be integrated directly giving:-

$$f = pr/2D \quad \dots 2.4$$

Equation 2.2 then gives the value of f at the wall of the tube. In order that D may take any value it is assumed that the pressure gradient is constant along the tube.

The total rate of flow down the tube is given by:-

$$q = \int_0^R 2\pi r v \, dr \quad \dots 2.5$$

where v is the velocity of the fluid at distance r from the axis. Integrating by parts:-

$$q = \left[\pi r^2 v \right]_0^R - \int_0^R \pi r^2 \frac{dv}{dr} \, dr \quad \dots 2.6$$

The first term is zero if it is assumed that the fluid is at rest at the wall, i.e., that $v = 0$ when $r = R$.

As $g = -dv/dr$, by changing the variable to f by equation 2.4, equation 2.6 becomes:-

$$p^3 q = 8\pi D^3 \int_0^f r^2 \, df \quad \dots 2.7$$

$$\text{or} \quad 3p^3q = 8\pi D^3 \int_0^{f_R^3} g \, d(f^3) \quad \dots 2.8$$

If g is an analytic function of f , i.e., is single-valued in the range considered, then

$$3 \frac{d(p^3q)}{d(f_R^3)} = 8\pi D^3 g_R \quad \dots 2.9$$

From equation 2.2 this becomes:-

$$3 \frac{d(p^3q)}{d(p^3)} = \pi R^3 g_R \quad \dots 2.10$$

$$\text{or} \quad (3q + p \frac{dq}{dp}) = \pi R^3 g_R \quad \dots 2.11$$

which is equation 2.1.

It is sometimes convenient to use a variable q' in the place of q , where:-

$$q' = q / \pi R^3 \quad \dots 2.12$$

and to use f instead of p . Equation 2.11 can then be put in the form:-

$$g = 3q' + f \frac{dq'}{df} \quad \dots 2.13$$

which now represents the flow properties of the fluid, the right hand side of the equation being the flow function when q' has been experimentally determined as a function of f .

2. The sample fluid.

Certain assumptions made in the above theory limit the type of fluid whose flow function can be determined by means of flow down a tube. In order that the pressure gradient may be constant along the tube it is necessary that the characteristics of the fluid shall not change during its passage down the tube: that is, the fluid must be instantaneously thixotropic. Such a fluid was produced by dispersing suitable solid particles in a suitable liquid medium. The details of its production are given in Appendix I.

As it has been found that the nature of the sample fluid determines, to some extent, the way in which equations 2.1 and 2.2 are applied and some details in the construction of instruments for measuring the flow function, its main characteristics will be given here. These are that it behaves as a solid body for shearing stresses below a certain value f_y , the yield value, and as a fluid for which g is a function of f for f greater than f_y , and as f becomes very large g becomes a proportion of f .

A peculiarity of the samples used in these experiments is the existence of two distinct yield values: a dynamic yield value, f_d , and a static yield

value, f_s . If a portion of the material is subjected to a gradually increasing shearing stress, it will not flow until the stress has reached a certain value, the static yield value: if a portion of the material is flowing under the action of a shearing stress, it will not cease to flow until the stress has been reduced to a certain value, the dynamic yield value. It is found that f_s is greater than f_d .

Thus, for such a fluid, the flow function is not single-valued at $g = 0$. The values $g = 0$, $f = f_d$ belong to the flow function: the values $g = 0$, $f_d < f \leq f_s$ do not. As will be shown below, the second set of values can be eliminated by adopting a suitable experimental procedure.

3. Assumptions which govern instrument design.

The first assumption governing the design of the tube instrument is that the tube shall be a right circular cylinder. Accordingly, such a tube is used in the instrument.

In deriving the expression $f = pr/2D$, it is assumed that the pressure over any plane perpendicular to the axis of the tube is constant. In the case of a sample with a yield value, there will be a central

region of plug flow down the whole length of the tube. At r less than a certain value r_y , determined by f_y , q , the sample will be in the solid state, and the pressure over a plane perpendicular to the axis of the tube may not be constant, as the material is capable of withstanding a certain pressure without necessarily transmitting this pressure as it is transmitted in a fluid.

The fundamental shape of a tube instrument is a reservoir, containing a supply of the sample, and connected to the tube, over the whole, or part of which the pressure is measured. The other end of the tube is open to the atmospheric pressure. The sample flows from the reservoir to the tube, and the solid plug down the centre of the tube will be driven down the tube partly by the direct (solid) thrust on it from the material coming from the reservoir. This thrust will not necessarily be the theoretical force on the plug, $\pi r_y^2 p$, and the value of r_y will not necessarily be the value given theoretically by the relation $f_y = p r_y / 2D$. In order to remedy this improper pressure distribution it is necessary to bring the sample to the fluid state at all r at the entry of the tube, so that there is no direct thrust

on a solid plug, and so that the pressure can be transmitted as in a fluid to all parts of a plane perpendicular to the axis of the tube at this point.

The pressure to be measured is the pressure difference between two planes at a distance D apart: i.e., it can be the pressure difference between a point on the wall of the tube at the open end (atmospheric pressure) and a point on the wall of the tube at a distance D from the open end. If the whole of the tube is longer than D , the sample can be brought to the fluid condition at all r at some point between the reservoir end of the tube and distance D from the open end. By measuring p between two such corresponding points, the pressure required to accelerate the sample from the reservoir into the tube, and the pressure required for the non-uniform region of flow between reservoir and tube, are not included in the measured pressure.

It is found that such a sample as is used in these experiments tends to 'slip' at a smooth wall. The assumed mechanism is a layer of the liquid medium, exuded from the sample, between the sample proper and the wall, acting as a lubricant. This effect can be observed most conveniently by containing the sample

between two parallel plates, the existence of the yield value maintaining the sample in position, and applying a tangential force to one plate. With smooth plates it can be seen that movement of a plate can take place without any movement in the sample, and that that plate is covered by a layer of the medium, and that no sample has adhered to it.

As the tube was to be of glass, the above experiment was performed with glass plates. In order to prevent this film of liquid acting as a lubricant, the surfaces of the plates were roughened by scratches perpendicular to the direction of the applied force, to such a degree that no slipping took place. The tube wall was then treated in the same way. Thus it can be assumed that no slipping took place in these experiments: i.e., that $v = 0$ at $r = R$.

4. Assumption which governs measuring technique.

The remaining assumption to be considered is that the flow function is single-valued. The experimental procedure for excluding the unwanted values $g = 0$, $f_d < f \leq f_s$ will now be described.

If the tube is filled with sample at the maximum rate of flow for an experiment, then since the sample

has all been brought to the fluid state before entering the tube, the solid region is formed from fluid sample. The shearing stress at the boundary between solid and fluid regions is therefore f_d , and the shearing stress within the solid region is less than f_d . Hence no part of the sample has $g = 0, f > f_d$. If the rate of flow, q , is now reduced, the radius of the solid region is increased. This increase is formed from fluid sample; hence the shearing stress at the boundary is still f_d , and within the solid region is less than f_d . If successively decreasing values of q are taken, $f \leq f_d$ for $g = 0$, and the unwanted values are therefore excluded.

If the tube is filled at a low rate of flow, the unwanted values are again excluded, but if the rate of flow is then increased, these values will be introduced into the sample in the tube at the time of the increase. They will be introduced because an increase in q will cause an increase from f_d in the shearing stress at r' , the position of the boundary: if the increase brings the shearing stress at r' to a value less than or equal to f_s , the boundary will remain at r' with $g = 0, f_d < f \leq f_s$ for the solid region; if greater than f_s , the boundary will move to a value of

r less than r' , with the shearing stress at the boundary equal to f_s and the unwanted values again included. However, sample supplied to the tube after the increase is made has been in the fluid state and will, therefore, form a boundary where the shearing stress is f_d . This change in radius of the solid region will travel down the tube until the whole of the boundary suffers a shearing stress equal to f_d , and the unwanted values are again excluded.

In practice the method of decreasing values of q was used, as the reservoir did not contain sufficient sample to allow the shearing stress at the boundary to be brought to f_d for each value of q .

CHAPTER III

THE ROTARY FLOW: THEORY AND ASSUMPTIONS.

1. Flow between concentric cylinders.

The theory of the determination of g and f at the inner cylinder, g_a , f_a , in terms of the couple, C , acting on a length H of the cylinders, and the angular velocity of the outer cylinder, W , was first given by Thornton (1948) in the form:-

$$g_a = 2C \frac{dW}{dC} \quad \dots 3.1$$

$$f_a = \frac{C}{2\pi a^2 H} \quad \dots 3.2$$

when it is assumed that the rate of shear at the outer cylinder, g_b , is zero, where a , b , are the radii of the inner and outer cylinders respectively. The derivation of these formulae will be given here, special attention again being paid to the assumptions made in their derivation.

If it is assumed that all forces are in equilibrium, the couple exerted by the flowing fluid on any cylindrical surface, of length H , within the

fluid and coaxial with the bounding cylinders, is the same. Hence, if C is the couple on the inner cylinder then the shearing stress f , at radius r , is given by:-

$$C = 2\pi r^2 H f \quad \dots 3.3$$

Equation 3.2 then gives the value of f at the inner cylinder.

For rotational flow, $g = r \, dw/dr$, where w is the angular velocity and g the rate of shear of the fluid at radial distance r . Hence,

$$dw = g \, dr/r \quad \dots 3.4$$

If the inner cylinder is at rest, and the outer cylinder has angular velocity W , integration gives:-

$$\int_0^W dw = \int_a^b \frac{g \, dr}{r} \quad \dots 3.5$$

As C is the same for all r , differentiation of equation 3.3 gives:-

$$dr/r = -\frac{1}{2} \, df/f \quad \dots 3.6$$

Therefore

$$W = - \int_{f_a}^{f_b} \frac{1}{2} \frac{g \, df}{f} \quad \dots 3.7$$

If $g = 0$ for $f \leq f_b$, this can be written:-

$$W = \int_0^{f_a} \frac{1}{2} \frac{gdf}{f} \quad \dots 3.8$$

If g is single-valued in the range considered, then

$$\frac{dW}{df_a} = \frac{1}{2} \frac{g_a}{f_a} \quad \dots 3.9$$

From equation 3.2:-

$$df_a / f_a = dC/C \quad \dots 3.10$$

which on substitution in equation 3.9 gives equation 3.1.

In general, if f_a is replaced by f and g_a by g in equation 3.9, the relation:-

$$g = 2f \frac{dW}{df} \quad \dots 3.11$$

is obtained, which represents the flow properties of the fluid, the right hand side being the flow function when W has been experimentally determined as a function of f .

2. The sample fluid.

In the case of the rotary instrument, a normally thixotropic fluid can be used if it is brought to its equilibrium rate of shear for each reading; but as the

tube instrument requires an instantaneously thixotropic fluid, only this type of fluid, as described in Chapter II, 2, need be considered here.

It has been assumed that the rate of shear at the outer cylinder is zero: this will be so if the shearing stress at the outer cylinder, f_b , is less than or equal to the yield value of the sample fluid, f_y , for the maximum couple attained in an experiment.

$$\text{Now } C_{\max} = 2\pi a^2 H f_{a(\max)} = 2\pi b^2 H f_{b(\max)} \quad \dots 3.12$$

$$\text{therefore } f_{b(\max)} = \frac{a^2}{b^2} f_{a(\max)} \quad \dots 3.13$$

hence $f_{b(\max)}$ can be made less than f_y by making a/b sufficiently small. In the instrument to be described $b^2 = 10 a^2$ so that $f_{a(\max)}$ cannot be greater than ten times the yield value.

3. Assumptions which govern instrument design.

The instrument is so designed that the outer cylinder, which contains the sample, rotates about a vertical axis, and that the inner cylinder, which is suspended in it, can be aligned on the same axis. There will thus be a region round the lower end of the inner cylinder in which the flow cannot be treated as

that between concentric cylinders. This region of improper flow is inherent in the nature of the instrument: the elimination of its effect will be discussed below.

The considerations of slip at the boundary walls for the tube instrument apply also to this instrument. As the cylinders were to be of brass, the experiment with parallel plates described in Chapter II, 3 was performed with brass plates, and the same remedy applied. It can then be assumed that $w = W$ at $r = b$, and $w = 0$ at $r = a$.

4. Assumptions which govern measuring technique.

If the region of improper flow at the lower ends of the instrument cylinders is considered to extend for a distance y from the lower end of the inner cylinder, then the flow pattern to which the theory applies will occur above this level. If the instrument is filled first to one level, and then to another level, then provided that the immersion of the inner cylinder is greater than y in each case, and that the speed of the outer cylinder is the same in each case, the difference between the couples obtained corresponds to a region of

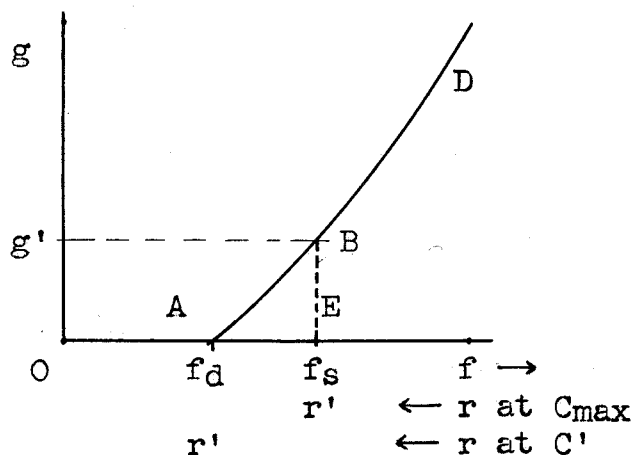
proper flow, the height of which is the difference between the two levels. In this way the effect of the region of improper flow can be eliminated.

In obtaining equation 3.9 it is assumed that g is a single-valued function of f . As in the case of the tube instrument, the unwanted values $g = 0$, $f_d < f \leq f_s$ can be excluded by a suitable experimental procedure which will now be described.

If the outer cylinder is rotated at the maximum speed for an experiment, and the corresponding couple is C_{\max} , then that part of the sample for which $r > r'$, where r' is given by $C_{\max} = 2\pi r'^2 H f_s$, does not suffer a shearing stress greater than f_s , and therefore does not flow, and that part for which $r < r'$ does flow. Let the flow function be represented by the curve OABD in Fig I, where the ordinate is g , and the abscissa f , or r at a given C . For $C = C_{\max}$, the boundary between solid and fluid states is at r' , i.e., where $f = f_s$, so that the flow of the sample is represented by the curves OE, BD in Fig I. Hence, as $r \rightarrow r'$ from $r < r'$, $g \rightarrow g'$, where g' is the value of g for which $f = f_s$ in the flow function, i.e., the point B in Fig I; and as $r \rightarrow r'$ from $r > r'$, $g = 0$. There is therefore a discontinuity BE in the rate of shear at

the boundary, and the values $g = 0$, $f_d < f \leq f_s$ are operative.

Fig I.



If C is now reduced from C_{max} , the boundary will remain at $r = r'$ until the shearing stress there is reduced to f_d , i.e., to the point A in Fig I, and then $f \leq f_d$ for $g = 0$. Further reduction in C will then move the boundary to smaller values of r , the shearing stress at the boundary remaining at f_d , and within the solid region at less than f_d . When $f = f_d$ at $r = r'$, let $C = C'$; then $C' = 2\pi r'^2 H f_d$. Hence for $C < C'$ the unwanted values are excluded, as the flow of the whole sample is then represented by the curve $OABD$ in Fig I.

From the above, the relation between C_{max} and C' can be obtained, for:-

$$C_{\max} = 2\pi r'^2 H f_s \quad \dots 3.14$$

and
$$C' = 2\pi r'^2 H f_d \quad \dots 3.15$$

therefore
$$C' = C_{\max} \frac{f_d}{f_s} \quad \dots 3.16$$

Hence if successively decreasing values of W are taken, the unwanted values are excluded for $C \leq C_{\max}(f_d / f_s)$.

In the case of increasing values of W , W_s , the boundary between solid and fluid regions is at $f = f_s$, since this shearing stress is required to increase the radius of the fluid region: for decreasing values of W , W_d , the boundary is at $f = f_d$ for $C \leq C'$. Then, since the lower limit of the integral in equation 3.8 can be the greatest value of f for which $g = 0$:-

$$W_d = \int_{f_d}^{f_a} \frac{1}{2} \frac{gdf}{f} \quad \dots 3.17$$

and
$$W_s = \int_{f_s}^{f_a} \frac{1}{2} \frac{gdf}{f} \quad \dots 3.18$$

Hence for a given value of f_a ,

$$W_d - W_s = \int_{f_d}^{f_s} \frac{1}{2} \frac{gdf}{f} = W' \quad \dots 3.19$$

where W' is a constant, as the integral depends only on the properties of the fluid.

Differentiation of equation 3.19 with respect to C gives:-

$$\frac{dW_d}{dC} = \frac{dW_s}{dC} \quad \dots 3.20$$

so that g_a can be computed from either the W_d curve for $C \leq C'$, or the W_s curve.

In the transition region between C_{max} and C' for decreasing values of W , W_t , the boundary conditions are $w = W$ at $r = r'$ and $w = 0$ at $r = a$, and equation 3.5 becomes:-

$$W_t = \int_a^{r'} \frac{gdr}{r} \quad \dots 3.21$$

In practice it was found that in taking an increasing set of values the lower part of the W_s curve did not correspond to a value of $f = f_s$ at the boundary. For, in taking an increasing set (of values), the outer cylinder is initially at rest, and is then given a small angular velocity. The sample is all in the solid state, and the rotation of the outer cylinder is given to the inner, until its deflection against the restoring couple of its suspension corresponds to a shearing stress f_s at its surface. Flow then takes place. The yield value is reduced to f_d , and this causes, in practice, a fairly rapid decrease in the deflection. This decrease means that the reading at this speed does not belong to the

increasing set, owing to the rise and subsequent fall in the relative angular velocity of the cylinders during the decrease in the deflection. Subsequent readings will not belong to this set until the shearing stress at the boundary between fluid and solid states is again f_s . As there appears to be no criterion for determining the position of the boundary after the initial decrease in the deflection, there must be some doubt as to the validity of the readings for the lower values of W_s .

Fig II

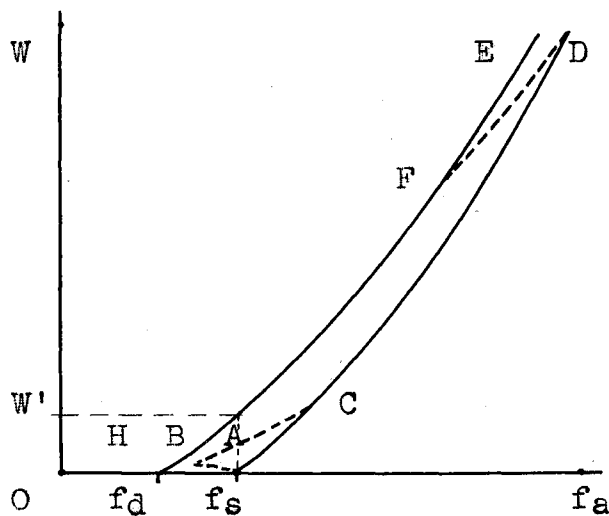


Fig II shows the results to be expected from the above theory. The ordinate is W , and the abscissa f_a , which is proportional to the deflection. For the curve ACD , the shearing stress at the boundary is f_s

(i.e., increasing values); for the curve EFH, it is f_d (i.e., decreasing values). If, for an increasing set of values, the outer cylinder is given a small angular velocity, the deflection reaches A, where $f_a = f_s$; it then falls, as described, to some value represented here by B. If W is now increased, the corresponding values of f give the curve BC until the shearing stress at the boundary is f_s , i.e., at the point C. Further increase gives the curve CD up to D, where $f_a = f_a(\max)$. A decrease in W now gives the transition stage, the curve DF. Along this curve the shearing stress at the boundary falls, until at the point F it reaches f_d . Further decrease gives the curve FH down to H, where $f_a = f_d$ and $W = 0$.

In order to calculate g_a , the value of dW/df_a can be taken from the part CD of the experimental increasing curve BCD, and from the part FH of the experimental decreasing curve DFH. Within the range of f_a between C and F, the values of dW/df_a from both curves are equal, as the separation of the curves, W' , is constant. If the point A has not been determined experimentally, the value of f_s can be found from the separation W' , as $f_a = f_s$ when $W_d = W'$.

CHAPTER IV

METHODS FOR COMPARING THE RESULTS FROM THE INSTRUMENTS.

1. Direct comparison.

In order to compare the flow functions as derived from the two instruments separately it is necessary only to obtain from each the values of g for a set of values of f , and display them on the same graph. If all points lie on the same smooth curve (within the limit of experimental error) then the flow functions are said to agree. There is a disadvantage in this method: it is that the direct procedure involves the drawing of tangents to the experimental curves in order to evaluate dq'/df and dW/df . This is not usually a very accurate procedure, as small irregularities in the curve may produce comparatively large variations in the estimated gradient. There is also some doubt as to the direction that the curve is taking at the extreme values, particularly at the upper end. The position of the discontinuity shown at F in Fig II is not immediately obvious from the plotted points and attempts to fit the points in this region to a smooth

curve again introduces errors in the value of the gradient.

To overcome these objections methods have been developed by which comparison can be made without having to estimate the gradient of the experimental curves. In one case the experimental q' -values can be transformed into the corresponding W -values, which can then be compared with the experimental W -values: in the other case, the experimental W -values can be transformed into the corresponding q' -values.

In these methods the flow function is not computed from the experimental curves: their sole purpose is to make a more accurate comparison between the results from the two instruments. Both cases are given, although only one is needed in practice. The choice of method depends on the completeness of the experimental curves at their lower ends. In the case of the instruments to be described the W - f curves are more complete in this respect than the q' - f curves. Hence q' -values were derived from the W - f curve. This case will, therefore, be considered first.

2. Derivation of q'-values from the W-f curve.

For the tube instrument, from equation 2.13,

$$g_R = 3q' + f_R \frac{dq'}{df_R} \quad \dots 4.1$$

For the rotary instrument, from equation 3.11,

$$g_a = 2f_a \frac{dW}{df_a} \quad \dots 4.2$$

$$\text{If } f = f_R = f_a \quad \dots 4.3$$

$$\text{then } g_R = g_a \quad \dots 4.4$$

$$\text{and } 3q' + f \frac{dq'}{df} = 2f \frac{dW}{df} \quad \dots 4.5$$

from equations 4.1 and 4.2. Equation 4.5 can be put in the form:-

$$\frac{d(f^3 q')}{df} = 2f^3 \frac{dW}{df} \quad \dots 4.6$$

If, at a shearing stress $f = f_0$, W has the value W_0 and the corresponding value of q' is q'_0 , equation 4.6 can be integrated to give:-

$$\int_0^{f_0^3 q'_0} d(f^3 q') = 2 \int_0^{W_0} f^3 dW \quad \dots 4.7$$

$$\text{Hence } q'_0 = \frac{2}{f_0^3} \int_0^{W_0} f^3 dW \quad \dots 4.8$$

From the experimental results, W can be plotted as a function of f^3 and the integral in equation 4.8 can be evaluated by counting squares or by some more exact method. A value of f_0 is chosen and the integral evaluated between the limits shown: the value of q'_0 thereby obtained is the value corresponding to f_0 . In this way a number of values of q'_0 and f_0 can be obtained, and the graph relating them compared with the experimental q' - f curve.

3. Derivation of W-values from the q' - f curve.

Alternatively, equation 4.5 may be written in the form:-

$$2 \frac{dW}{df} = 3 \frac{q'}{f} + \frac{dq'}{df} \quad \dots 4.9$$

Integrating, as in 2., between limits represented by the corresponding values W_0 , q'_0 , f_0 , equation 4.9 becomes:-

$$2 \int_0^{W_0} dW = 3 \int_0^{f_0} \frac{q'}{f} df + \int_0^{q'_0} dq' \quad \dots 4.10$$

or

$$2W_0 = 3 \int_0^{f_0} \frac{q'}{f} df + q'_0 \quad \dots 4.11$$

From the experimental results the right hand side of equation 4.11 can be evaluated for any value of f_0 , and hence the corresponding value of W_0 obtained. These W -values can then be plotted as a function of f and the curve obtained compared with the experimental W - f curve.

4. Method for incomplete curves.

A less complete way of making the comparison, if the lower ends of the experimental curves are in doubt, or missing, is to select some value of f , f_1 , which corresponds to a reliable point on the lower part of the experimental curve under consideration, and to use this value as the lower limit of integration in equation 4.8 or 4.11. If this is done, however, an arbitrary constant is introduced which can only be evaluated from the experimental curve which it is desired to obtain. For example, if the method of 3. is being used, the right hand side of equation 4.10 can be evaluated for any value of the lower limit. The left hand side will, however, contain a term W_1 (the lower limit) which is the value of W at $f = f_1$. This can only be found from the experimental W - f curve.

However, the other points of the derived curve should agree with the experimental curve for any chosen value of the lower limit: thus non-agreement is demonstrated, but agreement is not completely conclusive.

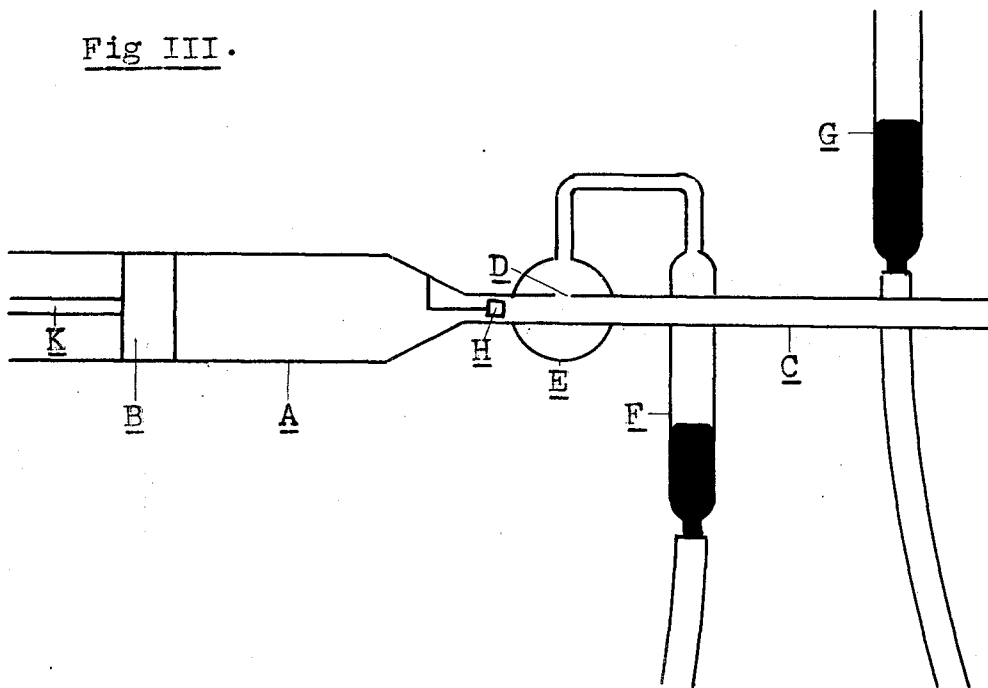
CHAPTER V

THE TUBE INSTRUMENT: DESCRIPTION.

1. The essentials of the instrument.

The essentials of the tube instrument are shown in Fig III. The reservoir, A, is a cylindrical glass tube down which a close-fitting plunger, B, can be

Fig III.



driven at a number of predetermined rates. The tube, C, also of glass, is connected directly to the reservoir. Hence, if U is the velocity of the

plunger, and d the diameter of the reservoir, q will be given by the relation:-

$$q = \frac{1}{4} \pi d^2 U \quad \dots 5.1$$

and a number of predetermined values of q will be obtained.

The excess pressure, p , in the material, due to the flow, at a distance D from the end of the tube open to the atmosphere, is equal to the pressure exerted by the wall of the tube on the material at this point. Hence, if a small portion of the tube wall is removed at this point, and an external air pressure, of magnitude p , applied at the hole so made, the flow will not be disturbed: the pressure in the material due to the flow can then be found by measuring the applied pressure. In the instrument, there is a hole, D , bored in the wall of the tube near the reservoir end. This hole and a short portion of the tube containing it are surrounded by a small closed chamber, E , which is connected to a variable manometer, $F G$. This hole is the pressure-measuring hole.

In order that the sample shall be in the fluid state at all r at some point in the tube before the pressure-measuring hole, a constriction, H , is

introduced which causes the sample to be supplied to the operative part of the tube through a narrow annulus bordering the wall of the tube. As the material for the flow down the axis of the tube has then to flow from the wall to the axis, the sample must be in the fluid state at all r in a small region immediately following this constriction.

The inner wall of the tube is roughened by scratches in a direction perpendicular to the direction of flow. This was done by filling the tube with a mixture of emery powder and water, and rotating in it a short brass cylinder of diameter slightly less than that of the tube. The abrasive used was the same as that used in the pilot experiment with the parallel plates, and the same degree of roughening was applied. This roughening removed a large part, but not all, of the original surface of the wall: the original surface remaining acts as a guide for the flow, and the depressions serve to anchor the material and to prevent the formation of a smooth film of the medium.

The basis of the experimental procedure is to set q at its maximum value and to adjust the pressure in the chamber, by means of the movable limb, G , of the manometer, until the boundary between the material in

the tube and the air in the chamber is stationary and at the position formerly occupied by the tube wall at the hole. This pressure can then be measured on a manometer. q is now reduced to the next lower value and the manometer $F G$ readjusted for equilibrium at the hole, and p again measured. In this way a value of p is obtained for each value of q . From these values of p and q , f_R and q' are calculated, and the graph relating them drawn.

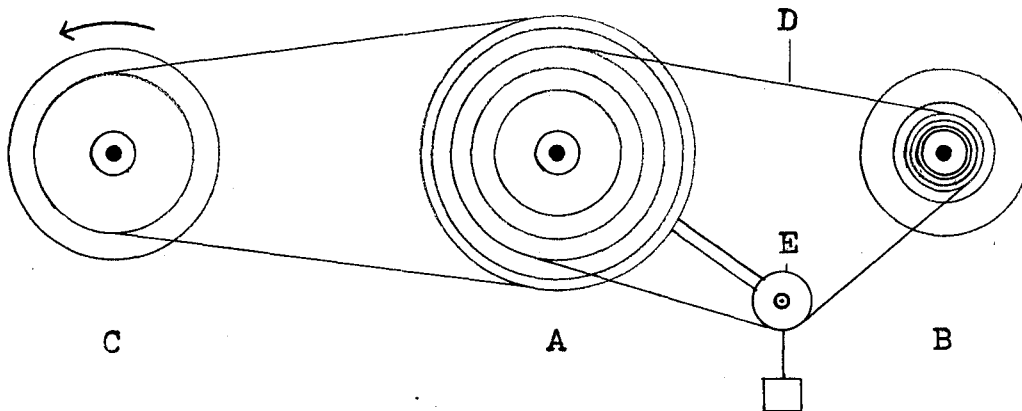
2. The plunger-driving mechanism.

The plunger-driving mechanism consists of a constant speed motor driving a pulley system from which a number of speeds can be selected for application to the gear box that changes the rotation of the drive into the lateral motion of the rod carrying the plunger. Fig IV shows the pulley system and Fig V the gear box for driving the plunger rod.

The pulley system comprises three wheels: wheel C is mounted on the motor spindle, wheel B on the gear box, and wheel A idles. Wheels A and B each have six grooves with radii, in decreasing magnitude, A_1, A_2, \dots, A_6 ; B_1, B_2, \dots, B_6 , respectively. When the belt,

D, connects grooves A1 and B6 the maximum speed is obtained. The next lower speed is obtained by slipping the belt from B6 to B5; the next by slipping

Fig IV.



the belt from A1 to A2; then from B5 to B4; and so on. In this way eleven speeds are obtained which are numbered as shown in Table I.

Table I - Pulley system speed numbers.

Speed No.	6	$5\frac{1}{2}$	5	$4\frac{1}{2}$	4	$3\frac{1}{2}$	3	$2\frac{1}{2}$	2	$1\frac{1}{2}$	1
Wheel A:-	A1	A1	A2	A2	A3	A3	A4	A4	A5	A5	A6
Wheel B:-	B6	B5	B5	B4	B4	B3	B3	B2	B2	B1	B1

This gives eleven values for n , the ratio of the speed of B to that of A. The radii of the grooves are such

that, if A rotates with constant speed, the speeds of B are approximately in arithmetical progression. Wheel A has a seventh groove by which it is driven by a belt from wheel C: three radii, C1, C2, C3, are available on C, allowing a variation of the range of the eleven speeds given by A and B. m is the ratio of the speed of A to that of C, and has three values.

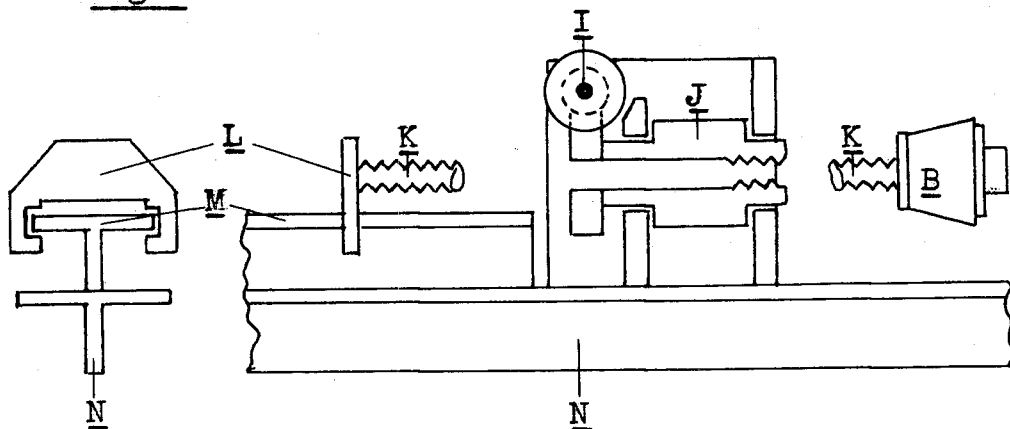
The belt connecting A and C is kept at a suitable tension by the position of the motor: that between A and B by means of a weighted idling pulley E. Each belt is made from a single length of thread wound round the wheels about twelve times, each successive turn being wound toroidally round the turns already on. The ends are then knotted. This gives a belt of the required size and strength, and the small knot does not cause any appreciable vibration as it meets the grooves.

The spindle I on which the wheel B is mounted rotates the cylinder J (see Fig V.) by means of a worm drive. This cylinder has a tapped hole down its axis, through which passes the screwed rod K, carrying the plunger B. This rod is prevented from rotating by the guide L running along the slide M: hence the rotation of I gives a translation to B along the reservoir.

The gear box and the reservoir are mounted on the 'T'-section girder N.

The plunger consists of a tapered rubber bung held between brass washers: the larger end of this bung has

Fig V.



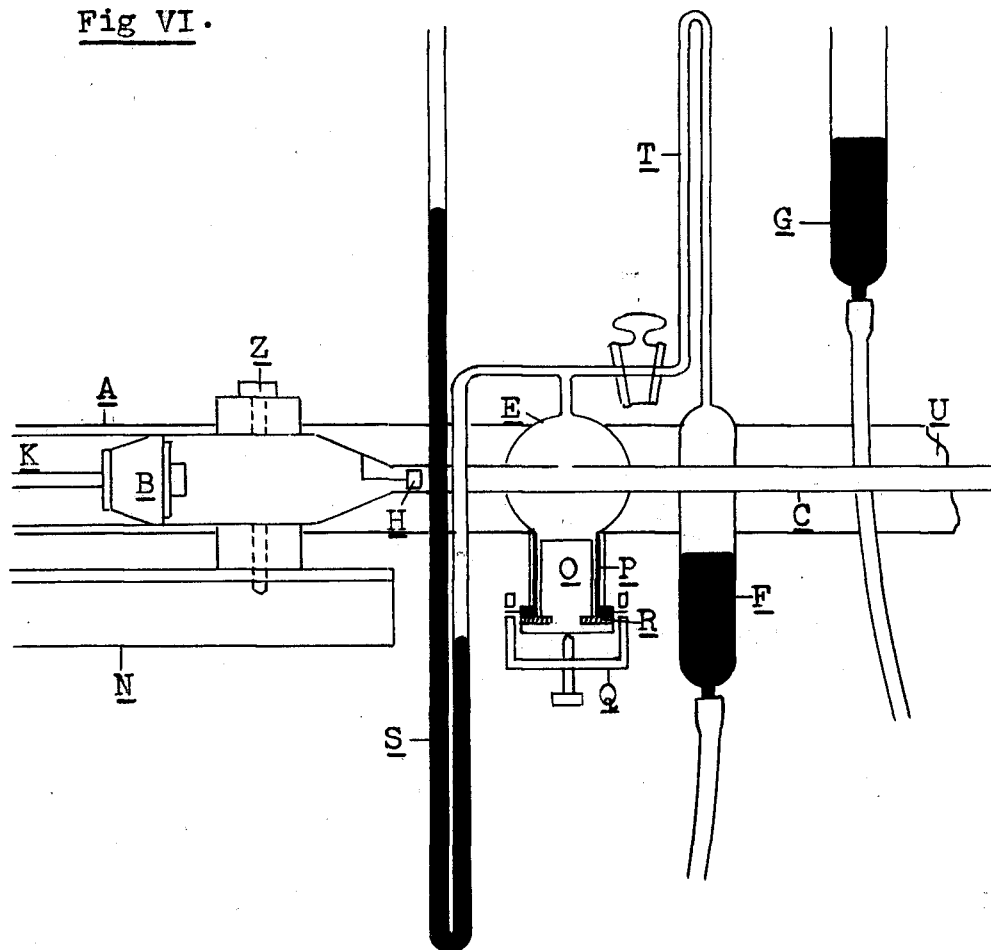
a normal diameter slightly greater than the diameter of the reservoir, and this ensures a leak-proof sliding fit. The plunger can be dismounted from the rod K.

3. The reservoir and tube assembly.

The reservoir and tube assembly is shown in Fig VI and consists of the reservoir, the tube, the pressure chamber, a fixed mercury manometer for measuring the pressure, and the variable mercury manometer, one limb

of which can be raised or lowered, for adjusting the pressure in the chamber. The reservoir and the tube have already been described.

Fig VI.



The pressure chamber consists of a bulb blown on the end of a piece of wide bore glass tube. Two holes, of diameter slightly greater than the external

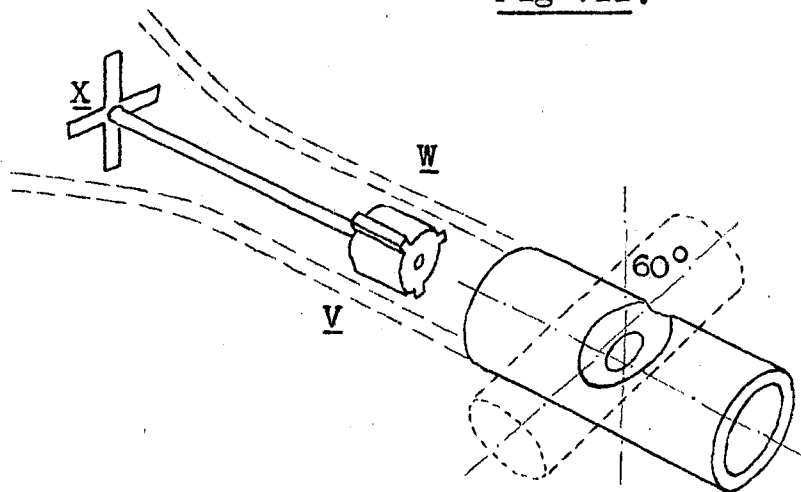
diameter of the tube C, were made through the wall of the bulb at opposite ends of a diameter perpendicular to the axis of the wide bore tube. By means of these holes, the bulb was slipped over the tube C so that the hole in this tube was at the centre of the bulb. The bulb was sealed in place on the tube by means of wax, to avoid any deformation of the tube by glass-to-glass sealing.

A short length of the wide bore tube was left on the bulb to serve as a suitable exit through which any material escaping into the bulb can be removed at the end of an experiment. A removable seal was made in this opening by means of a plug Q (see Fig VI) which is a sliding fit in a brass insert P, sealed into the glass tube. The plug is held in place by means of a screw through the bridge Q which is suspended from the insert P by means of two diametrically opposed pins. By filling the narrow space between plug and insert with the sample, and by means of the rubber washer R, an effective removable seal was made which requires only a small couple to make or break it: thus there is no danger of fracture to the glass assembly.

The hole through the wall of the tube C was made by rotating on it a brass cylinder supplied with a

suitable abrasive. This cylinder was of the same diameter as the internal diameter of the tube, and was held with its axis perpendicular to the axis of the tube. This action produces a hole with bevelled edges

Fig VII.



which allow accurate observation of the alignment of the surface of the sample with the tube wall. It also gives a hole which is narrow in the direction of the flow, so that there is a negligible pressure drop across the hole, but the hole is large enough for the purpose of measurement. (The diameter of the tube is about 5 mm. and the hole made is about 2 mm. wide in the direction of the tube, and 3 mm. perpendicular to this direction.) The tube is mounted in the

instrument so that the axis of the cylinder forming the cut in the tube is inclined at about 60° to the vertical. This allows any material escaping through the hole during an experiment to fall away from the hole, so that observation is not impeded. The shape of the hole is indicated in Fig VII.

The chamber is connected, by means of narrow-bore glass tubing, to the two manometers. The fixed manometer, shown at S in Fig VI, is used for measuring the pressure in the chamber and has a millimetre scale attached to it. The tube connecting the fixed limb, F, of the variable manometer to the chamber makes the upward loop shown at T, and includes a glass tap. The purpose of the loop is to prevent mercury from F and G overflowing into the chamber and contaminating the sample, in the event of a sudden fall in the pressure in the chamber owing to leakage or other causes. The glass tap allows the chamber to be opened to atmospheric pressure, or isolated from the variable manometer. The dimensions of the variable manometer are such that, when the pressure in the chamber is as great as is required, the fixed limb, F, is full of mercury: this gives the greatest sensitivity to the pressure control.

The constriction, H, is shown in detail in Fig VII. It consists of a short cylinder, V, connected by a thin rod to the cross X. Three studs, as at W, serve to locate the axis of V along the axis of the tube. The constriction is kept in place by the flow of the sample past it, as it brings the cross to bear on the narrowing part of the reservoir. It is then easily removed for cleaning purposes at the end of an experiment.

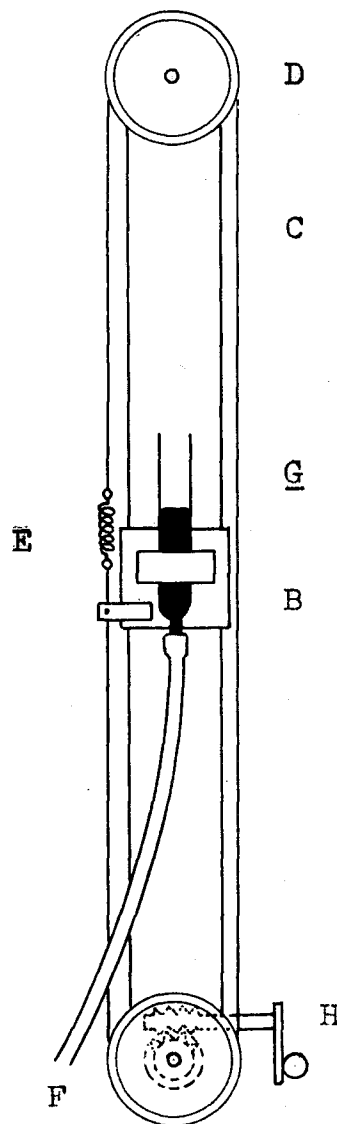
The reservoir and tube are mounted on a light rigid girder, U (shown in Fig VI), together with the fixed manometer and the fixed limb of the variable manometer. The variable limb is normally mounted separately from this assembly, but it can be attached to it. The whole assembly is then mounted on the girder N of the plunger-driving mechanism, and is connected to it by means of four screws, as at Z, through the wooden blocks that hold the reservoir to the girder U.

4. The manometer lift.

The manometer lift is shown in Fig VIII. Its purpose is to raise or lower the limb G of the variable

manometer so that the pressure in the chamber can be adjusted. As this pressure must be capable of fine adjustment, the apparatus described below was constructed. The lift consists of a vertical post, A, on which can slide, without rotating, a carriage, B, which carries the movable limb G. The position of the carriage is controlled by a cord, C, which passes over pulleys, D and F, at the upper and lower ends of the post A. This cord is kept taut by a spring, E, and is attached to the carriage. The upper pulley wheel idles, and the lower is rotated by a handle, H, through a worm drive. This drive permits precise adjustment of the carriage, and hence precise control of the pressure,

Fig VIII.



and allows the carriage to remain in any position in which it is set. The limb G is fixed to the carriage by means of a single screw, so that it can readily be removed and attached to the reservoir and tube assembly when the instrument is dismantled for filling or cleaning as described in Chapter VII.

5. The complete instrument.

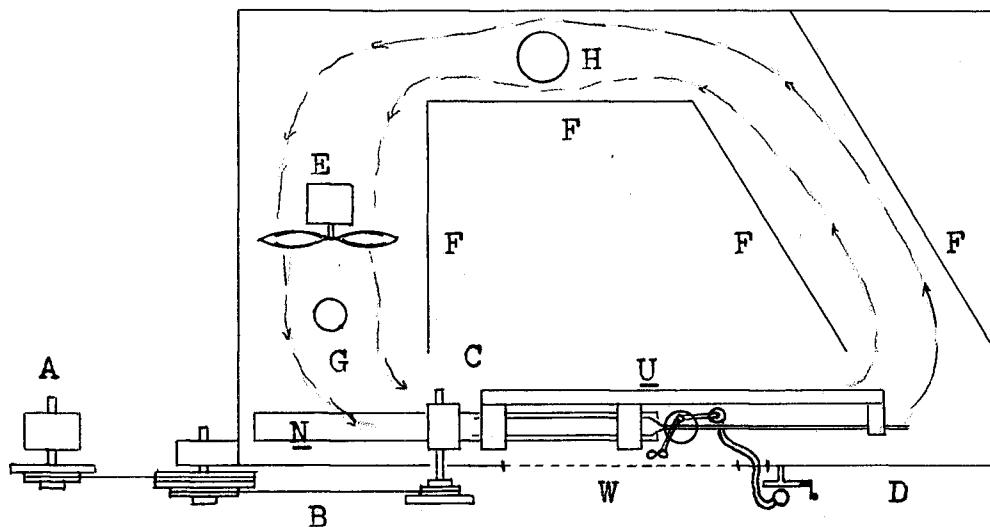
The plunger-driving mechanism and the reservoir and tube assembly are mounted in a constant temperature air-bath which is in the form of a rectangular box. The manometer lift and the pulley system are mounted on the outside of this box. The driving motor is mounted separately from the rest of the instrument in order to minimise the effects due to any vibration from it.

The instrument is mounted along one side of the box. A glazed window permits observation of the pressure chamber and the fixed manometer, and a door allows the reservoir and tube assembly to be removed for filling. The disposition of the various parts is shown diagrammatically in Fig IX. The driving motor is shown at A, and the pulley system at B, the axle of

the gear box passing through the air-bath wall. The reservoir and tube assembly is shown at C, and the positions of the window and door at W and D.

Air is circulated in the box by means of a fan, E.

Fig IX.



By means of the baffles, F, which reach from floor to roof of the box, the air is made to circulate first past a thermal regulator, G; then along the whole length of the instrument; then past a heater, H, and back to the fan. In this way all the air in the box is kept moving, and at the correct temperature.

The temperature regulation is effected by means of

a mercury-toluene regulator operating a 100-watt electric lamp through a 'Sunvic' electronic relay.

In the case of the samples of the type used in these experiments, a small change in shearing stress may produce a large change in the rate of shear, especially near the yield value. The minimisation of vibration is therefore important, as vibration can contribute to the shearing stress through the inertia of the material. To this end the motor is mounted separately, and the apparatus is designed so that the rotating parts run at small speeds. The fan used for circulating the air in the box is also run at a low speed, and is of a large size so that its effectiveness is not impaired.

It was found, with the speeds used, that there was no appreciable vibration at the lower speeds: at the higher speeds some vibration could be felt, but in this region it would have the least effect on the rate of flow. The effect of the vibration present was examined with the tube full of the sample and the plunger disconnected from the driving rod. The pressure in the chamber was increased until flow along the tube from the hole commenced; the pressure was then reduced until flow stopped, and then increased

to within about one per cent of its former value. Starting the driving motor and the fan motor did not cause the sample to flow, but a light tap on the tube with a pencil did: it was therefore assumed that the amount of vibration present in an experiment did not have an appreciable effect.

The manometer lift is mounted on the outside of the box in a position in which it can conveniently be operated by one hand as the pressure-measuring hole is observed. The pulley system is in a convenient position for slipping the belt from one groove to another with the other hand when the speed has to be changed.

C H A P T E R VI

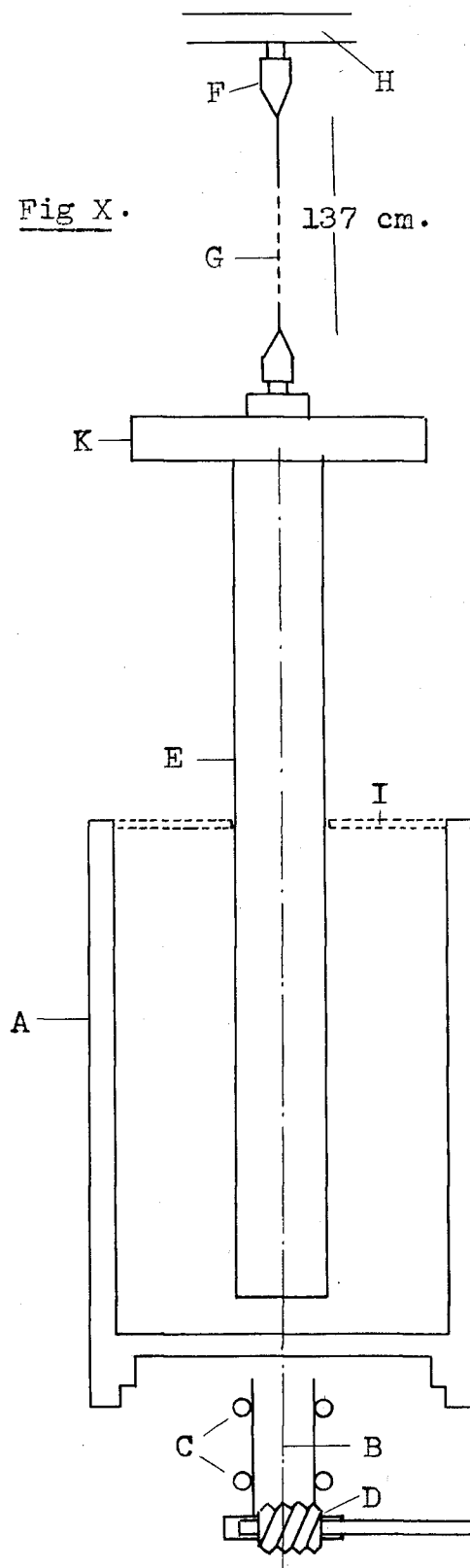
THE ROTARY INSTRUMENT: DESCRIPTION.

1. Essentials and initial adjustment.

The essentials of the rotary instrument are shown in Fig X where the inner and outer cylinders are drawn half their actual size. The outer cylinder, A, contains the sample, and is able to rotate about a vertical axis, B, in the bearings, C. These bearings are mounted on the baseplate, which can be adjusted by means of three levelling screws so that the axis B is vertical. This position is determined by placing a sensitive spirit-level across the upper rim of the outer cylinder. This cylinder is driven from a variable speed motor, through a system of pulleys and gears, of which the worm drive, D, is a part. The motor and pulley wheels are mounted separately from the operative part of the instrument. The angular velocity of the motor spindle is measured: that of the outer cylinder is determined from a knowledge of the various pulley and gear ratios.

The inner cylinder, E, is suspended from a clamp, F, by means of a torsion wire, G. The position of this clamp relative to a rigid support, H, also mounted on the baseplate, can be adjusted by means of screws so that the inner cylinder can be made coaxial with the outer. This position is determined by inserting a plate, I, in the top of the outer cylinder. This plate has a hole, concentric with its outer edge, and of diameter about 1 mm.

Fig X.



greater than that of the inner cylinder. The position of the upper clamp is adjusted until the gap between the plate and the cylinder appears to be of constant width. A constant length of torsion wire is used. If necessary, the clamp F can be moved up or down to adjust the gap between the lower ends of the cylinders. This gap is usually kept at a fixed value.

The couple exerted on the inner cylinder by the flowing material when the outer cylinder rotates is measured by the angular deflection of the inner cylinder against the restoring couple of the torsion wire. A circular scale, K, graduated in degrees, is mounted on the inner cylinder and is read by means of a telescope.

When the inner cylinder was set coaxial with the outer cylinder, and the instrument then filled with the sample, it was not found possible to set the inner cylinder in such a position that the deflection remained steady when the outer cylinder was rotated at constant speed. The least variation from the mean deflection was about $\pm \frac{1}{2}$ degree. The reading recorded was the mean deflection. It was found that this mean reading was independent of the position of the axis of the inner cylinder with respect to the axis

of the instrument, even for considerable maladjustment of the inner cylinder (a variation of up to ± 5 degrees). The small variations obtained were therefore not considered to introduce any error. This property of the instrument arises from the use of a long suspension wire: maladjustment of the inner cylinder gives no appreciable change in the flow pattern, only a precession of this pattern around the axis of rotation of the outer cylinder. An inner cylinder constrained in its axis and not concentric with the outer cylinder would appreciably alter the flow pattern.

In order to prevent slipping, the inner cylinder was roughened in the same way, and, as far as could be judged, to the same degree, as the brass parallel plates used in the pilot experiment described in Chapter II, 3. It was not found necessary to roughen the outer cylinder as no slipping was observed at this point.

The basis of the experimental procedure is to set W at its initial value and to observe the scale reading. W is then given other values, according to the programme used, and the scale readings taken. Owing to the presence of a yield value, the zero on

the scale is determined from the mean of readings taken at a given speed with opposite directions of rotation. The actual deflections of the inner cylinder can then be determined. From the calibration constant of the wire, from the depth of immersion, and from the end correction, the shearing stress at the inner cylinder, f_a , can be found. W is then plotted as a function of f_a , and from the curve obtained the flow function is determined.

2. The variable speed motor and drive.

The variable speed motor is a B.T.-H. 'Emotrol' equipment. By means of a potentiometer, the speed can be controlled continuously over the range 150 to 3 000 revolutions per minute. In order to increase the range at the instrument, a pulley system which will give a 1:1 or 20:1 speed ratio is included between it and the motor. The design of the instrument proper includes some gearing which gives a further reduction in speed. The pulleys and belts were made in the same way as those described for the tube instrument.

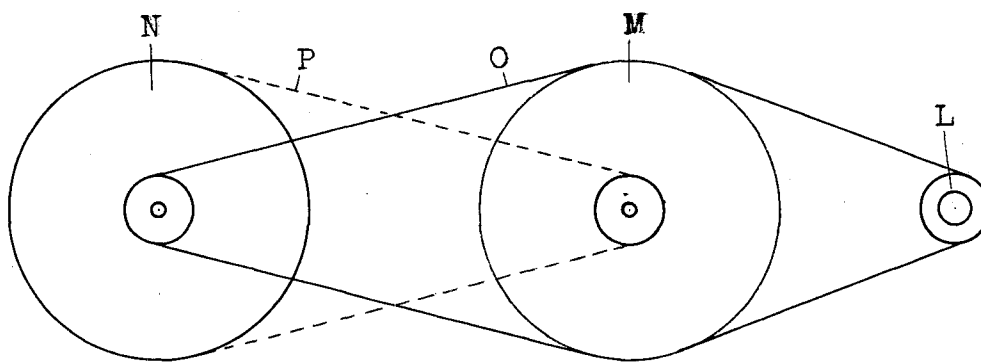
The speed of the motor can be measured by two different methods. It is found that the voltage

across the armature of the motor is closely proportional to its speed: thus a measure of the armature voltage can be taken as a measure of the speed of the motor. Calibration of this voltage at several values is effected by means of a stroboscopic disc attached to the motor spindle, and illuminated by a neon lamp run from the supply mains. The advantage of this method is that it uses the same standard of time (the frequency of the supply mains) as does the tube instrument: a disadvantage is that a certain amount of drift occurs in the voltage readings and frequent recalibration is necessary. A less fundamental method, but one that proves as accurate, is the use of a mechanical tachometer which can be brought to bear on the motor spindle, and the speed read off directly. It is found that the two methods are in agreement, and both have been used.

The pulley system is shown in Fig XI. The motor spindle carries a pulley wheel, L, from which an idling wheel, M, is driven: this gives a speed reduction of $\sqrt{20}:1$. Wheel M has two grooves, the radii of which are in the ratio of $\sqrt{20}:1$. The two grooves on wheel N are exactly similar to those on wheel M. Thus the belt connecting these wheels can be put in either of

the positions O and P. The position O gives a step up of $\sqrt{20}:1$ in speed, and is called the fast setting: the position P gives a step down of $\sqrt{20}:1$, and is called the slow setting.

Fig XI.

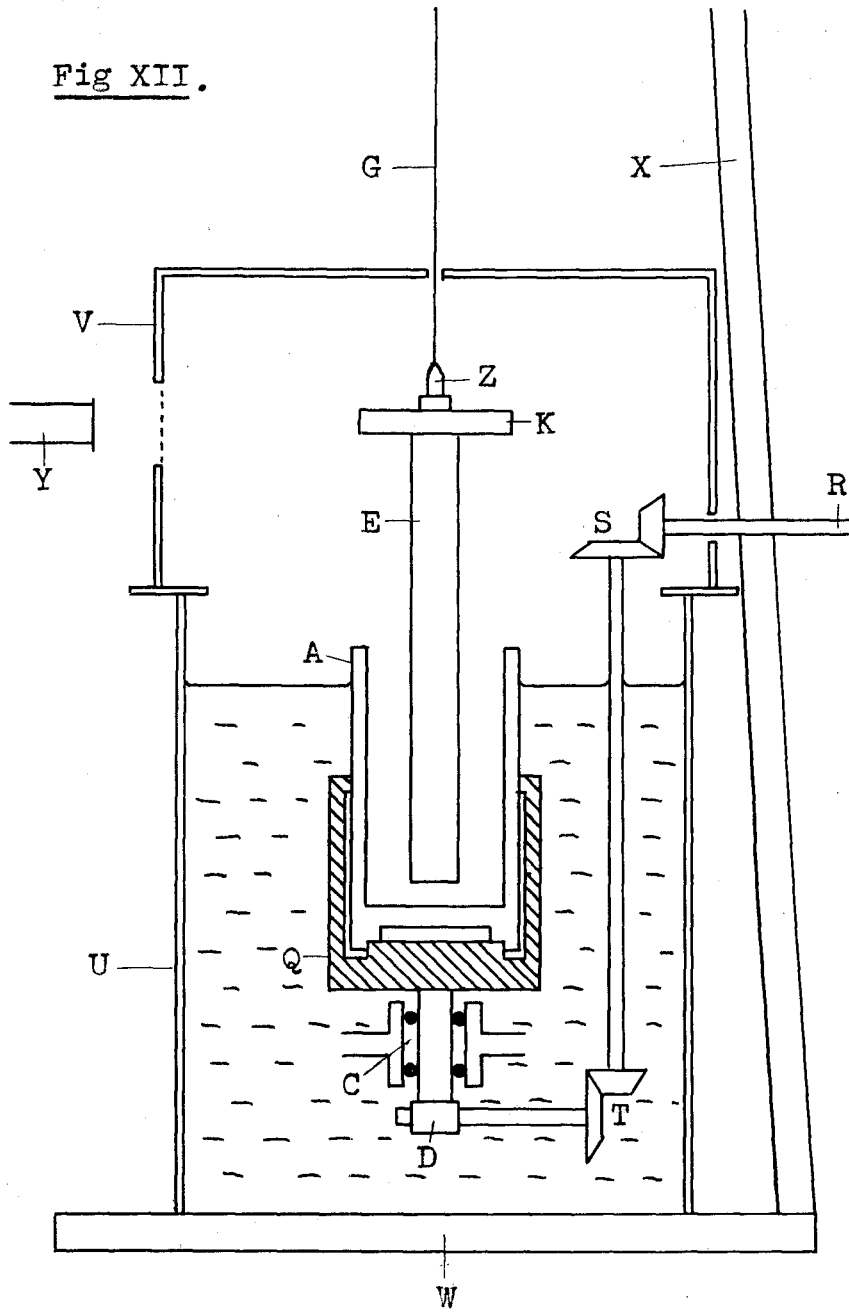


As in the case of the tube instrument, the motor and the pulley system are mounted separately from the rest of the apparatus in order to minimise any effects due to their vibration. No such effects were detected.

3. The instrument proper.

This part of the instrument is shown in Fig XII and consists of the concentric cylinders; some gearing

Fig XII.



for driving the outer cylinder; the suspension for the inner; and a constant temperature enclosure. The outer cylinder A is held in a cup, Q, from which it can be removed for ease of filling and cleaning. This cup is mounted in the bearings C, and is surrounded by a constant temperature oil-bath. The drive from the spindle R, on which the pulley N is mounted (see Fig XI), is by means of the train of gears shown at S, T, and D. The outer cylinder, which is slightly tapered on its outer surface, fits firmly into the cup Q (shown shaded in the figure). This cylinder can be withdrawn by attaching a handle to its upper rim.

The apparatus for keeping the temperature of the oil-bath constant is mounted in the annular space between the outer cylinder and the cylindrical container, U. The oil is driven round this space by means of a propeller so that it circulates continuously past heater, mercury-toluene thermo-regulator, thermometer, and propeller. The samples used are poor conductors of heat. In order to prevent a temperature difference across the sample it is necessary to enclose the non-immersed portion of the inner cylinder in an air-bath at the same temperature as the oil-bath. This is done by closing the top of the container U with

an asbestos-sheet box, V, including a small heater, fan, and thermo-regulator. The general principles of its construction are the same as for the box enclosing the tube instrument.

The support for the inner cylinder (shown at H in Fig X) is mounted on a tripod, the feet of which are firmly attached to the baseplate W, and the legs of which (one is shown at X in Fig XII) are blocked in, as far as possible, with sheet metal in order to make the structure rigid. The inner cylinder is suspended from this support by means of a phosphor-bronze wire of such a radius that the deflections of the cylinder are of the order of 100° for the sample used. The scale K is viewed through a window by means of the telescope Y. The wire is attached to the cylinder by means of a small chuck, Z, in order that the cylinder may be removed for cleaning. Provision is made for ensuring that the same length of wire is again in operation whenever the cylinder is replaced.

CHAPTER VII

EXPERIMENTAL PROCEDURES.

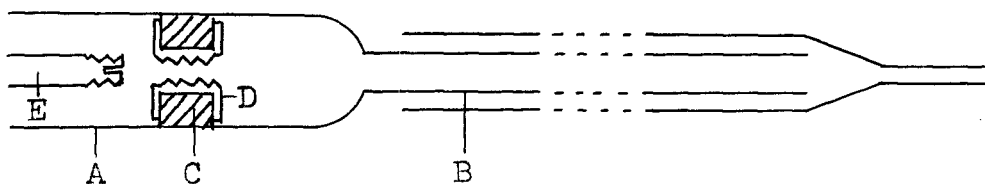
1. Filling the instruments.

It is essential that the samples in the instruments should be free from included air bubbles. A sample with an appreciable yield value will not readily flow, under the action of gravitational forces alone, into a tube such as is used for the reservoir of the tube instrument. This instrument is therefore filled by means of a supplementary reservoir, or 'filler', into which flow is caused by forces on the sample greater than those due to gravity. In this way air bubbles are not included, and the sample can then be transferred to the reservoir. With the samples used in these experiments it is possible to fill the rotary instrument directly by pouring from a container.

If a small volume of the sample is placed on a surface, it will retain its shape by virtue of its yield value: if the surface is accelerated, and the acceleration is great enough, the inertia of the

material will bring into play at the surface a force which is greater than the yield value, and the greater part of the material will then move relative to the

Fig XIII.



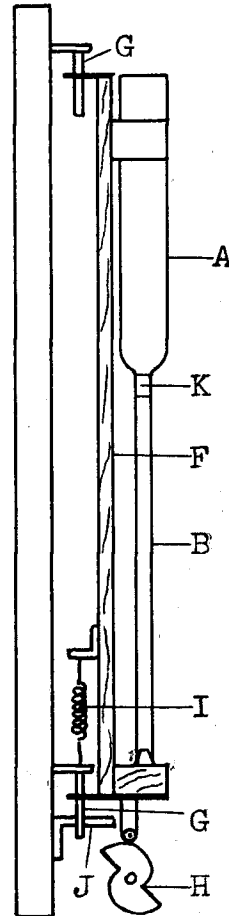
surface. If the surface is now returned to its original position with an acceleration less than the amount required for flow, and this cycle is repeated, the material will flow along the surface in a series of steps: if this cycle is repeated rapidly, the flow of a liquid under the action of gravity is simulated. This principle is used in filling the filler.

The filler is shown in Fig XIII. It consists of a wide glass tube A (length 18 cm. and diameter 3 cm.) which can contain sufficient sample to fill the reservoir (length 28 cm. and diameter 2 cm.), and which is connected to a narrower glass tube B (length 28 cm. and diameter 1 cm.) which can be inserted into the reservoir to reach its join with the measuring

tube. The wide tube is furnished with a plunger, C, which has a brass centre, D, with a threaded hole along its axis. The plunger is pushed down the tube by a handle, E, which can be screwed into the hole in the brass centre, at the same time sealing this hole.

For filling, the filler (see Fig XIV) is mounted on a carriage, F, which is given the motion described above along the slides, G. The cam, H, which is driven from a motor at a speed of 100 r.p.m., drives the carriage back against the spring, I, and then releases it to be brought back towards its original position by the action of the spring: this is the period of low acceleration. The carriage is then brought to a sudden standstill by

Fig XIV.



a stop, J: this is the period of high acceleration during which the sample moves some distance down the wall of the filler. The carriage is mounted vertically, and, as it oscillates, the sample is fed a small amount at a time to the lip of the tube A. From there it moves down the tube wall to the join with the tube B. It is found difficult to fill the narrower tube, B, in this way without including air bubbles, and so a small bung is placed in this tube at the join: it is shown at K.

When the filler has been filled in this manner, the plunger C is inserted in the open end of A and pushed in far enough for the sample to start escaping from the hole in D. This ensures that there is no air left in the filler: the handle is now attached and the plunger depressed, pushing the bung K down the tube B until the material fills this tube: the bung can then be removed. The whole of tube B is now inserted into the reservoir and the plunger again depressed: the material escapes into the reservoir. As the reservoir is filled, the filler is withdrawn to keep pace with the advancing material until the reservoir has been filled completely. The plunger of the plunger-driving mechanism is now inserted into the open end of the

reservoir, care being taken not to entrap any air in this process. The tube and reservoir assembly is then attached to the plunger-driving mechanism in the constant temperature air-bath.

Filling of the outer cylinder of the rotary instrument can be achieved by direct pouring, with the cylinder in situ if the sample is 'fluid' enough. In the case of less 'fluid' samples the cylinder can be removed from the instrument and filled again by pouring, with a certain amount of extra agitation.

2. Procedure for comparative experiments.

The following procedure is adopted to ensure that the parts of the sample in the two instruments have the same properties. The sample is contained in an airtight can and kept at 25°C.: before the experiment it is thoroughly stirred to avoid sedimentation effects. All the other apparatus is also kept at the same temperature. The filler is filled as described above, and returned to the air-bath: the process of filling takes a few minutes, and hence some cooling occurs and some time in the air-bath is necessary to bring the temperature to its former value. Meanwhile

the rotary instrument is filled: this process can be completed within a minute, so the cooling is less than in the former case. The reservoir and tube assembly is now removed from the air-bath, filled from the filler, and then returned to the air-bath: this process takes a few minutes, and again some cooling occurs; also the sample in the filler may not yet have reached temperature equilibrium with the air-bath. In order to make good any temperature losses, both instruments are left for a few hours before any readings are taken. This time is long enough for any temperature deficiency to be made up, but not long enough for any effects due to sedimentation or ageing to become appreciable. Readings can then be taken.

The rotary instrument was first run at a constant speed for about 30 minutes and the deflection observed in order to detect the presence of any normal thixotropy. With the samples used here the deflection remained constant. Readings were then taken on both instruments as described below. At the end of the experiments the temperature of the sample in each instrument was measured, and found to be within 0.1°C . of the nominal temperature, indicating that the above precautions were sufficient.

3. Readings on the tube instrument.

The method of filling given above ensures that the reservoir is filled as far as its join with the measuring tube. The driving motor is now started and the sample commences to flow down the tube: when it reaches the pressure-measuring hole the motor is stopped and the instrument is then ready. Because of the considerations given in Chapter II, 4., decreasing values of the speed are usually taken in order to determine the flow function, and hence this procedure will be given here. The procedure for increasing values is similar except that sufficient time must be allowed between readings for the proper conditions to be established.

The motor is started with the pulley system set to give the maximum rate of flow: sample then starts to escape from the pressure-measuring hole. By means of the manometer lift, the pressure at the hole is increased to prevent this escape. As the length of the tube filled by the sample increases, the pressure required to prevent escape of the sample increases until the whole of the tube has been filled: the pressure required to align the boundary between air and

sample with the tube wall is now found by slight variation of the pressure. If the pressure is too great, the sample will begin to disappear into the hole: if the pressure is too small, the sample will escape slowly from the hole. The pressures at which these two effects become evident are found: usually it is difficult to determine any difference between them on the fixed manometer (read to within about 0.1 mm. in a few centimetres). When the pressure has been balanced, the height of the mercury column in one limb of the fixed manometer is read; this reading then gives the value of p for the value of q given by the setting of the pulley system.

In order to take a reading at the next lower speed, the pressure in the chamber is reduced, and, as the sample starts to escape through the pressure-measuring hole, the belt of the pulley system is moved to the appropriate groove for the new speed, and the equilibrium at the hole re-established. The manometer is again read.

If the speed is reduced before the pressure, the reduced pressure in the sample causes the boundary between air and sample at the hole to disappear into the hole so that air enters the tube: the column of

sample in the tube is therefore shortened, the pressure in the chamber remaining sensibly constant, and hence the tube tends to empty rapidly. With practice, it is possible to judge the amount by which the pressure has to be reduced between speeds, and to change the speed as the pressure is being reduced so that there is little chance of the above state of affairs arising.

By continuing in this manner, values of p can be obtained for all values of q given by the pulley system. As the time available for taking all these readings is limited by the amount of the sample in the reservoir, it is usually found possible to read only one limb of the fixed manometer for each speed. The value of p is therefore calculated by doubling the difference between this reading and the zero position of the manometer.

If some air does enter the tube during the speed change, and the pressure can be reduced quickly enough to establish the proper rate of flow, it is necessary to wait until the air in the tube escapes from the open end of the tube. The distance that the plunger has to travel in order to send an air bubble down the tube is found to be about 2 cm.: a scale is therefore placed along the reservoir, and if an air bubble enters the

tube, the plunger is allowed to travel this distance before further readings are taken.

At the end of a set of readings, the pressure chamber is opened to the atmosphere by means of the glass tap; the manometer lift is returned to its lowest level; and the motor set in reverse to withdraw the plunger.

The actual values of q , the total rate of flow, are obtained by means of a prior calibration from the pulley grooves used: the values of p are determined from the height of the fixed mercury manometer. The calibration of the instrument also gives the factors for converting p -values into f_R -values, and q -values into q' -values. The relation between q' and f_R can thus be plotted, and from the curve obtained the flow function can be determined.

4. Readings on the rotary instrument.

With this instrument it is first necessary to determine the end correction to be applied in order to eliminate the effect of the region of improper flow at the lower end of the inner cylinder. The motor spindle is therefore furnished with a stroboscopic

disc which, when illuminated by means of a neon lamp run from the supply mains, enables a number of different speeds to be selected. The instrument is filled to various levels and the deflection of the inner cylinder read at each of the selected speeds for each level of filling: these deflections are plotted on a graph against the actual immersion for each speed. Thus the nature of the end correction can be investigated. It is found, with the samples used here, that it is equivalent to an extra depth of immersion which is sensibly independent of speed or immersion.

The speeds given by the stroboscopic disc are also used for finding the zero on the scale attached to the inner cylinder, as this cylinder is usually inserted after the outer is filled. For each of these speeds the values of the deflection are found with the motor running forward and in reverse: the zero at each speed is obtained and the mean taken.

A set of readings is now taken for increasing, or for decreasing, values of the variables. For increasing readings, the speed is set at a low value with the pulley system in its slow setting. The speed of the motor and the deflection of the inner cylinder

are determined. For the next reading, the speed of the motor is increased so slowly that the inertia of the inner cylinder does not carry the deflection past its equilibrium value, otherwise the boundary between the fluid and solid states of the material will not be at the position given by the theory for increasing values. Proceeding in this manner, values of the deflection are obtained for a number of values of the speed for the slow setting of the pulley system: the setting of the pulley system is now changed and the process continued. When the maximum speed is attained, a set of readings for decreasing values can be taken in a similar manner.

The values of the shearing stress at the inner cylinder are obtained from the deflections by means of the calibration of the suspension wire, the radius of the cylinder and the corrected immersion. The values of the speed of rotation of the outer cylinder are obtained from the motor speeds by means of the calibration of the pulley system and the value of the reduction ratio of the instrument gearing. The relation between W and f_a can thus be plotted, and from the curve obtained the flow function can be determined.

CHAPTER VIII

CALIBRATIONS OF THE INSTRUMENTS.

1. Tube instrument: methods.

Two distinct methods were used for this instrument. In the first method, the speed, M , of the driving motor was taken as 100 r.p.m.: the rate of flow, q , was determined from this value by measuring the pulley ratios, m and n ; the distance the plunger moves for one revolution of the spindle of the plunger-driving mechanism, s ; and the area of cross-section of the reservoir, $\frac{1}{4}\pi d^2$. The velocity of the plunger, U , is therefore given (with M in revs. per sec.) by:-

$$U = M m n s \quad \dots 8.1$$

and hence the rate of flow, from equation 5.1, is given by:-

$$q = \frac{1}{4}\pi d^2 M m n s \quad \dots 8.2$$

The pressure, p , is calculated from the difference in levels, h , of the mercury manometer by the relation:-

$$p = h \rho g \quad \dots 8.3$$

where ρ is the density of mercury at the temperature of the air-bath, and g is the acceleration due to gravity.

The length of the tube, D , was measured directly: the radius of the tube, R , was determined by direct measurement, and also from the volume per unit length of the tube. Using these values of R and D , the coefficients relating q and q' , and p and f_R , can be obtained from equations 2.12 and 2.2 respectively.

In the second method an oil of known viscosity was used in the instrument, and Poiseuille's Law:-

$$q = \frac{\pi p R^4}{8 \eta D} \quad \dots 8.4$$

applied to determine the value of R^4/D . By weighing the efflux in a given time, and using the density of the oil, the efflux volume in unit time, q , was found. p was determined from the height of a manometer containing the oil. The viscosity of the oil, η , was measured in a calibrated Ostwald Viscometer. D was again measured directly, and from the value of R^4/D obtained from equation 8.4, R was calculated. The coefficients relating q and q' , p and f_R , were then calculated as above.

The set of values of q given by the pulley ratios n , with $m = 1$, were also determined by measuring the velocity of the plunger and the cross-section of the reservoir. The velocity of the plunger was found by measuring the time taken for it to move through a known distance: the area of cross-section of the reservoir was calculated from the measured rates of flow in the application of equation 8.4, and the corresponding velocities of the plunger.

A comparison is made of the results of the two methods.

2. Tube instrument: first method.

(a) The speed of the motor.

The driving motor is of the synchronous type, and as, for the purpose of this calibration, the frequency of the mains supply from which it is energised is taken to be 50 c.p.s., then the speed of the motor is 100 r.p.m.. Hence:-

$$\underline{M} = \underline{\frac{5}{3}} \underline{\text{ rev. per sec.}}$$

(b) The pulley ratios m.

To determine m, marks were made on the peripheries of the wheels C and A of Fig IV and were aligned with fixed pointers. Wheel A was taken through a number of complete revolutions which brought the mark on C close to its pointer. The whole number of revolutions of C were counted. The fraction of a revolution is given by $e = x/2\pi X$, where x is the distance between mark and pointer, and X is the distance of the mark from the axis of the wheel: x was measured with a ruler, and eight determinations were made.

The values of m for the two radii of C used (C2 and C3) are given in Table II. The distance X was 5.70 cm., hence $e = x/35.8$.

Table II - Values of m.

	<u>C2.</u>	<u>C3.</u>
Revolutions of A:-	7	8
Revolutions of C:-	12 + e	39 - e
Mean values of x:-	0.74 ± 0.17	0.65 ± 0.25
Mean values of e:-	0.021 ± 0.005	0.018 ± 0.007
<u>Values of m:-</u>	<u>0.5824</u>	<u>0.2052</u>

The motor can also be connected directly to the wheel A: this arrangement, for which $m = 1$, will be called CO.

(c) The pulley ratios n.

The pulleys A and B were so constructed that their ratios are approximately in arithmetical progression. The values of n were determined in the same way as the values of m. As in the above case, the spread of the individual determinations of x were small, and will not be given. The values of n are given in Table III.

Table III - Values of n.

<u>Speed No.</u>	<u>Revs. of A.</u>	<u>Revs. of B.</u>	<u>n.</u>
6	8	40.07	5.001
$5\frac{1}{2}$	4	18.10	4.525
5	13	53.01	4.077
$4\frac{1}{2}$	13	47.02	3.617
4	9	28.08	3.120
$3\frac{1}{2}$	6	15.99	2.665
3	10	21.96	2.196
$2\frac{1}{2}$	11	19.04	1.731
2	13	16.04	1.234
$1\frac{1}{2}$	12	9.00	0.750
1	38	10.00	0.263

(d) The movement of the plunger, s.

The tapped cylinder which drives the plunger rod rotates at one-eighth of the speed of wheel B owing to the worm drive in the plunger-driving mechanism. The plunger-driving rod has a 2 B.A. thread which is nominally 31.4 t.p.i.. The distance between 192 threads was measured to be 15.52 ± 0.01 cm. (which gives 31.42 ± 0.02 t.p.i.), and hence, for one revolution of the cylinder, the plunger will move 0.08083 ± 0.00005 cm. Hence,

$$\underline{s = 0.01010 \pm 0.00001 \text{ cm. per rev.}}$$

(e) The cross-section of the reservoir, $\frac{1}{4}\pi d^2$.

The diameter of the reservoir was determined by means of internal calipers: their separation, after withdrawal, being measured with a micrometer. Column A gives the readings near the open end, and B the readings near the closed end for the vertical direction; columns C and D give readings near the open and closed ends respectively for the horizontal direction.

<u>A</u>	<u>B</u>	<u>C</u>	<u>D</u>
1.894	1.900	1.899	1.903
1.895	1.902	1.899	1.903
1.896	1.901	1.900	1.903
1.897	1.902	1.898	1.904
1.894	1.900	1.901	1.905
1.896	1.899	1.902	1.903

Hence, the mean diameter = 1.900 ± 0.001 cm.

Therefore:- $\frac{1}{4}\pi d^2 = \underline{2.835 \pm 0.003 \text{ cm}^2}$.

(f) The length of the tube, D.

The distance between the open end of the tube, and the centre of the pressure-measuring hole was found to be 33.4 cm.. As the hole extends for about 0.2 cm. in the direction of the tube, the value of D is given as:-

$$\underline{D = 33.4 \pm 0.1 \text{ cm.}}$$

(g) The radius of the tube, R.

The open end of the tube was fitted with a small bung, and the tube and reservoir assembly set at about 45° to the vertical. Mercury was then poured into the tube, via the reservoir, until its level reached the pressure-measuring hole. The length of the column was measured, the bung removed, and the mass of the mercury determined: the estimation of the length was to about

0.1 cm. owing to the shape of the meniscus at the hole.
Five determinations were made:-

<u>Length of column.</u>	<u>Mass of Hg.</u>	<u>Mass per cm.</u>
33.2 cm.	83.80 grm.	2.524
33.1	83.31	2.517
33.0	83.23	2.523
33.1	83.47	2.523
33.1	83.41	2.521

Hence, mean mass per cm. = 2.522 ± 0.003

The temperature of the mercury was about $22^{\circ}\text{C}.$, hence its density was taken as 13.54. The value of R^2 obtained from the volume of 1 cm. of the tube is then:-

$$R^2 = 0.05929 \pm 0.00007 \text{ cm}^2.$$

giving:- $\underline{R = 0.2435 \pm 0.0002 \text{ cm.}}$

A cathetometer measurement of the open end of the tube, before the tube was roughened, gave:-

$$R = 0.2423 \pm 0.0005 \text{ cm.}$$

(h) The values of q' .

Equation 8.2 gives the value of q , and from equation 2.12, the value of q' can be found. From

these equations:-

$$q' = \frac{1}{\pi R^3} \frac{1}{4} \pi d^2 M m n s \quad \dots 8.5$$

From the value of R given in (g), $1/\pi R^3 = 22.05 \pm 0.03$. The value of $\frac{1}{4} \pi d^2$ is taken from (e), M from (a), and s from (d). From these values, $q' = 1.052 m n$. The values of m and n are taken from Tables II and III, and the values of q' given in Table IV.

Table IV - Values of q and q'.

<u>Speed No.</u>	<u>q'</u>	<u>q'</u>	<u>q'</u>	<u>q</u>
	<u>C 0</u>	<u>C 2</u>	<u>C 3</u>	<u>C 0</u>
6	5.264	3.069	1.079	0.2387
5½	4.762	2.776	0.976	0.2160
5	4.291	2.502	0.880	0.1946
4½	3.807	2.219	0.780	0.1726
4	3.284	1.914	0.673	0.1489
3½	2.805	1.615	0.575	0.1272
3	2.311	1.348	0.474	0.1051
2½	1.822	1.062	0.374	0.0826
2	1.299	0.757	0.266	0.0589
1½	0.789	0.460	0.162	0.0358
1	0.278	0.161	0.057	0.0126

(i) The relation between h and f_R .

For experiments carried out at 25°C., the relation between h and p, from equation 8.3, is:-

$$p = 1.327 \cdot 10^4 h \text{ dynes per cm}^2.$$

Since $f_R = pR/2D$, the relation between h and f_R is:-

$$\underline{f_R = 48.4 h \text{ dynes per cm}^2.}$$

The least accurate measurement in this determination is the value of D, but this is known to within less than 1%, which is the accuracy desired in the calibration.

3. Tube instrument: second method.

(a) The density and viscosity of the oil.

The density of the oil was determined at two temperatures in the range used in the experiments to be described below. The results can be represented by:-

$$\text{density at } t^\circ\text{C.} = 0.9012 - 0.00065 t$$

The viscosity of the oil was determined by means of an Ostwald Viscometer. This viscometer carries a N.P.L. calibration, hence the viscosities at various temperatures in the range used could be measured to within a few parts in a thousand. The details will

not be given here. From the kinematic viscosity obtained and the density of the oil, the viscosities calculated can be represented by:-

$$\log_{10} \eta = 1.451 - 0.0335 t$$

where t is the temperature in degrees centigrade, and η is the viscosity in poise.

(b) The application of Poiseuille's Equation.

In order to use an oil in the instrument, a modification is necessary:

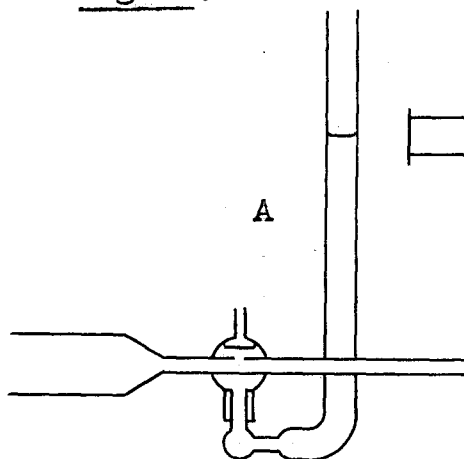
it is shown in Fig XV.

The mercury manometers were dispensed with, and the pressure was measured from the height of the oil in the vertical tube, A, which had a

diameter of 1 cm.. The

tube A was joined to the pressure chamber by a connection as wide and as short as possible, so that equilibrium conditions were established without undue delay. A speed was selected which brought the level in A near to the upper end of the tube, and a

Fig XV.



preliminary experiment was conducted to determine this level. In this experiment, the reservoir was filled, the driving motor started, and the oil allowed to flood the pressure chamber (which was open to the atmosphere) until it reached some level above the pressure-measuring hole. The chamber was then closed and the oil allowed to flow along the measuring tube and also up the vertical tube. When the measuring tube was full, its open end was closed to allow the oil to fill the vertical tube more quickly. After each few millimetres rise in the level in A, the oil was allowed to flow along the measuring tube also for a short time: the level in A at which a fall first occurred on allowing this flow then gave an approximate value of the equilibrium level. The instrument was then refilled under sufficient pressure to bring the oil in the vertical tube up to this level, and the motor started. By adopting this procedure, the equilibrium conditions could be established before the plunger reached the end of its traverse. The experiment was then repeated at a different speed. If h is the difference in the levels between the two speeds, which were Nos. 3 and $1\frac{1}{2}$ with $m = 1$, then from equation 8.4:-

$$\begin{aligned}
 q_3 - q_{1\frac{1}{2}} &= \frac{R^4}{D} \frac{\pi \rho' h g}{8\eta} \\
 &= \frac{R^4}{D} \frac{\pi h g}{8\nu} \quad \dots 8.6
 \end{aligned}$$

where ρ' is the density, and ν the kinematic viscosity, of the oil.

The values of h were measured by means of a cathetometer. The values of q_3 and $q_{1\frac{1}{2}}$ were determined by weighing the amount of efflux in a given time, and using the density of the oil at the appropriate temperature. These results are shown in Table V.

Table V - Values of q_3 and $q_{1\frac{1}{2}}$.

<u>Speed No.</u>	<u>Mass of oil in grms.</u>	<u>Temp. °C.</u>	<u>Density of oil.</u>	<u>Time in secs.</u>	<u>q cc/sec.</u>
3	44.52	19.2	0.8887	480	0.1044
3	39.09	18.2	0.8894	420	0.1047
$1\frac{1}{2}$	22.96	19.5	0.8885	720	0.03590
$1\frac{1}{2}$	28.68	19.5	0.8885	900	0.03588

These results give: - $q_3 = 0.1045$; $q_{1\frac{1}{2}} = 0.0359$

Hence, $q_3 - q_{1\frac{1}{2}} = 0.0686 \pm 0.0001$

Five experiments to determine the value of h/ν were then carried out: the details are given in Table VI, where h_3 and $h_{1\frac{1}{2}}$ are the cathetometer readings at the two speeds and ν is the kinematic viscosity (see (a)).

Table VI - Values of h/ν .

<u>Expt.</u>	<u>h_3.</u>	<u>$h_{1\frac{1}{2}}$.</u>	<u>h.</u>	<u>$^{\circ}\text{C}$.</u>	<u>ν.</u>	<u>h/ν.</u>
1.	35.45	22.03	13.42	17.8	8.05	1.666
2.	34.24	21.63	12.61	18.5	7.62	1.655
3.	34.41	21.59	12.82	18.3	7.74	1.657
4.	34.96	21.72	13.24	18.1	7.87	1.682
5.	34.75	21.58	13.17	18.3	7.74	1.702

Thus the mean value of $h/\nu = 1.67 \pm 0.02$.

Using equation 8.6, the value of R^4/D is given by:-

$$\underline{R^4/D = (1.065 \pm 0.01) 10^{-4} \text{ cm}^3.}$$

(c) The radius of the tube.

Using the result of (b), and the length of the tube given in 2.(f), the following result is obtained:-

$$\underline{R = 0.2443 \pm 0.0007 \text{ cm.}}$$

(d) The relation between h and f_R .

The values of R and D again give the relation between h and f_R as in 2.(i). The relation is:-

$$\underline{f_R = 48.5 h \text{ dynes per cm}^2.}$$

(e) The velocity of the plunger.

The velocity of the plunger for the various speed numbers with $m = 1$ was found by determining the time taken for the plunger to travel between two fixed marks on the reservoir. The results obtained are included in Table VII. Apart from the last result, that for speed No. 1, the distance travelled was 13.10 cm.; for the last result, the distance was 4.11 cm.. The spread of the individual readings indicates that the experimental error is about $\pm \frac{1}{2}\%$.

(f) The cross-section of the reservoir.

Using the values of the rate of flow for speeds Nos. 1 $\frac{1}{2}$ and 3 given in (b), and the values of the velocity of the plunger given in (e), the area of cross-section of the reservoir can be found from the relation:- $q = \frac{1}{4}\pi d^2 U$.

Speed No. 3:- $q/U = 2.843$; hence $d = 1.903$.

Speed No. 1 $\frac{1}{2}$:- $q/U = 2.836$; hence $d = 1.900$.

Thus the mean value of $d = 1.901 \pm 0.002$; and
 the mean value of $\frac{1}{4}\pi d^2 = 2.840 \pm 0.004$.

Table VII - The plunger velocity and values of q.

Speed No.	Time in secs.		Mean Time.	U.	q(2).	q(1).
	Reverse	and Forward.				
6	157.2 156.8	156.4 156.4	156.7	0.08360	0.2374	0.2387
5½	172.8 173.2	173.0 173.0	173.0	0.07573	0.2151	0.2160
5	193.0 193.4	192.6 193.4	193.4	0.06784	0.1927	0.1946
4½	218.2 218.0	217.6 217.4	217.8	0.06016	0.1711	0.1726
4	252.6 252.4	251.4 251.2	251.9	0.05201	0.1477	0.1489
3½	294.2 292.6	292.0 292.6	292.8	0.04474	0.1271	0.1272
3	356.2 357.6	356.2 356.4	356.6	0.03675	0.1043	0.1051
2½	451.6 450.8	450.6 448.0	450.3	0.02910	0.0826	0.0826
2	628.4 630.0	626.4 628.6	628.3	0.02084	0.0606	0.0589
1½	1037.5 1035.0	1030.0 1035.0	1034.4	0.01266	0.0360	0.0358
1	915.0	916.2	915.6	0.00449	0.0127	0.0126

(g) The values of q.

From the values for the velocities of the plunger given in Table VII, and the value for the area of cross-section of the reservoir from (f), the values for the rates of flow for all speeds can be found. They are given in Table VII under q(2).

4. Comparison of the two methods.

The values of q from the first method, q(1), and the values from the second method, q(2), are both given in Table VII. Since no two corresponding values differ by more than 1%, the values of q' given in Table IV can be taken as correct.

The values for R, $\frac{1}{4}\pi d^2$, and f_R/h also agree between the two methods. Since the determination of R was more accurate in the first method, the relation between h and f_R is taken from 2.(i). It is:-

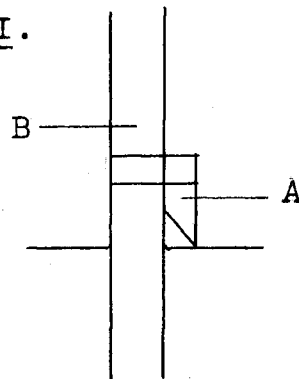
$$\underline{f_R = 48.4 h \text{ dynes per cm}^2.}$$

5. Rotary instrument: methods.

For this instrument the required relations are that between the deflection θ of the inner cylinder and the shearing stress f_a at its surface, and that between the speed S of the driving motor (r.p.m.) and the angular velocity W of the outer cylinder. The first relation depends on the torsion constant c of the suspension wire (the couple per degree of deflection), and the area of the inner cylinder in contact with the sample (corrected for end effects). The second relation depends on the pulley and gear reductions between the driving motor and the outer cylinder.

The torsion constant was determined by suspending a body of known moment of inertia on the wire, and measuring the period of torsional oscillations. The radius of the inner cylinder was measured directly: the actual immersion was determined at the end of an experiment by clipping a pointer, shown at A in Fig XVI, to the inner cylinder B, and sliding the pointer down until it

Fig XVI.



touched the surface of the sample. When the cylinder was removed, the distance between the point and the bottom of the cylinder was measured. The experimentally determined end-correction was then added to give the effective immersion for substitution in the expression for f_a .

In the case where the speed of the motor was measured by means of a tachometer, it was necessary only to calibrate the pulley wheel ratios as the gearing reduction was known. In the case where the speed was measured from the voltage across the armature of the motor, it was necessary to calibrate this voltage with reference to the mains frequency by means of the stroboscopic disc on the motor spindle.

The calibration was checked by filling the instrument with the oil used in the calibration of the tube instrument, and determining its viscosity: the result is compared with the value obtained in the Ostwald Viscometer.

6. Rotary instrument: first method.

(a) The torsion constant of the suspension wire.

The moment of inertia, I , of the inner cylinder

was calculated from its dimensions and mass. These quantities were measured to within one part in a thousand: to three significant figures,

$$I = 789 \text{ c.g.s. units.}$$

The times for five sets of 250 oscillations were:-

$$294.6, \quad 294.8, \quad 294.8, \quad 294.8, \quad 294.6 \text{ secs.}$$

The clock used was corrected by reference to a standard clock, and the corrected mean period, T , found. The result was:-

$$T = 1.177 \pm 0.001 \text{ secs.}$$

Using the relation $T = 2\pi\sqrt{(I/c')}$, where c' is the torsion constant in dyne cm. per radian, the values of c' and c were found, giving:-

$$c' = 2.25 \times 10^4 \text{ dyne cm. per radian,}$$

$$\text{and} \quad c = 392.5 \pm 0.5 \text{ dyne cm. per degree.}$$

(b) The expression for the shearing stress.

The shearing stress at the surface of the cylinder is given by:-

$$f_a = \frac{c\theta}{2\pi a^2 H} \quad \dots 8.7$$

The diameter of the inner cylinder was measured by means of a micrometer: its value was 2.543 cm. at all points. Hence, the radius,

$$a = 1.2715 \text{ cm.}$$

Thus, from equation 8.7, and the above results:-

$$\underline{f_a = 38.6 \frac{\theta}{H} \text{ dynes per cm}^2.}$$

where H is the corrected immersion, and the numerical constant is given to three significant figures.

(c) The pulley and gear ratios.

The values of the pulley ratios were found in the same manner as in the tube instrument calibration (see 3 above), and to a similar degree of accuracy: the details will not be given. The results are:-

Fast setting ratio:- 1:1.225

Slow setting ratio:- 1:23.4

These figures give the ratio between the speed of the motor spindle and the input drive of the instrument. Within the instrument the following gear reductions operate (see Fig XII):-

24:62, 24:62 (bevel gears), and 1:16 (worm gear).

The total gear reduction is therefore 1:106.8.

Using the above values, the relations between W , the angular velocity of the outer cylinder in radians per sec., and S , the speed of the motor in r.p.m., are:-

$$\text{Fast setting:- } W = 8.00 \cdot 10^{-3} S, \text{ and}$$

$$\text{Slow setting:- } W = 0.419 \cdot 10^{-3} S.$$

to three significant figures. Also, for a given S :-

$$W\text{-slow} = 0.0524 W\text{-fast}.$$

(d) The stroboscope.

This consists of a disc, mounted on the motor shaft, and illuminated by a neon lamp run from the supply mains of nominal frequency 50 c.p.s.. There are six rings of alternate black and white segments on the disc: the number of black segments, N , with their corresponding speeds are given in Table VIII below.

The voltage across the armature, V , was measured on a three-range voltmeter: the ranges were selected so that the speeds 2, 4, and 6 fell near the upper ends, and 1, 3, and 5, therefore, near the middle, of the three ranges respectively. The speed was determined from the voltage by means of proportion from the two calibration speeds in any range: the lower

ends of the ranges, and the zeros, were not used.

Table VIII - Stroboscope speeds.

<u>Ring No.</u>	<u>N.</u>	<u>S.</u>	<u>W-fast.</u>	<u>W-slow.</u>
1.	32	187.5	0.150	0.0079
2.	16	375	0.300	0.0157
3.	12	500	0.400	0.0210
4.	6	1000	0.800	0.0419
5.	4	1500	1.200	0.0629
6.	2	3000	2.400	0.126

As the voltages corresponding to the speeds given in the above table did not remain constant from one experiment to another, their values cannot be given here: they were determined for each experiment, and the speeds calculated accordingly. These changes were less than 2%. In one experiment the speed of the outer cylinder was also measured for each reading by timing a convenient number of revolutions: the difference between the two values obtained was less than 2% in each case.

In later experiments, a tachometer was used to measure the speed of the motor: this tachometer could

be read to within 1% for the motor speeds used. The readings on the tachometer agreed with the speeds given in Table VIII.

7. Rotary instrument: second method.

In order to check the above calibration, an oil of known viscosity (see 3.(a)) was used in the instrument. The deflection of the inner cylinder was measured by using a lamp, mirror, and scale. The viscosity was determined from the formula:-

$$\eta = \frac{c\theta}{4\pi WH} \left\{ \frac{1}{a^2} - \frac{1}{b^2} \right\} \quad \dots 8.8$$

where the various constants are as follows:-

Radius of inner cylinder:-	a = 1.271 cm.
Radius of outer cylinder:-	b = 4.440 cm.
Speed at Ring 5, hence	W = 1.200 rad./sec.
Distance of mirror from scale:-	L = 109.2 cm.
Torsion constant of the wire:-	c' = 2.25 10 ⁴ dyne cm./rad.

The deflection was measured for two immersions:-



<u>Immersion.</u>	<u>Deflection:</u>		<u>Mean Deflection.</u>
	<u>Left.</u>	<u>Right.</u>	
11.10 cm.	12.7 cm.	13.0 cm.	12.85 cm.
3.25	4.6	4.6	4.60 cm.

where these readings were reproducible. Hence the angular deflection per unit length of the inner cylinder is given by the difference in the mean deflections divided by the difference in the immersions and twice the mirror-scale distance, giving:-

$$\theta/H = 0.00481 \pm 0.00003$$

Substituting the above values in equation 8.8, the viscosity of the oil is given as:-

$$\eta = 4.11 \pm 0.03 \text{ poise.}$$

The viscosity of the oil as determined in the Ostwald Viscometer at the temperature of the above experiment, 25.0°C., is:-

$$\eta = 4.12 \text{ poise.}$$

Thus the correctness of the calibration is demonstrated.

C H A P T E R IX

FIRST COMPARATIVE EXPERIMENT - EXPERIMENT A.

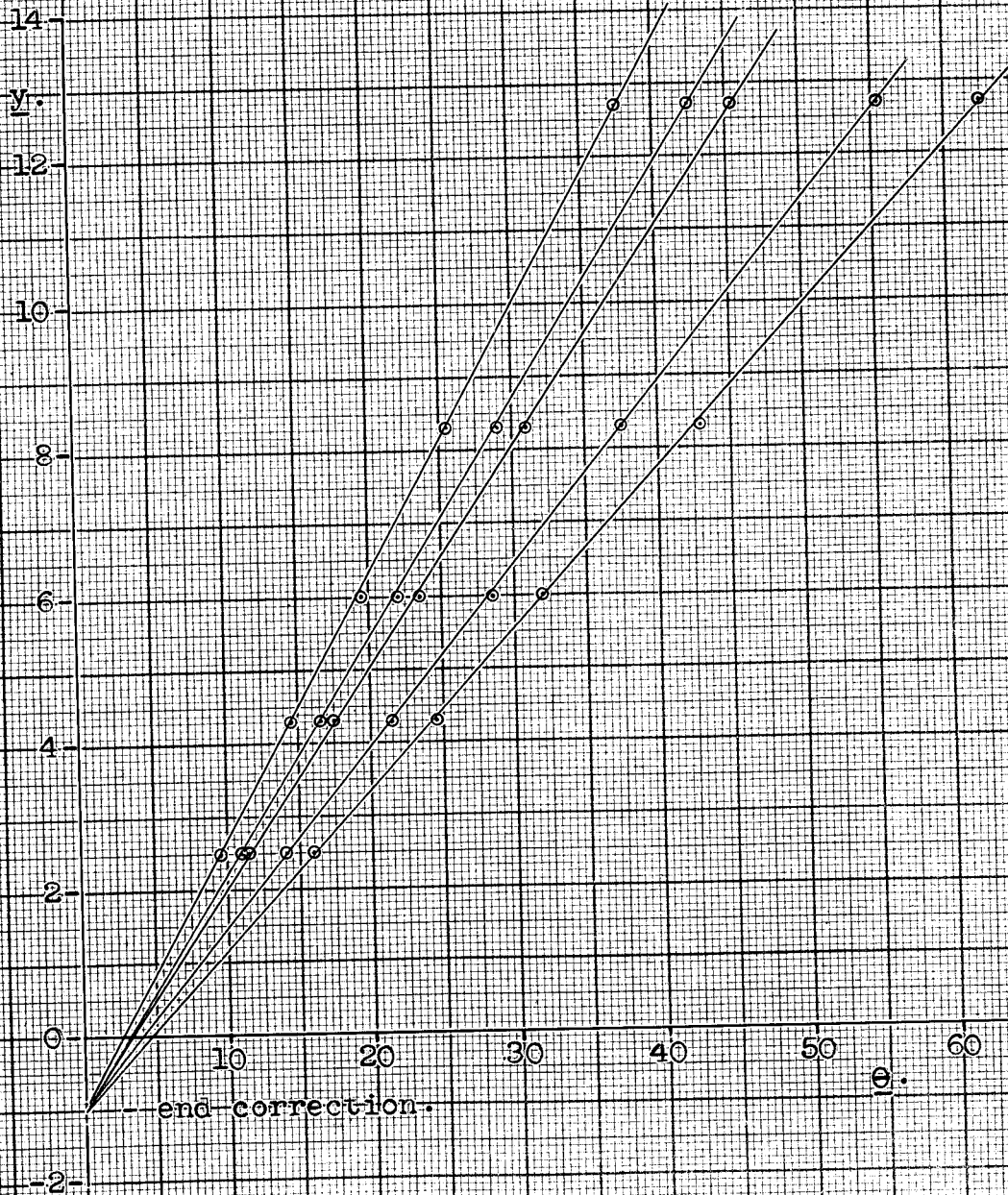
1. The end correction in the rotary instrument.

The deflections at five of the calibration speeds were measured for five depths of immersion of the inner cylinder at a temperature of 25°C. From these results it is possible to determine the end correction at five values of the angular velocity of the outer cylinder, and thus examine its variation with this velocity.

The zero on the scale was the same for all readings and was determined by taking the deflections at five speeds with the rotation in the forward and reverse directions. These results gave:-

<u>Ring.</u>	Scale:-		<u>Zero.</u>
	<u>Reverse.</u>	<u>Forward.</u>	
5.	245.5	10	307.7
4.	254	3	308.5
3.	263.5	354	308.7
2.	267	350.5	308.7
1.	272	346	309.0

Graph I - Actual immersion y v. deflection θ .



The zero is the mean of the reverse and forward scale readings: the mean zero = 308.5. This value was subtracted from all readings to give the deflection θ .

The actual immersion of the inner cylinder was measured by means of the pointer (A in Fig XVI). The following table gives the values of θ (in degrees) at the five speeds for the five values of y , the actual immersion.

	<u>Values of y in cm.</u>				
<u>Ring.</u>	<u>2.5</u>	<u>4.3</u>	<u>6.0</u>	<u>8.3</u>	<u>12.7</u>
5.	16.0	24.5	32.0	43.0	62.5
4.	14.0	21.5	28.5	37.5	55.5
3.	11.5	17.5	23.5	31.0	45.5
2.	11.0	16.5	22.0	29.0	42.5
1.	9.5	14.5	19.5	25.5	37.5

These values of θ are plotted against y on Graph I. For each speed, the intercept on the y -axis of the best straight line through the five points gives the end correction for that speed. In order of decreasing speed, these end corrections are:-

1.05, 0.98, 0.98, 1.06, 1.01 cm.

The end correction is therefore sensibly independent of speed so that it is permissible to add the mean

end correction to the actual immersion to obtain H , the effective immersion.

2. Results from the rotary instrument.

(a) Experimental results.

Two different inner cylinders, A and B, were used: cylinder A (used in the calibration) was rough, as described in Chapter III, 3.; cylinder B was smooth, but had grooves 1 mm. wide and deep, cut parallel to its generators, with a separation of 1 mm.. The two cylinders had the same radius. Two sets of readings were taken with cylinder A. It will be seen that there is little difference between the values of the shearing stress for cylinders A and B, and that the second set of readings agrees with the first set.

The results are given in Table IX. The angular velocity of the outer cylinder, W , was measured by the voltage across the armature: this is given in arbitrary units under V . R is the stroboscope ring number (see Table VIII), θ the deflection, and f_a the shearing stress at the inner cylinder. V was set to the values given in the first column (apart from the calibration speeds) and the values of θ obtained.

Graph II - Rotary instrument: Experiment A.

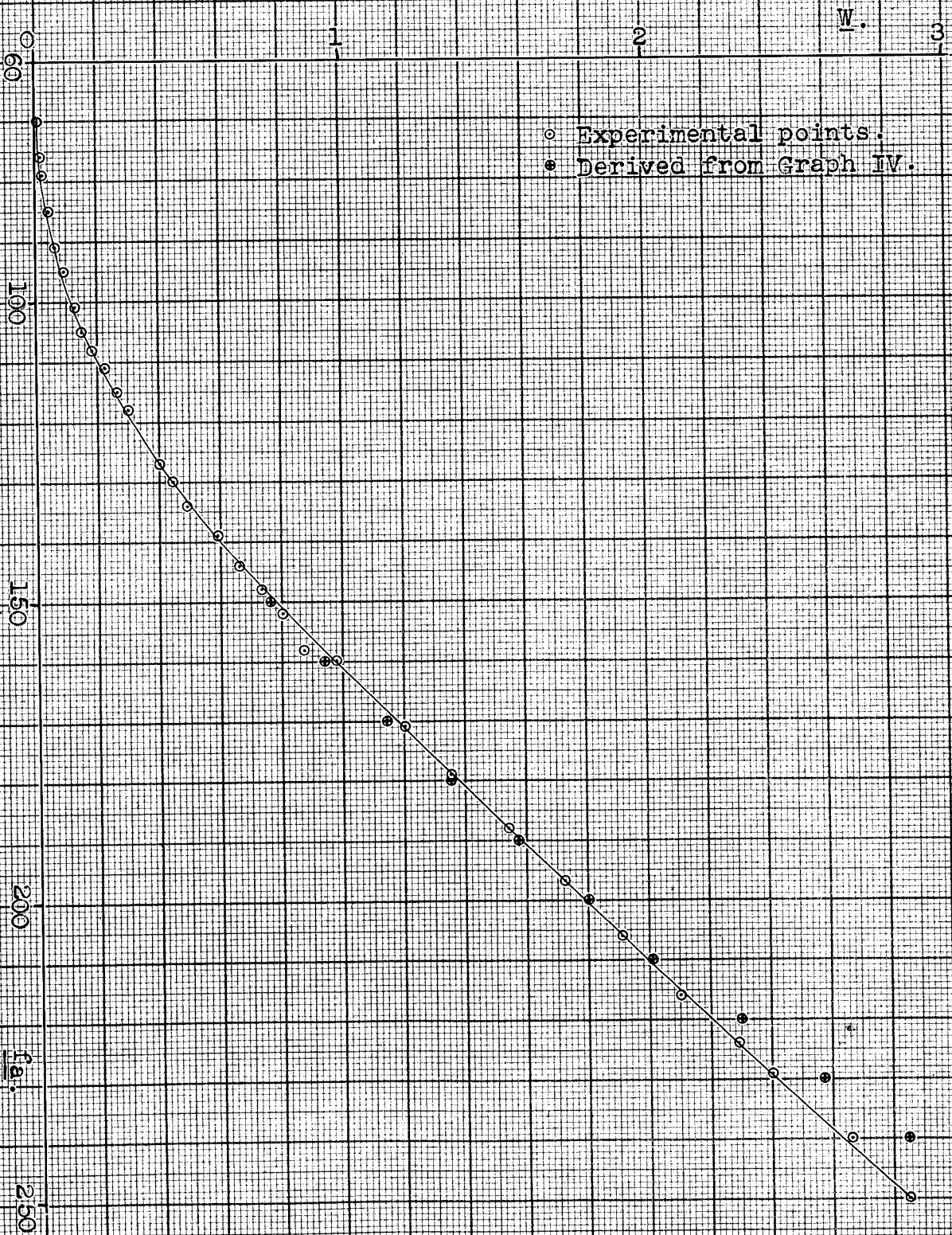
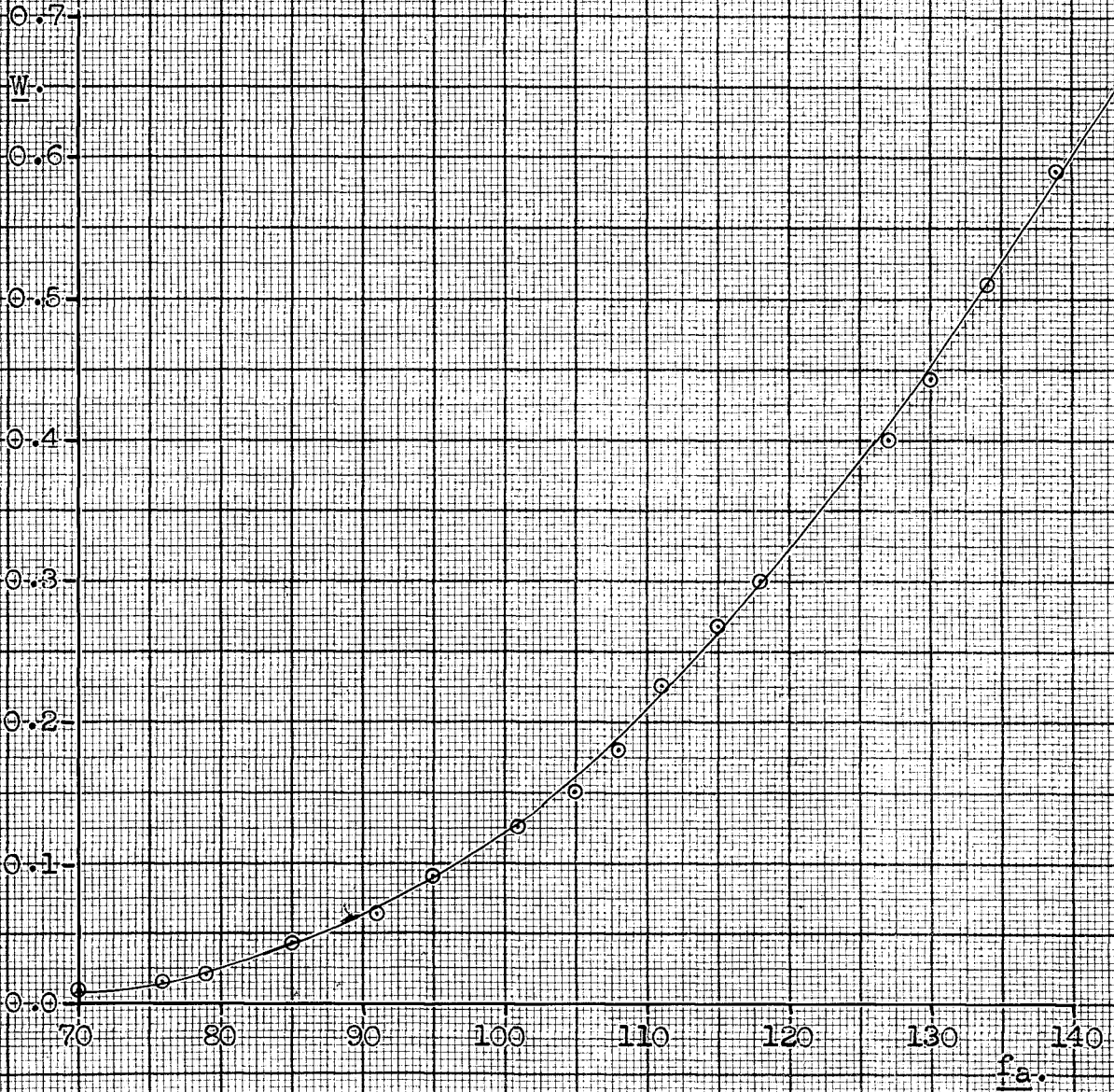


Table IX - Results from the rotary instrument.

<u>V.</u>	<u>R.</u>	<u>$\Theta(A1)$</u>	<u>$\Theta(A2)$</u>	<u>$\Theta(B)$</u>	<u>$f_a(A)$</u>	<u>$f_a(B)$</u>	<u>W.</u>
<u>Fast setting:</u>							
7.5	-	90	88.5	87	250	246	2.85
7.0	-	87	84.5	85	240	240	2.66
6.30	6	82.5	81	81	229	229	2.40
6.0	-	80.5	79.5	78.5	224	222	2.29
5.5	-	78	76	76.5	216	216	2.10
5.0	-	74.5	73	73	206	206	1.91
4.5	-	71.5	69.5	70	197	198	1.72
4.0	-	68	66	66.5	188	188	1.54
3.5	-	64.5	63.5	64	179	181	1.35
3.10	5	61.5	60.5	61	171	172	1.20
2.5	-	57.5	57	57.5	160	162	0.98
6.0	-	56.5	56	56	158	158	0.87
5.50	4	54.5	54.5	54.5	152	154	0.80
5.0	-	53	53	52.5	148	148	0.73
4.5	-	51.5	51.5	52	144	147	0.66
4.0	-	49.5	50	50	139	141	0.59
3.5	-	48	48	48	134	136	0.51
3.0	-	46	46.5	46	130	130	0.443
2.70	3	45.5	45.5	45.5	127	129	0.400
7.30	2	42	42.5	42.5	118	120	0.300
6.5	-	41	41.5	41.5	115	117	0.267
5.5	-	39.5	40	40	111	113	0.224
4.5	-	38.5	38.5	39	108	110	0.181
3.80	1	37.5	37.5	37.5	105	106	0.150
<u>Slow setting:</u>							
-	6	36	36	37	101	105	0.126
4.5	-	34	34	34	95	96	0.090
-	5	32.5	33	32	91	91	0.063
-	4	30.5	30.5	30	85	85	0.042
-	3	28.5	28	28.5	79	81	0.021
-	2	27.5	26.5	27.5	76	78	0.015
-	1	25.5	24.5	26	70	74	0.008

Graph III - Lower part of Graph II.



The following data are used:-

$$\text{Calibration equation:- } f_a = 38.6 \theta/H.$$

$$\text{Immersion, cylinder A:- } = 12.80 \text{ cm.}$$

$$\text{Immersion, cylinder B:- } = 12.65 \text{ cm.}$$

$$\text{End correction:- } = 1.00 \text{ cm.}$$

$$\text{Hence, for cylinder A:- } f_a = 2.80 \theta.$$

$$\text{for cylinder B:- } f_a = 2.83 \theta.$$

W is calculated by proportion from the calibration speeds.

$$\text{For Voltmeter Range 1:- } W = 0.375 V + 0.04$$

$$\text{Range 2:- } W = 0.143 V + 0.014$$

$$\text{Range 3:- } W = 0.0429 V - 0.013$$

The results in Table IX were taken in the order shown (i.e., decreasing values). $f_a(A)$ is calculated from the mean of $\theta(A1)$ and $\theta(A2)$. The whole $W-f_a$ curve is plotted on Graph II: the lower part is plotted on Graph III in order to obtain the flow function more accurately at these values.

(b) Determination of the flow function.

The flow function is given by:-

$$g_a = 2f_a \frac{dW}{df_a}$$

Graph IV - Values of g from both instruments: Expt A

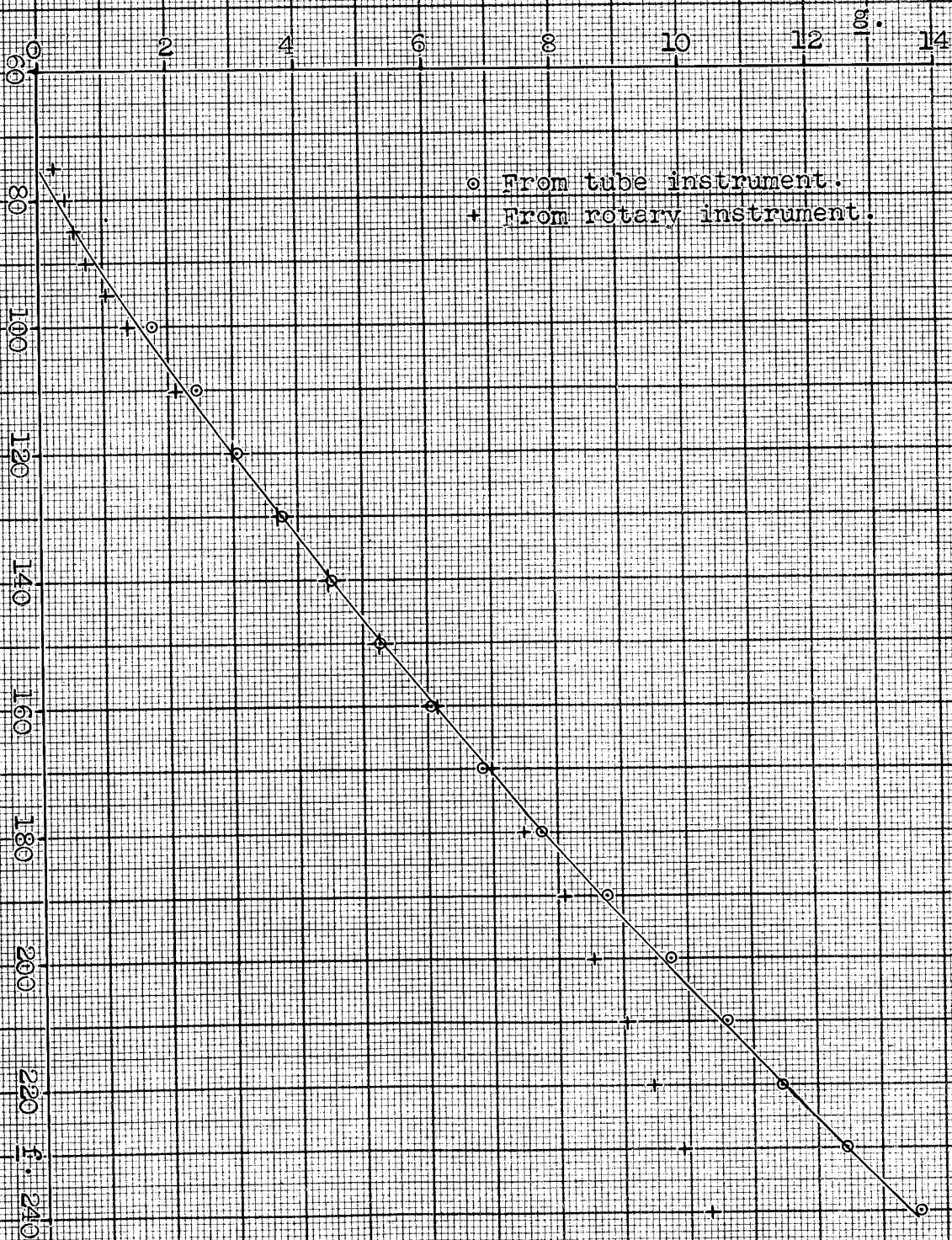


Table X - Values of g_a : Experiment A.

<u>f_a.</u>	<u>$g_a(\text{III})$</u>	<u>$g_a(\text{II})$.</u>	<u>f_a/g_a.</u>	<u>g_a/f_a.</u>
75	0.23		320	0.0031
80	0.43		188	0.0053
85	0.57		149	0.0067
90	0.74		122	0.0082
95	1.07		89	0.0112
100	1.36	1.42	72	0.0139
110	2.16	2.06	52	0.0192
120	3.04	2.96	40	0.0250
130	3.72	3.66	35	0.0286
140		4.48	31.2	0.0321
150		5.25	28.5	0.0351
160		6.15	26.0	0.0385
170		7.00	24.2	0.0413
180		7.49	24.0	0.0417
190		8.10	23.5	0.0425
200		8.52	23.5	0.0425
210		9.04	23.2	0.0430
220		9.46	23.2	0.0430
230		9.89	23.2	0.0430
240		10.31	23.2	0.0430
250		10.75	23.2	0.0430

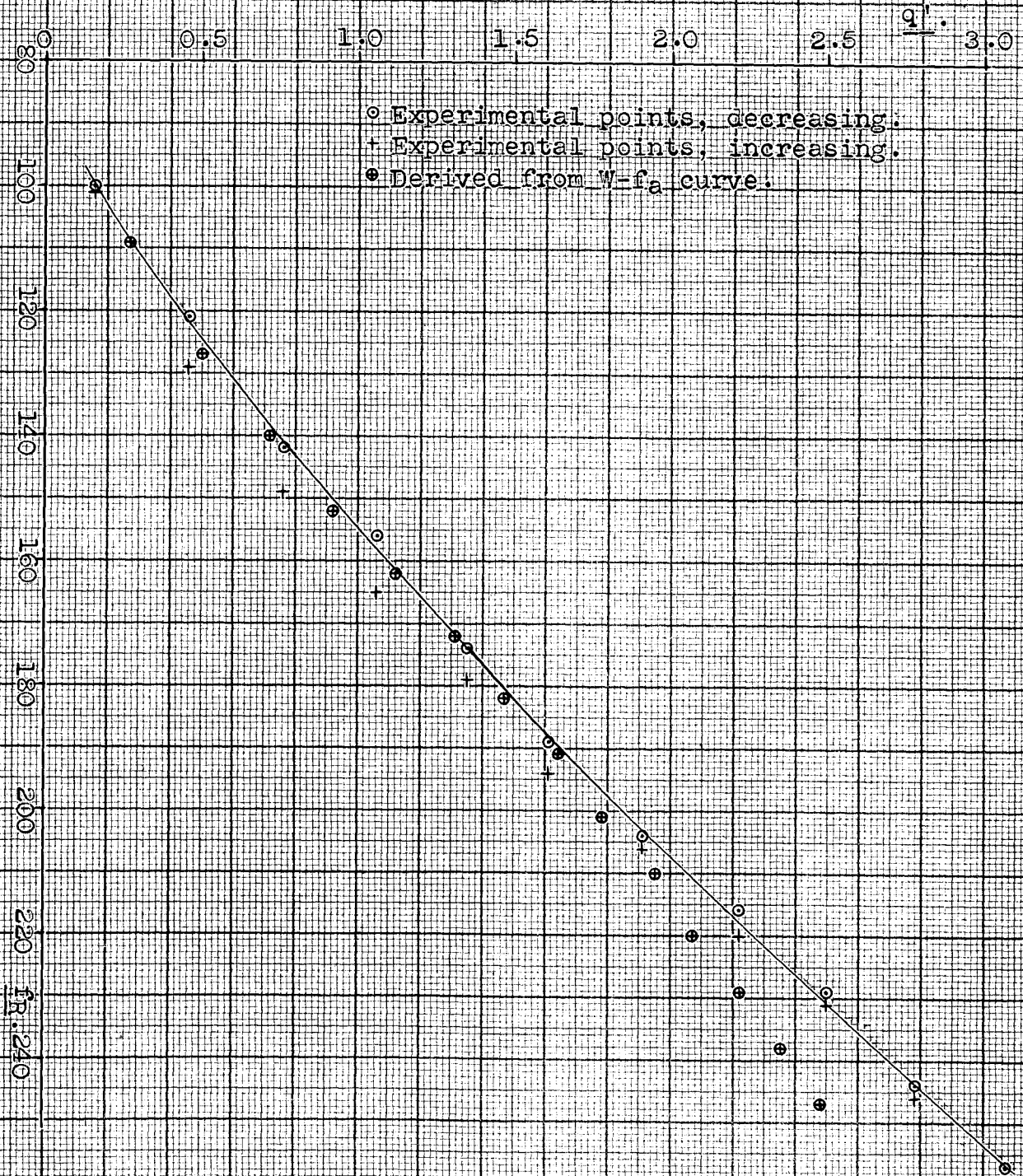
The values of g_a at a number of values of f_a are obtained from Graphs II and III. For each value of f_a a straight edge is laid against the curve, and the value of dw/df_a evaluated from its position. The results are given in Table X, together with the corresponding values of the viscosity (f_a/g_a), and the fluidity (g_a/f_a). Above $f_a = 200$ the $W-f_a$ curve cannot be distinguished from a straight line. The values of g_a are plotted on Graph IV; the viscosity and fluidity on Graph VII.

3. Results from the tube instrument.

(a) Experimental results.

Readings were taken for both increasing and decreasing values of the variables. Pulley ratio C2 was used: the values of q' are taken from Table IV. The values for h increasing, h_s , and h decreasing, h_d , are obtained by doubling the difference between the zero on the scale (17.85 cm.) and the manometer readings. The results indicate a small, but significant, difference between the increasing and decreasing values. The values of f_R are calculated from h by the calibration equation:- $f_R = 48.4 h$.

Graph V - Tube instrument: Experiment A.



The results are given in Table XI. Both sets are plotted on Graph V, but only the decreasing set is used in the determination of g_R .

Table XI - Results from the tube instrument.

S-N	Manometer readings.		h_s	h_d	q'	$f_R(s)$	$f_R(d)$
	<u>inc.</u>	<u>dec.</u>					
6	20.50		5.30		3.07	256	
$5\frac{1}{2}$	20.38	20.37	5.07	5.04	2.78	246	244
5	20.24	20.21	4.78	4.72	2.50	231	229
$4\frac{1}{2}$	20.12	20.09	4.54	4.48	2.22	220	216
4	19.98	19.96	4.26	4.22	1.91	206	204
$3\frac{1}{2}$	19.85	19.80	4.00	3.90	1.61	194	189
3	19.70	19.65	3.70	3.60	1.35	179	174
$2\frac{1}{2}$	19.55	19.46	3.40	3.22	1.06	165	156
2	19.39	19.31	3.08	2.92	0.76	149	141
$1\frac{1}{2}$	19.18	19.10	2.66	2.50	0.46	129	121
1	18.89	18.88	2.08	2.06	0.16	101	100

(b) Determination of the flow function.

The flow function is given by:-

$$g_R = 3q' + f_R \frac{dq'}{df_R}$$

The values of g_R for a set of values of f_R are

determined from Graph V. The values of the gradient are determined as above. The values of g_R are given in Table XII (together with the values of g_a for comparison), and are plotted on Graph IV. The viscosity and fluidity are also given and are plotted on Graph VII.

Table XII - Values of g_R : Experiment A.

f_R .	q' .	$3q'$.	$f_R \frac{dq'}{df_R}$	g_R .	g_a .	(f_R/g_R)	(g_R/f_R)
100	0.16	0.48	1.28	1.76	1.39	56.8	0.0176
110	0.30	0.90	1.53	2.43	2.11	45.3	0.0221
120	0.44	1.32	1.76	3.08	3.00	39.0	0.0256
130	0.59	1.77	1.97	3.74	3.69	34.8	0.0288
140	0.75	2.25	2.26	4.51	4.48	31.0	0.0323
150	0.92	2.76	2.50	5.26	5.25	28.5	0.0351
160	1.09	3.27	2.76	6.03	6.15	26.5	0.0377
170	1.26	3.78	3.06	6.84	7.00	24.9	0.0402
180	1.44	4.32	3.43	7.75	7.49	23.2	0.0430
190	1.64	4.92	3.84	8.76	8.10	21.7	0.0460
200	1.85	5.55	4.17	9.72	8.52	20.6	0.0486
210	2.06	6.18	4.42	10.60	9.04	19.8	0.0505
220	2.27	6.81	4.63	11.44	9.46	19.2	0.0520
230	2.48	7.44	5.00	12.44	9.89	18.5	0.0541
240	2.71	8.13	5.46	13.59	10.31	17.7	0.0566

4. Comparison of the results.

(a) Direct comparison.

The direct comparison of the flow functions as derived from the two instruments is given by the two sets of points on Graph IV.

It is estimated that tangents can be drawn to these curves to give the value of the gradient to within $\pm 2\%$: a similar variation may be introduced in drawing the curves through the experimental points. At the extremities of the curves the inaccuracy in the gradient of the drawn curves may be much greater, especially in the case of the tube instrument where there are fewer experimental points. It is probable, therefore, that the discrepancies between the g_R and g_a values for $f = 100, 110$ are due to this cause. If the value 4% is taken to be the maximum difference that can be called agreement, then the values in Table XII agree up to $f = 180$. Above this the difference is due to the existence of the static yield value in the rotary instrument.

(b) Indirect comparison.

The $W-f_a$ values from the rotary instrument have been transformed to $q'-f$ values by the method of

Chapter IV, 2: the values obtained are given in Table XIII and are plotted on Graph V with the experimental $q'-f_R$ values. The method of this transformation will be illustrated in a later experiment; the results only are quoted in Table XIII.

Table XIII - $q'-f$ values obtained from $W-f_a$ curve.

<u>f.</u>	<u>q'cal.</u>	<u>q'exp.</u>	<u>f.</u>	<u>q'cal.</u>	<u>q'exp.</u>
109	0.27	0.28	191	1.64	1.66
127	0.50	0.55	201	1.78	-
140	0.72	0.75	210	1.95	-
152	0.92	0.96	220	2.07	-
162	1.12	1.12	229	2.22	-
172	1.31	1.30	238	2.35	-
182	1.47	1.48	247	2.48	-

In drawing the $W-f_a$ curve, the existence of the discontinuity shown at F in Fig II is ignored, since its position cannot be found with any certainty from the plotted points. This has a greater effect on the gradient of the $W-f_a$ curve than on the value of the integral in equation 4.8, for shearing stresses in the neighbourhood of the discontinuity, and hence the

Graph VI - Values of $g_R/2f$.

0.030

$\frac{g_R}{2f}$

0.025

0.020

140

160

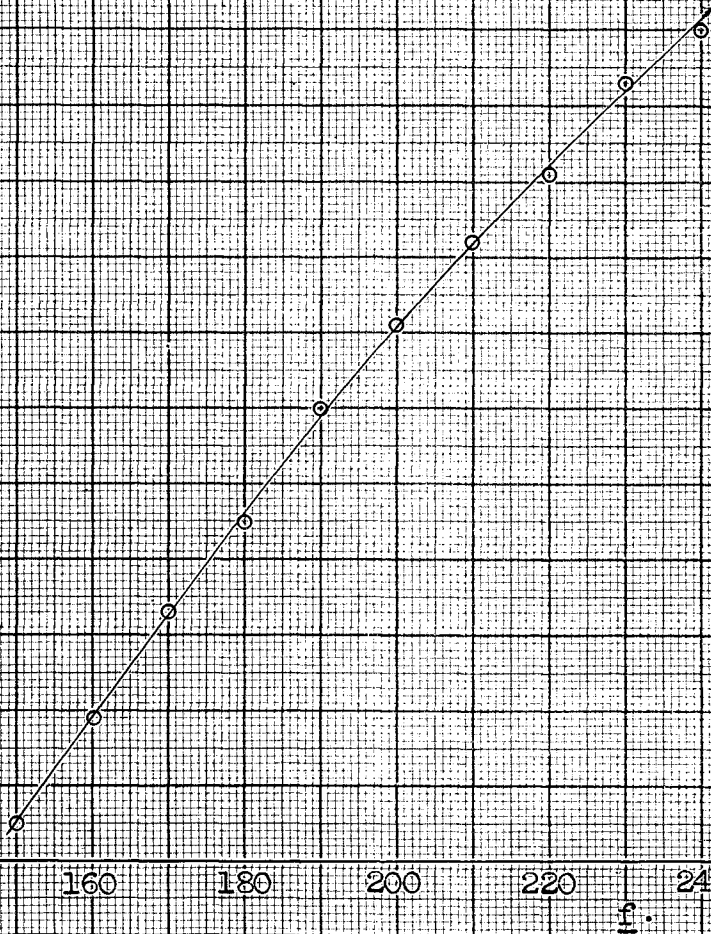
180

200

220

240

f



indirect method gives a more accurate measure of the shearing stress at the discontinuity. The fact that the values from the indirect method agree at the lower end of the curve indicates that the disagreement here in the direct method was due to incorrect curve drawing.

Since the curve for the tube instrument is correct, and the curve for the rotary instrument is correct at its lower end, the transformation of Chapter IV, 3. can be used to obtain the true $W-f_a$ curve above the discontinuity. Alternatively, equation 3.8 can be used, and the value of W calculated from the g_R-f_R curve: this method will be used. The value $f = 150$ is taken as the lower limit of integration, as the $W-f_a$ curve is correct at this point. Values of W are calculated from the expression:-

$$W = W_{f_a=150} + \int_{150}^f \frac{1}{2} \frac{gdf}{f} \quad \dots 9.1$$

Values of g are taken from the tube results on Graph IV and $\frac{1}{2}g/f$ calculated. This is plotted as a function of f on Graph VI: the integration is performed by considering the area under the curve between successive ordinates to be a trapezium. The results are given in

Graph VII - Viscosity and fluidity: Experiment A.

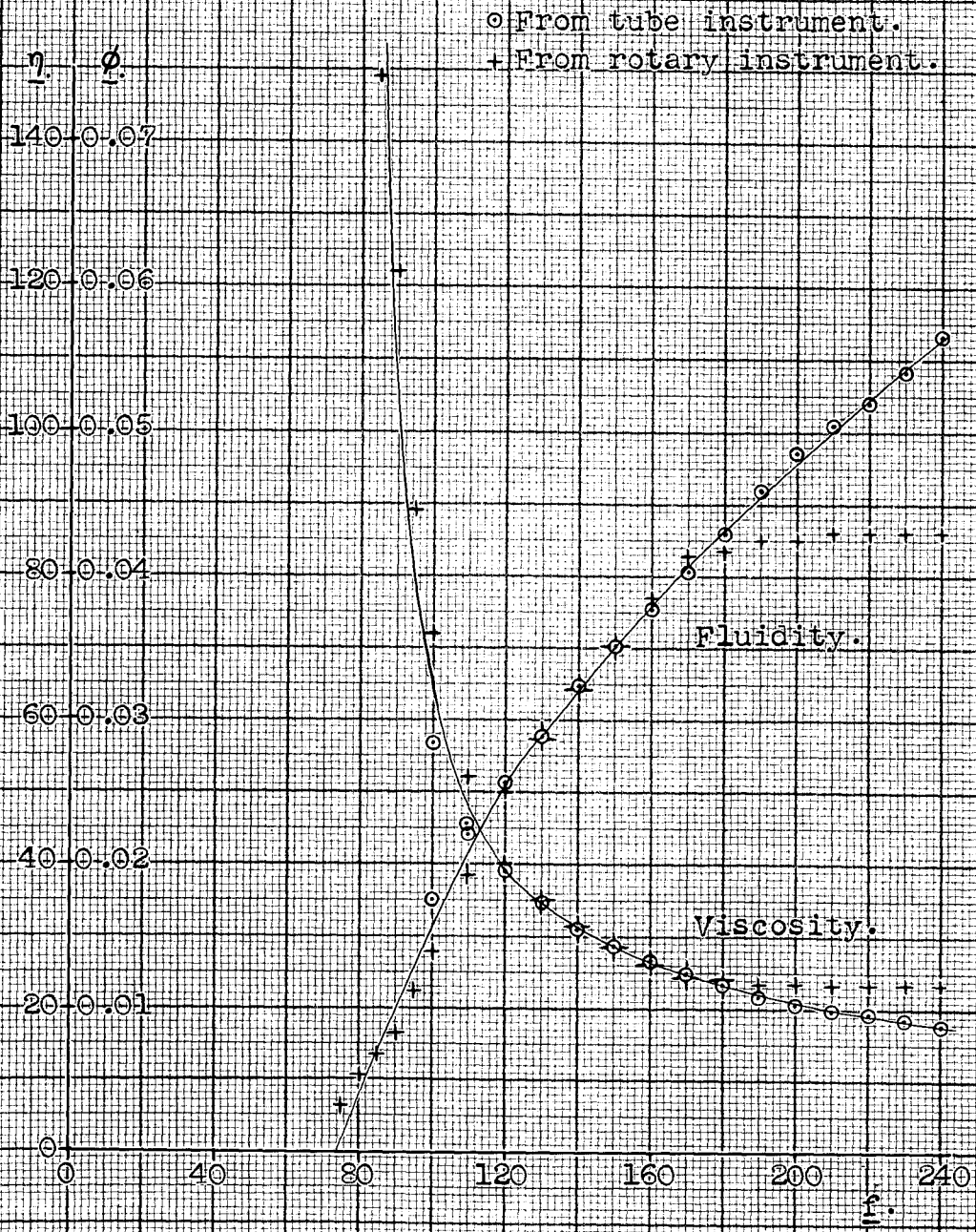


Table XIV, where $D(I)$ is the area under the curve between ordinates 10 units (dynes per cm^2 .) of f apart, and $I(W)$ is the value of the integral in equation 9.1 which is added to $W_{f_a=150} = 0.76$ (radians per sec.) to give the true value of W at the higher shearing stresses. The results are plotted on Graph II.

Table XIV - Derivation of W from g_R - f_R curve.

<u>f.</u>	<u>g.</u>	<u>$\frac{1}{2}g/f.$</u>	<u>$D(I).$</u>	<u>$I(W).$</u>	<u>$W.$</u>
150	5.25	0.0175	0.000	0.00	0.76
160	6.05	0.0189	0.182	0.18	0.94
170	6.90	0.0203	0.196	0.38	1.14
180	7.75	0.0215	0.209	0.59	1.35
190	8.75	0.0230	0.221	0.81	1.57
200	9.65	0.0241	0.234	1.04	1.80
210	10.60	0.0252	0.246	1.29	2.05
220	11.50	0.0261	0.257	1.54	2.30
230	12.55	0.0273	0.267	1.81	2.57
240	13.45	0.0280	0.277	2.09	2.85

The values of the viscosity and the fluidity obtained from the two instruments are plotted on Graph VII. The measure of agreement is again shown.

From the above results, the discontinuity in the $W-f_a$ curve (where $f_a = f_a'$) occurs at about $f_a' = 190$; from Table IX, $f_{a(\max)} = 250$; by extrapolation of the fluidity- f_a curve (Graph VII) to the f_a -axis, $f_d = 70$. Hence, since $f_{a(\max)} / f_a' = f_s / f_d$, $f_s = 90$. These values are only approximate, as the maximum value of f_a in Table IX may not correspond to $f_{a(\max)}$, but the order of the difference between f_s and f_d is indicated.

CHAPTER X

SECOND COMPARATIVE EXPERIMENT - EXPERIMENT B.

1. Experiment B.

In this experiment, the $W-f_a$ curves from the rotary instrument for both decreasing and increasing values were obtained and analysed. The sample used was the same as in Experiment A, but as Experiment B was performed six days later a small change in the properties of the sample could be expected. The methods for calculating the results are the same as in the previous experiment.

2. Results from the rotary instrument.

(a) Experimental results.

The following data are used:-

Calibration equation:- $f_a = 38.6 \Theta/H.$

Immersion:- $= 12.4 \text{ cm.}$

End correction:- $= 1.0 \text{ cm.}$

Hence:- $f_a = 2.88 \Theta.$

Graph VIII - Rotary instrument: Experiment B.

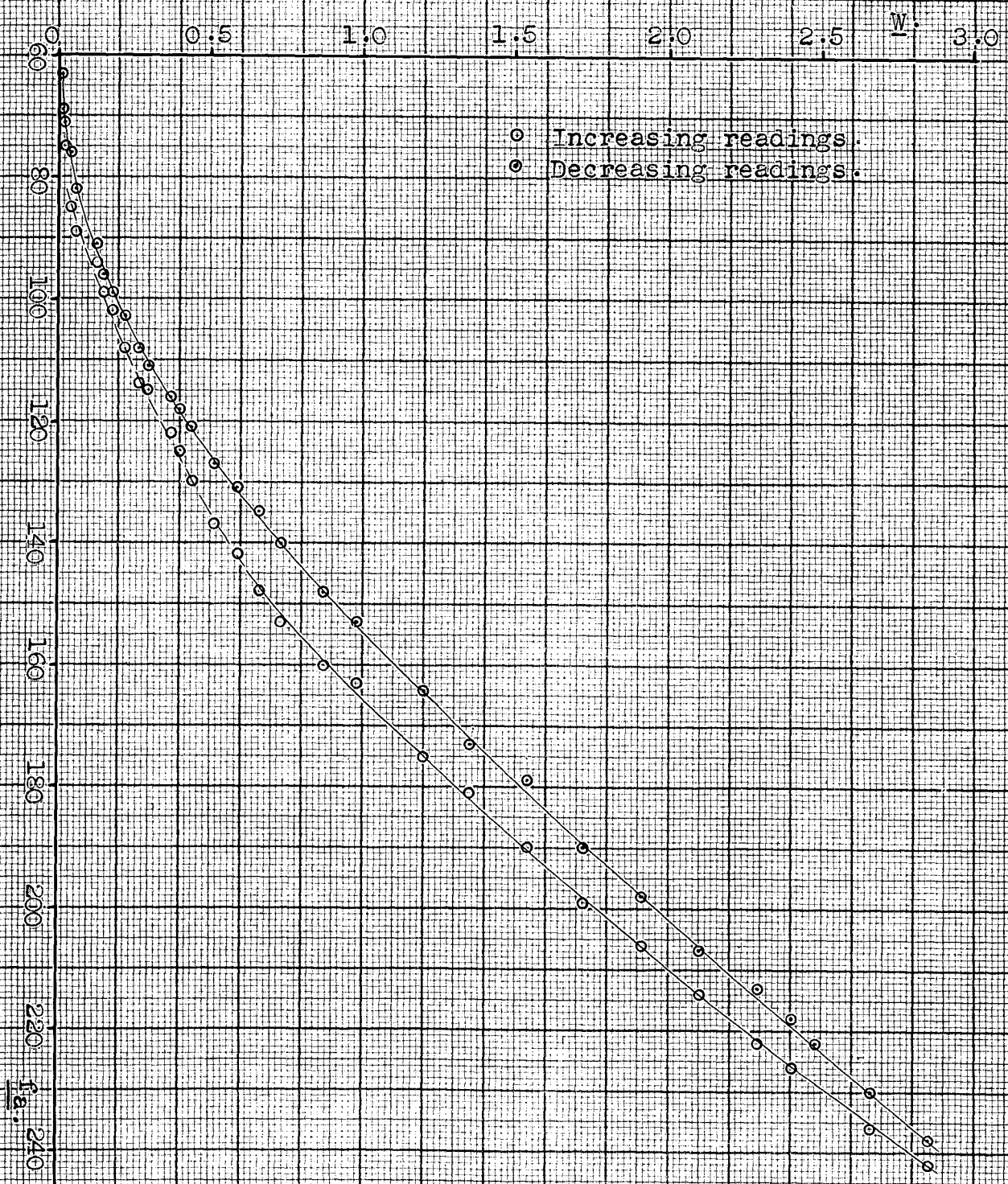
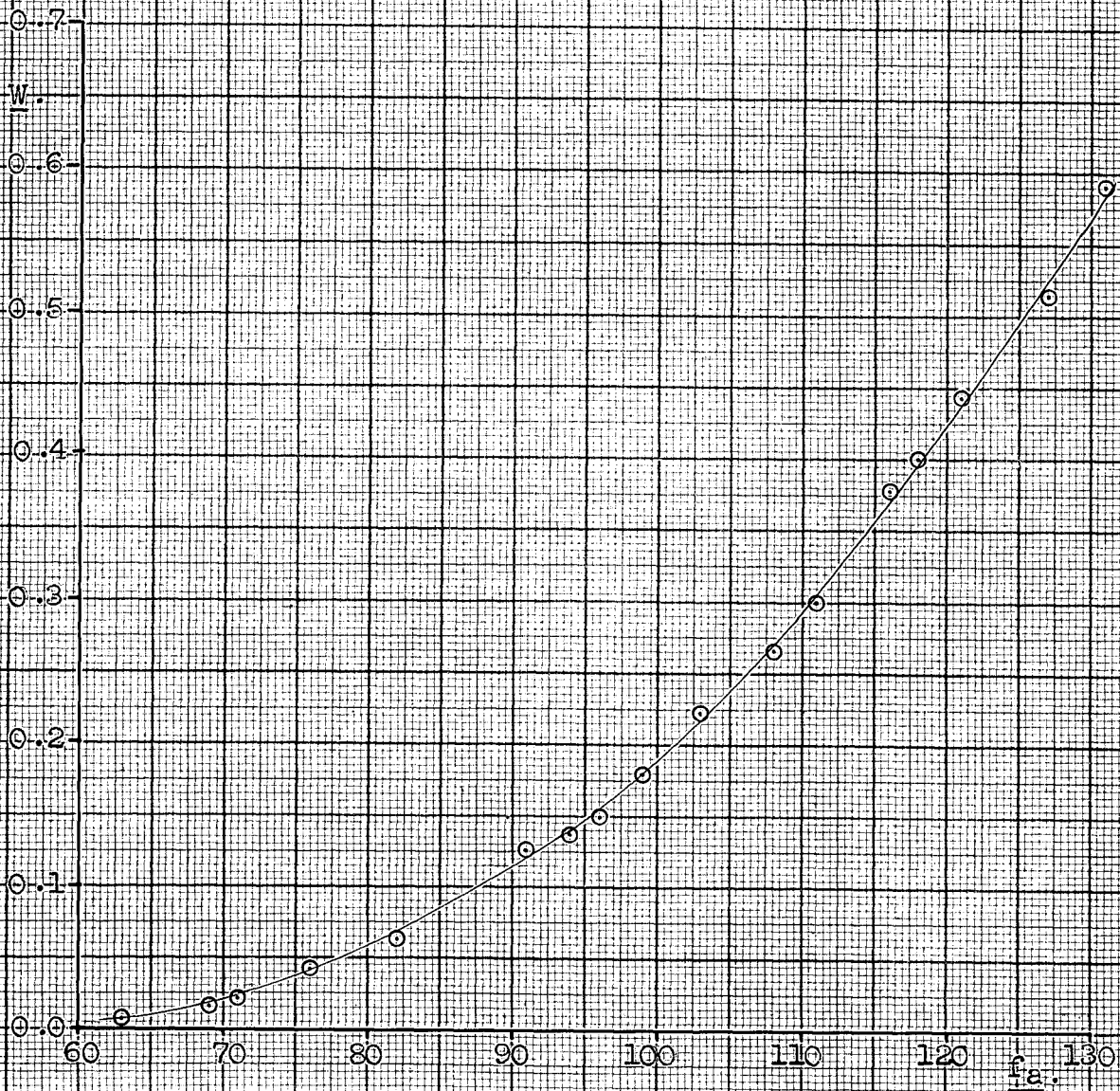


Table XV - Results from the rotary instrument.

<u>V.</u>	<u>B.</u>	<u>$\theta(d)-1$</u>	<u>$\theta(s)$</u>	<u>$\theta(d)-2$</u>	<u>$f_a(s)$</u>	<u>$f_a(d)$</u>	<u>W.</u>
<u>Fast setting:</u>							
7.5	-	82	84	83	242	238	2.85
7.0	-	79	82	80.5	236	230	2.66
6.5	-	76.5	-	78	-	222	2.48
6.30	6	75.5	78.5	76	226	218	2.40
6.0	-	73.5	77	74.5	222	213	2.29
5.5	-	71.5	74.5	72	214	207	2.10
5.0	-	68.5	71.5	69	206	198	1.91
4.5	-	65.5	69	66.5	199	190	1.72
4.0	-	62.5	66	62	190	179	1.54
3.5	-	60	63	60	181	173	1.35
3.10	5	57	61	57	175	164	1.20
6.7	-	53	56.5	53.5	163	153	0.98
6.0	-	51.5	55.5	51.5	160	148	0.87
5.50	4	50	54.5	50	157	144	0.80
5.0	-	48.5	53	48.5	153	140	0.73
4.5	-	47	51.5	47	148	135	0.66
4.0	-	45.5	49.5	45.5	142	131	0.59
3.5	-	44	47.5	44	137	127	0.514
3.0	-	42	45	42	130	121	0.443
2.70	3	41	43.5	41	125	118	0.400
2.5	-	40.5	42.5	40	122	116	0.372
7.5	-	38.5	-	38.5	-	111	0.308
7.35	2	38.5	40	38.5	115	111	0.300
6.5	-	37.5	39.5	37.5	114	108	0.265
5.5	-	36	37.5	35.5	108	103	0.222
4.5	-	34.5	35.5	34.5	102	99	0.179
3.85	1	33.5	34.5	33.5	99	96	0.150
3.5	-	33	31.5	32.5	91	94	0.136
<u>Slow setting:</u>							
7.5	-	32	33.5	32	96	92	0.149
-	6	31.5	32.5	31.5	94	91	0.126
-	5	28.5	31	28.5	89	82	0.063
-	4	26.5	29.5	26.5	85	76	0.042
-	3	24.5	26	24.5	75	71	0.021
-	2	24	25.5	24	73	69	0.016
-	1	22	22.5	22	65	63	0.008

Graph IX - Lower part of Graph VIII.



For Voltmeter Range 1:- $W = 0.375 V + 0.04$
 Range 2:- $W = 0.143 V + 0.014$
 Range 3:- $W = 0.0429 V - 0.015$

The results are given in Table XV. Starting at the maximum speed, a set of decreasing results was taken, $\theta_{(d)}-1$; then a set of increasing results was taken, $\theta_{(s)}$; and finally a further set of decreasing results, $\theta_{(d)}-2$. The value of the zero on the scale was determined as in Experiment A, and subtracted from the observed readings to give the values of θ in the Table. $f_a(d)$ is calculated from the mean of the decreasing sets.

All the above results are plotted on Graph VIII, and the lower decreasing values on Graph IX. The increasing results cannot be as dependable as the decreasing results, as any vibration will tend to shift an increasing value towards the decreasing curve.

(b) Determination of the flow function.

The values of g_a are found as in the previous experiment, and are given in Table XVI, together with the viscosity and fluidity. The values of g_a are plotted on Graph X; the viscosity and fluidity on Graph XII.

Graph X - Values of g from both instruments: Expt B.

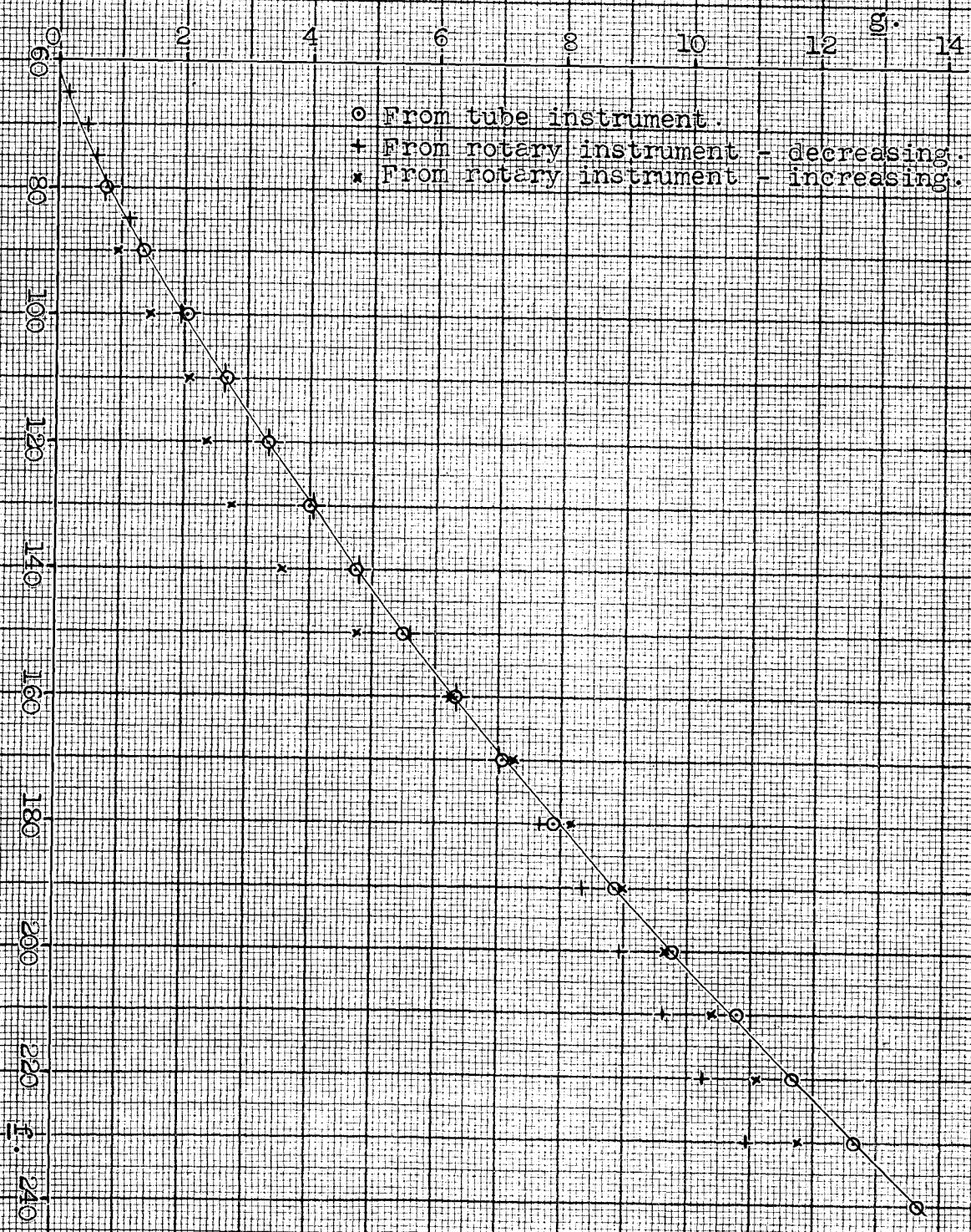


Table XVI - Values of g_a : Experiment B.

<u>f_a</u>	<u>$g_a(d)(IX)$</u>	<u>$g_a(d)(VIII)$</u>	<u>$g_a(s)(VIII)$</u>	<u>f_a/g_a</u>	<u>g_a/f_a</u>	
65	0.13			500	0.0020	1
70	0.46			152	0.0066	1
75	0.60			125	0.0080	1
80	0.74			108	0.0092	1
85	1.13			75	0.0133	1
90	1.30	1.26	0.92	69	0.0144	1
100	1.92	1.88	1.48	52	0.0192	1
110	2.62	2.66	2.07	42.0	0.0238	1
120	3.34	3.28	2.37	35.9	0.0278	1
130		4.05	2.78	32.1	0.0312	2
140		4.79	3.58	29.2	0.0342	2
150		5.61	4.77	26.8	0.0374	2
160		6.33	6.24	25.3	0.0396	2
170		7.01	7.25	23.5	0.0426	3
180		7.66	8.17	22.0	0.0454	3
190		8.32	8.97	21.2	0.0471	3
200		8.92	9.64	20.8	0.0482	3
210		9.62	10.38	20.2	0.0494	3
220		10.25	11.10	19.8	0.0504	3
230		10.95	11.75	19.6	0.0511	3

The numbers in the last column denote the columns from

which the value of g_a is taken in order to calculate the viscosity and fluidity, and from which values of g_a are taken for comparison with the results from the tube instrument. Columns 1 and 2 are the values of g_a obtained from Graphs IX and VIII respectively for the decreasing curve, and column 3 the values obtained from Graph VIII for the increasing curve.

3. Results from the tube instrument.

(a) Experimental results.

The results for decreasing values are given in Table XVII in the order in which they were taken. By using the pulley ratio C3 in addition to C2, the number of readings at the lower end of the range is increased, enabling g_R to be calculated more accurately at these values. The calculation of f_R from the manometer readings is as in Experiment A.

(b) Determination of the flow function.

The values of g_R are determined from the $q'-f_R$ curve as in the previous experiment. They are given, together with the values of g_a for this experiment, in Table XVIII and are plotted on Graph X.

Graph XI - Tube instrument: Experiment B.

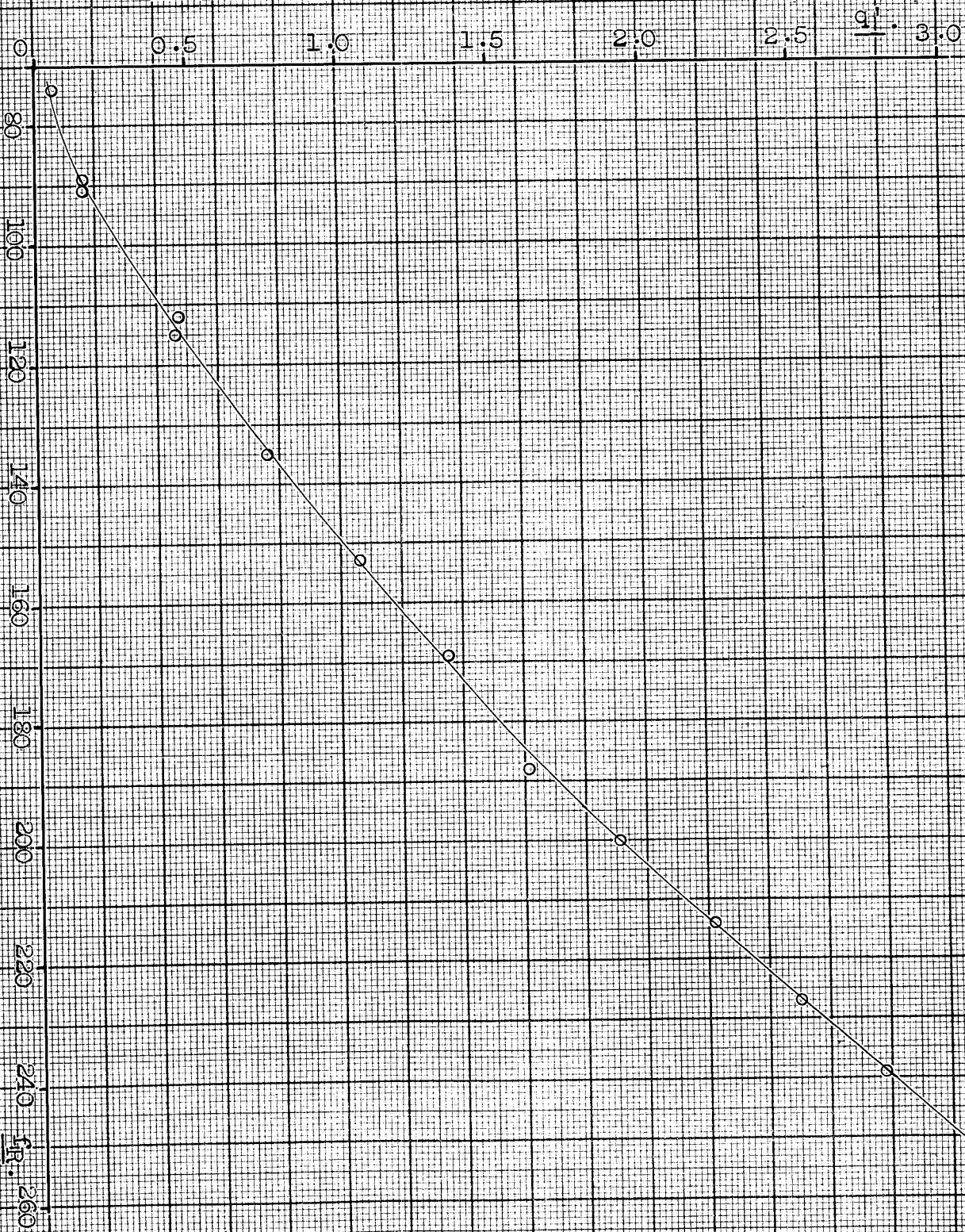


Table XVII - Results from the tube instrument.

<u>Speed No.</u>	<u>Pulley</u>	<u>Manometer reading</u>	<u>h.</u>	<u>q'.</u>	<u>f_R.</u>
6	C2	20.48	5.26	3.07	254
5½	C2	20.32	4.94	2.78	239
5	C2	20.20	4.70	2.50	227
4½	C2	20.06	4.42	2.22	214
4	C2	19.92	4.14	1.91	200
3½	C2	19.79	3.88	1.61	188
3	C2	19.60	3.50	1.35	169
2½	C2	19.43	3.16	1.06	153
2	C2	19.25	2.80	0.76	135
1½	C2	19.04	2.38	0.46	115
1	C2	18.79	1.88	0.16	91
3	C3	19.01	2.32	0.47	112
1½	C3	18.77	1.84	0.16	89
1	C3	18.61	1.52	0.06	74

The values of q' and f_R in the above Table are plotted on Graph XI. As in other results from the tube instrument, h is the height of the mercury manometer in cm.; q' is given in units of sec^{-1} , and f_R in dynes per cm^2 .

Graph XIII - Viscosity and fluidity: Experiment B.

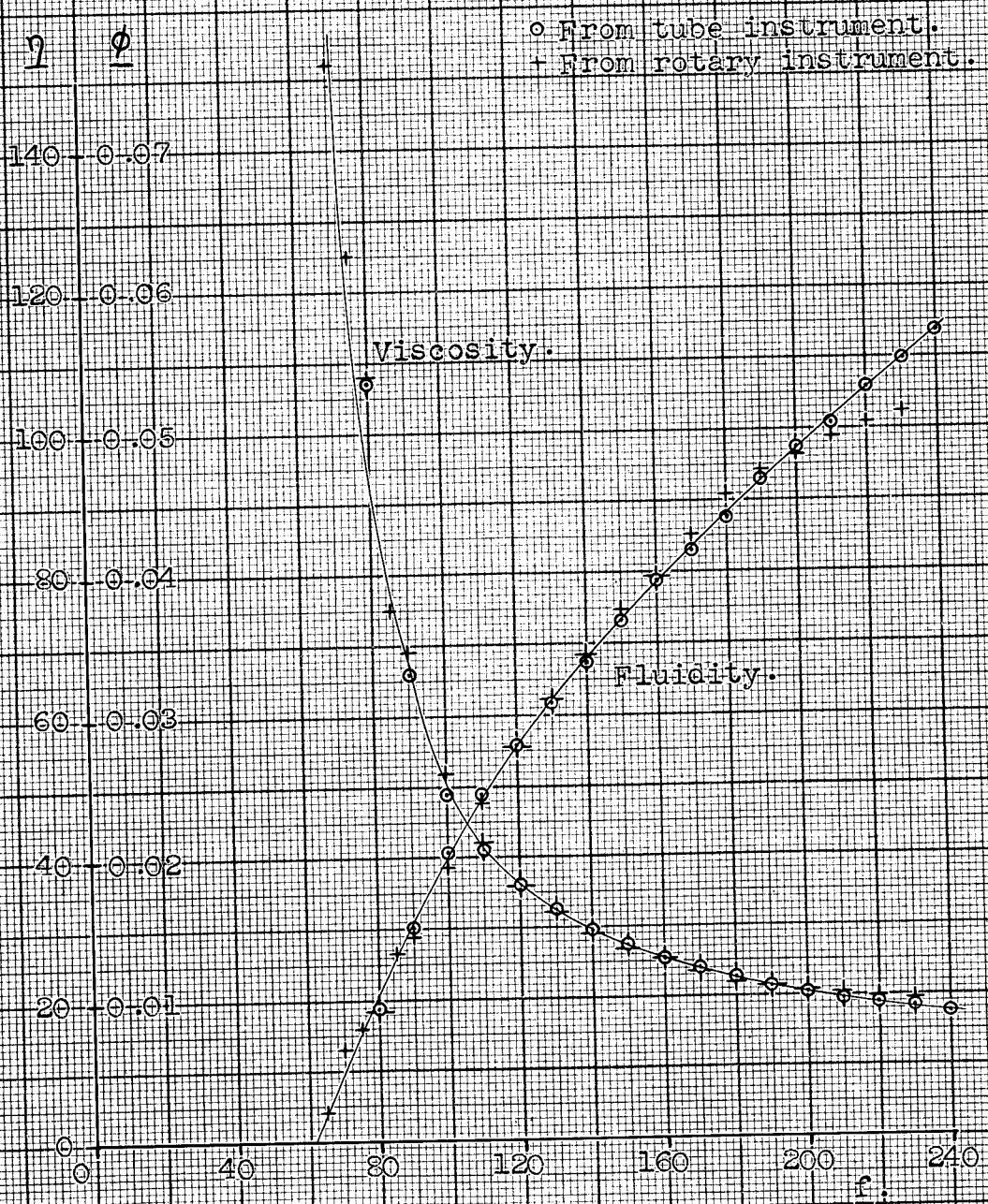


Table XVIII - Values of g_R : Experiment B.

f_R .	$3q'$	$f_R \frac{dq'}{df_R}$	g_R .	g_a .	$g_R - g_a$	f_R/g_R	g_R/f_R
80	0.24	0.51	0.75	0.74	1.4%	107	0.0094
90	0.51	0.85	1.36	1.30	4.5%	66	0.0151
100	0.84	1.19	2.03	1.92	5.6%	49	0.0203
110	1.20	1.48	2.68	2.62	2.3%	41.1	0.0244
120	1.62	1.70	3.32	3.34	-0.6%	36.1	0.0277
130	2.07	1.93	4.00	4.05	-1.2%	32.5	0.0308
140	2.52	2.20	4.72	4.79	-1.5%	29.6	0.0337
150	3.00	2.49	5.49	5.61	-2.2%	27.3	0.0366
160	3.51	2.80	6.31	6.33	-0.3%	25.4	0.0394
170	4.02	3.04	7.06	7.25	-2.7%	24.1	0.0415
180	4.56	3.33	7.89	8.17	-3.4%	22.8	0.0438
190	5.13	3.70	8.83	8.97	-1.6%	21.3	0.0465
200	5.73	4.02	9.75	9.64	1.1%	20.5	0.0487
210	6.36	4.43	10.79	10.38	3.9%	19.5	0.0504
220	6.99	4.66	11.65	11.10	4.8%	18.9	0.0529
230	7.68	4.95	12.63	11.75	7.2%	18.2	0.0549
240	8.31	5.31	13.62			17.6	0.0568

The values of g_R in the above Table are plotted on Graph X: the units are sec^{-1} , as in all other cases.

4. Comparison of the results.

(a) Direct comparison.

The results for the rotary instrument plotted on Graph X show that g_a can be evaluated from the decreasing curve below $f_a = 180$ (dynes per cm^2 .), and from the increasing curve above $f_a = 170$. The direct comparison is effected by comparing these values of g_a either with the values of g_R plotted on the same graph or with the values of g_R given in Table XVIII. The difference between g_R and g_a is given as a percentage in this table: these percentages show that the individual values of g_a and g_R have been determined to within $\pm 2\%$, except at the extremes of the range of shearing stresses, where a greater difference is to be expected.

(b) Indirect comparison.

By the method of Chapter IV, 3., the $q'-f_R$ values can be transformed to $W-f$ values, which can be compared with the experimental (decreasing) $W-f_a$ values up to a shearing stress of $f_a = 180$. Above this shearing stress, the transformation enables the decreasing curve to be extended to higher shearing stresses so that it can be compared with the increasing

curve. The difference between these curves will be examined in the next section.

The derivation of the W-f values is given in Table XIX. For a series of values of f_R , q' is

Table XIX - W-f values obtained from q' - f_R curve.

f_R .	q'	$3q'/f_R$.	$D(I)$.	I .	W .	$W(d)$.	$W(s)$
60	0	0	0	0	0	0	-
70	0.03	0.0013	0.0065	0.0065	0.02	0.02	-
80	0.08	0.0030	0.0215	0.028	0.05	0.05	-
100	0.28	0.0084	0.114	0.142	0.21	0.19	-
120	0.54	0.0135	0.219	0.361	0.45	0.43	-
140	0.84	0.0180	0.315	0.676	0.76	0.74	0.55
160	1.17	0.0219	0.399	1.075	1.12	1.12	0.88
180	1.52	0.0253	0.472	1.547	1.53	1.53	1.30
200	1.91	0.0286	0.539	2.086	2.00	1.96	1.76
220	2.34	0.0319	0.605	2.691	2.51	2.41	2.25
240	2.78	0.0348	0.667	3.358	3.07	2.89	2.80

obtained from Graph XI, and $3q'/f_R$ calculated. It is assumed that the dynamic yield value is 60 dynes per cm^2 . The differences between successive values of $3q'/f_R$ show that the curve relating $3q'/f_R$ and f_R has little curvature so that the integration in equation

4.11 can be performed (as in a previous example) by considering the area under the curve between successive values of f_R to be a trapezium. $D(I)$ gives these areas calculated in this way; I is the sum of the values of $D(I)$ up to the appropriate shearing stress; W is then given by $\frac{1}{2}(I + q')$. The values of $W(d)$ and $W(s)$ from Graphs VIII and IX are given for comparison: $W(d)$ and W agree to within 2% up to $f = 200$.

5. Discussion of the results.

It was shown in Chapter III, 4, that $W(d) - W(s)$ is a constant, W' , for a given shearing stress. The values of W' from the experimental curves for a number of shearing stresses are:-

<u>f_a</u> :-	<u>140</u>	<u>160</u>	<u>180</u>	<u>200</u>	<u>220</u>	<u>240</u>
<u>$W(d)$</u>	0.74	1.12	1.53	1.96	2.41	2.89
<u>$W(s)$</u>	0.55	0.88	1.30	1.76	2.25	2.80
<u>W'</u>	0.19	0.24	0.23	0.20	0.16	0.09

Since, from previous results, the correct parts of the increasing and decreasing curves overlap between shearing stresses 160 and 180 dynes per cm^2 ., the above table gives $W' = 0.24$ radians per sec..

The difference between the derived values of W and $W(s)$ are:-

f_a :-	<u>140</u>	<u>160</u>	<u>180</u>	<u>200</u>	<u>220</u>	<u>240</u>
W	0.76	1.12	1.53	2.00	2.51	3.07
$W(s)$	0.55	0.88	1.30	1.76	2.25	2.80
W'	0.21	0.24	0.23	0.24	0.26	0.27

This set of results shows that W' is reasonably constant from $f_a = 160$ to $f_a = 240$ with an average value of 0.25 radians per sec..

The static yield value can be obtained from these results since when $W(d) = W'$, then $f_a = f_s$. Hence from Graph IX, $f_s = 105$ dynes per cm^2 . The dynamic yield value can be obtained by extrapolation of the fluidity curve on Graph XII to the f -axis. The value obtained is $f_d = 62 \pm 2$ dynes per cm^2 .

From Chapter III, 4., equation 3.19 gives:-

$$W' = \frac{1}{2} \int_{62}^{105} \phi \, df.$$

By counting squares under the fluidity curve between these limits, the value of W' obtained is 0.25 ± 0.01 radians per sec., which agrees with the value of W' given by the difference between the derived values of W and the experimental $W(s)$ values.

Thus the characteristics of the sample can be described by the g-f curve obtained from the points plotted on Graph X and the values of f_d and f_s to an accuracy of $\pm 2\%$. At the greatest shearing stresses, where the differences between the results from the tube and rotary instruments differ by more than 4%, the tube results are the more accurate, since g_R depends only partly (see Table XVIII) on the value of a tangent to a curve, whereas g_a depends wholly on the value of a tangent.

6. Effect of change of temperature: Experiment C.

At the conclusion of Experiment B the sample in the rotary instrument was allowed to fall to room temperature (21.6°C.) and readings again taken with this instrument. The results will not be given here, but it was found, however, that the value of g for a given shearing stress was closely proportional to the viscosity of the liquid medium for changes in temperature, and that the yield value was little influenced by such changes. Hence, any inaccuracies in g due to temperature variations are the same as those in the viscosity of the medium. This was found

to be about 7% per degree change in temperature at 25°C.: thus, since the temperature was controlled to within $\pm 0.1^\circ\text{C}$., the inaccuracy in the flow function due to temperature effects is less than 1%, the inaccuracy of the calibration and the individual readings.

The effect of temperature on the flow properties of the type of sample used here will be discussed in more detail in a later chapter.

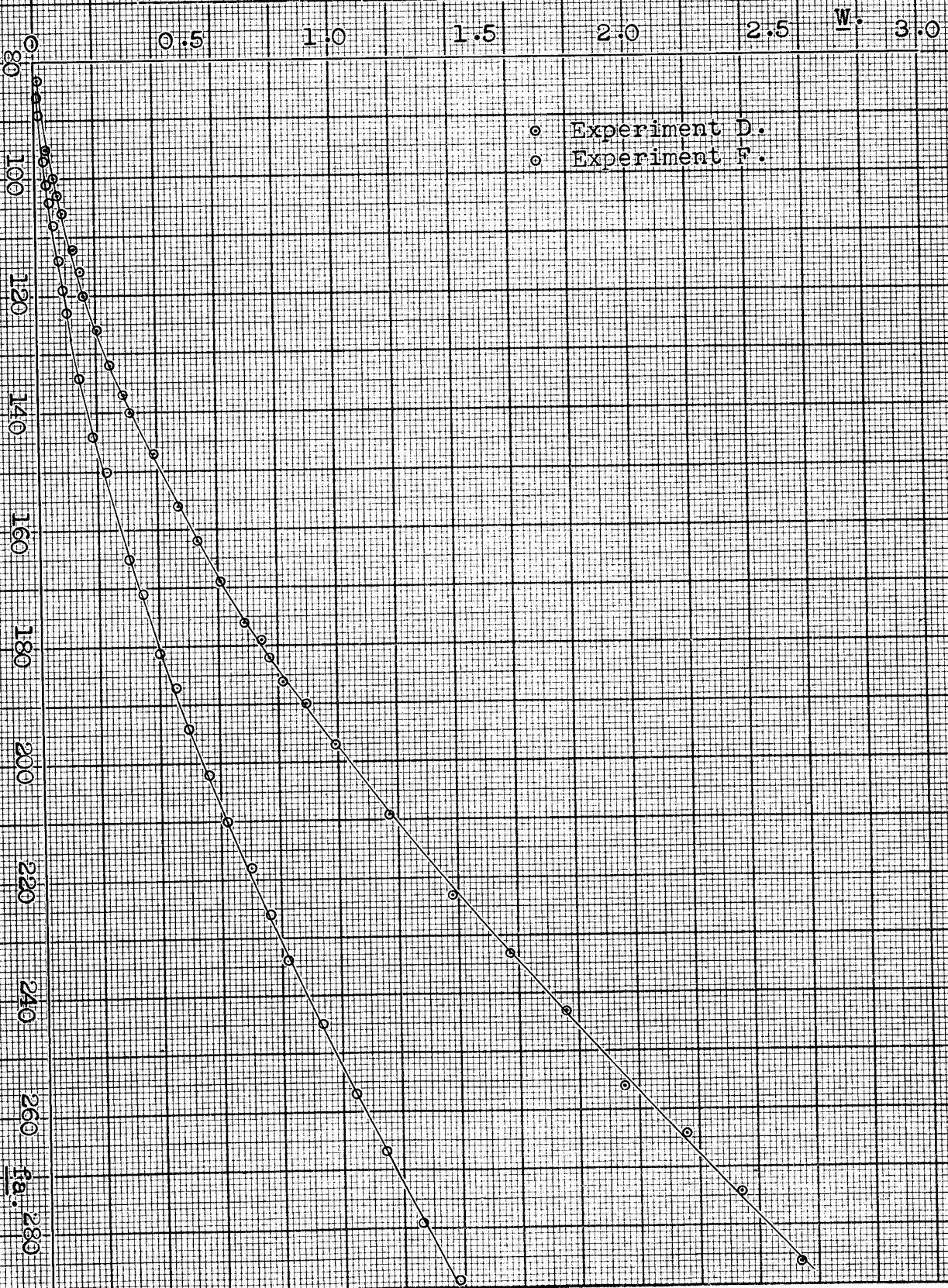
C H A P T E R X I

THIRD COMPARATIVE EXPERIMENT - EXPERIMENT D.

1. Experiment D.

The method of this experiment follows the same pattern as previous experiments. The temperature was again 25°C. It was found that the effects of the static yield value in the rotary instrument could be eliminated by switching on the driving motor to full speed: the resultant large overshoot of the initial reading was sufficient to give the condition that the shearing stress at the boundary between the fluid and solid states of the sample was the dynamic yield value. In this way a direct comparison could be effected between complete decreasing curves from both instruments. The sample used in this experiment was different from that used in the previous experiments: its flow properties were however similar, so that it was justifiable to use the end correction found in Experiment A in this experiment also. (From the immersions and deflections given in Chapter VIII, 7., the end correction is 1.1 cm. for a Newtonian fluid

Graph XIII - Rotary instrument: Experiment D.



compared with 1.0 cm. for the fluid of Experiment A.)

Direct and indirect comparisons are effected.

The values of q' , W , and g are again given in units of sec^{-1} , and f in dynes per cm^2 .

2. Results from the rotary instrument.

(a) Experimental results.

The following data are used:-

Immersion:- = 12.5 cm.

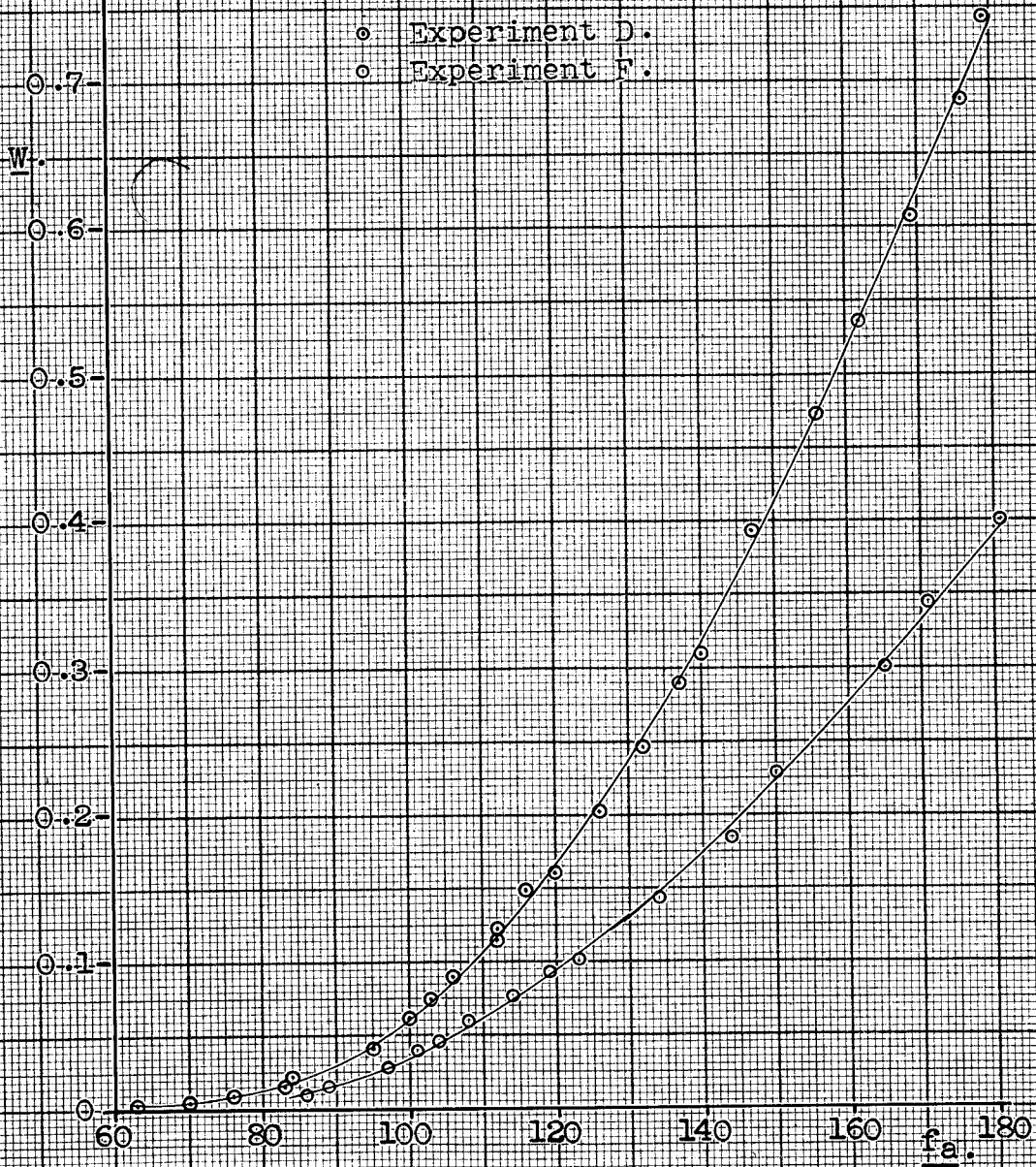
End correction:- = 1.0 cm.

Hence:- $f_a = 2.86 \theta$.

Table XX - Results from the rotary instrument.

<u>W.</u>	<u>f_a.</u>	<u>W.</u>	<u>f_a.</u>	<u>W.</u>	<u>f_a.</u>	<u>W.</u>	<u>f_a</u>
2.54	286	0.992	197	0.392	147	0.122	112
2.34	274	0.896	190	0.310	140	0.090	106
2.16	264	0.816	186	0.289	137	0.061	100
1.95	256	0.768	182	0.246	132	0.040	95
1.76	243	0.743	179	0.202	126	0.021	84
1.57	233	0.687	176	0.160	120	0.015	83
1.38	223	0.607	169	0.149	116	0.008	76
1.17	209	0.535	162	0.114	112	0.004	70
		0.472	156	0.074	103	0.002	63

Graph XIV - Lower part of Graph XIII.



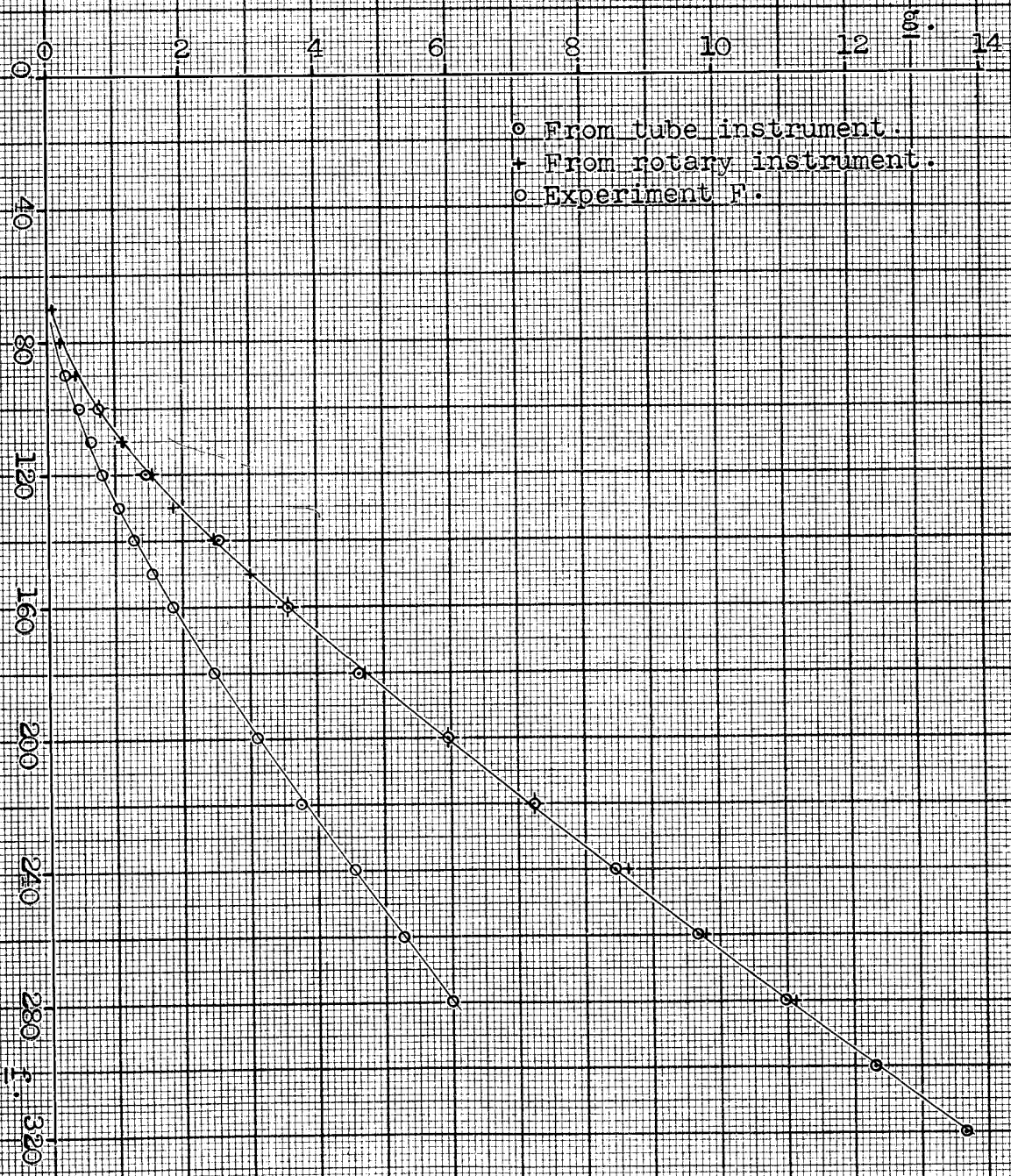
The speed of the motor was measured by means of the tachometer. The results obtained are given in Table XX, where the first three columns of pairs of

Table XXI - Values of g_a : Experiment D.

<u>f_a.</u>	<u>g_a(XIV).</u>	<u>g_a(XIII).</u>	<u>f_a/g_a.</u>	<u>g_a/f_a.</u>
70	0.08		830	0.0012
80	0.19		420	0.0024
90	0.41		220	0.0046
100	0.76		132	0.0076
110	1.12		98	0.0102
120	1.54		78	0.0128
130	1.87		69	0.0144
140	2.48		56.5	0.0177
150	3.00		50.0	0.0200
160	3.58		44.5	0.0224
180		4.71	38.2	0.0262
200		5.96	33.6	0.0298
220		7.26	30.3	0.0330
240		8.63	27.8	0.0360
260		9.78	26.6	0.0376
280		11.14	25.1	0.0398

values are for the fast setting, and the last column

Graph XV - Values of g from both instruments: Expt. D.



for the slow setting. The results are plotted in the usual way on Graphs XIII and XIV. (These graphs also include some results from a later experiment.)

(b) Determination of the flow function.

The values of g_a are found as in the previous experiments, and are given in Table XXI, together with the viscosity and fluidity. The values of g_a are plotted on Graph XV; the viscosity and fluidity curves are shown on Graph XVIII.

3. Results from the tube instrument.

(a) Experimental results.

The experimental results for the tube instrument (decreasing values) are given in Table XXII: they are calculated as before. The values of q' and f_R are plotted on Graph XVI.

(b) Determination of the flow function.

The values of g_R obtained from the $q'-f_R$ curve are given in Table XXIII, and plotted on Graph XV with the values of g_a : the viscosities and fluidities given in the same table are plotted on Graph XVIII.

Graph XVI - Tube instrument: Experiment D.

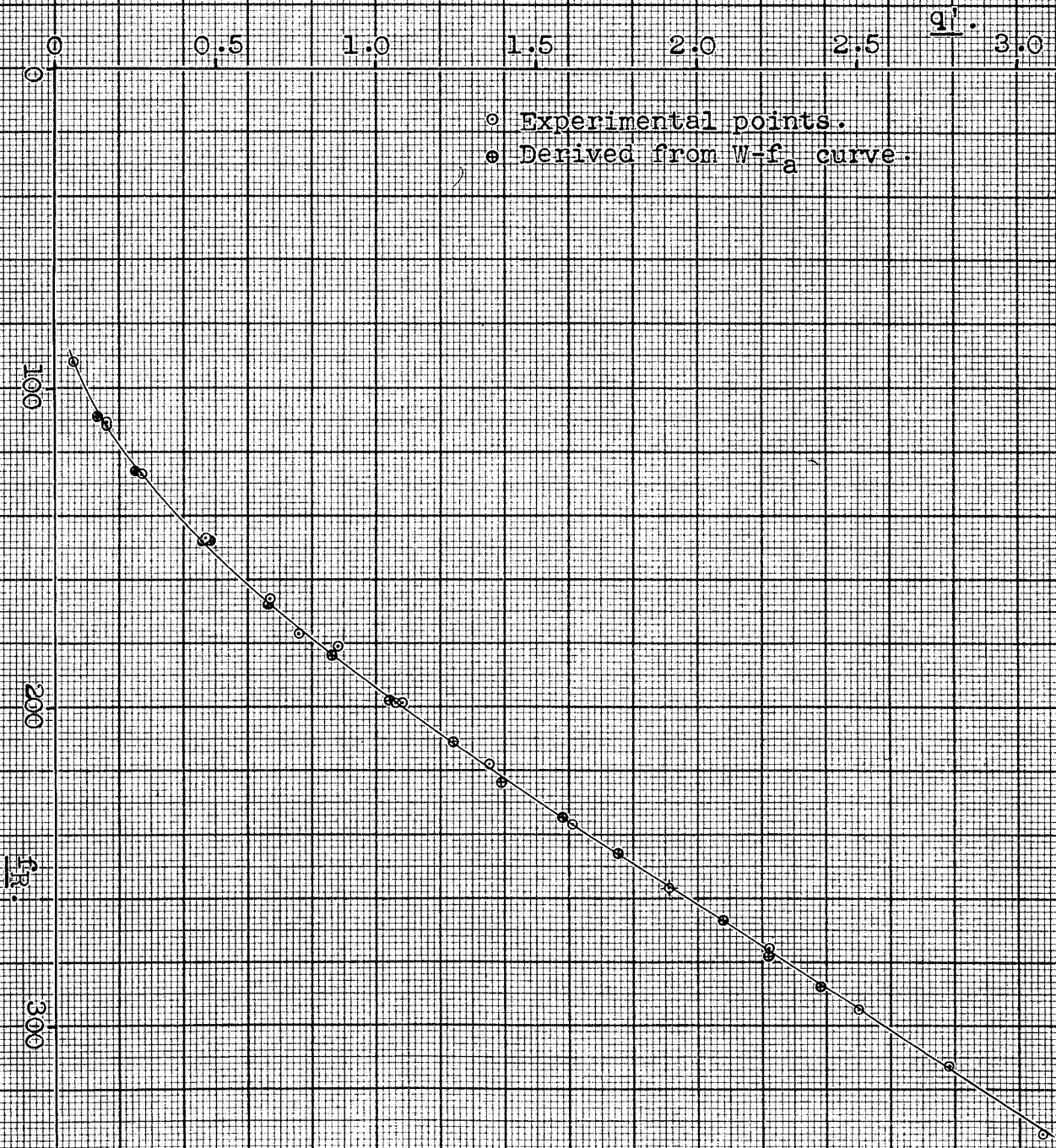


Table XXII - Results from the tube instrument.

<u>Speed No.</u>	<u>Pulley.</u>	<u>Manometer reading.</u>	<u>h.</u>	<u>q'.</u>	<u>f_R.</u>
6	C2	21.30	6.90	3.07	334
5½	C2	21.08	6.46	2.78	313
5	C2	20.90	6.10	2.50	295
4½	C2	20.70	5.70	2.22	276
4	C2	20.50	5.30	1.91	257
3½	C2	20.30	4.90	1.61	237
3	C2	20.10	4.50	1.35	218
2½	C2	19.90	4.10	1.06	199
2	C2	19.68	3.66	0.76	177
1½	C2	19.38	3.06	0.46	148
1	C2	19.00	2.30	0.16	111
6	C3	19.90	4.10	1.08	199
5	C3	19.72	3.74	0.88	181
4	C3	19.57	3.44	0.67	166
3	C3	19.37	3.04	0.47	147
2	C3	19.16	2.62	0.27	127
1½	C3	19.01	2.32	0.16	112
1	C3	18.80	1.90	0.06	92

Table XXIII - Values of g_R : Experiment D.

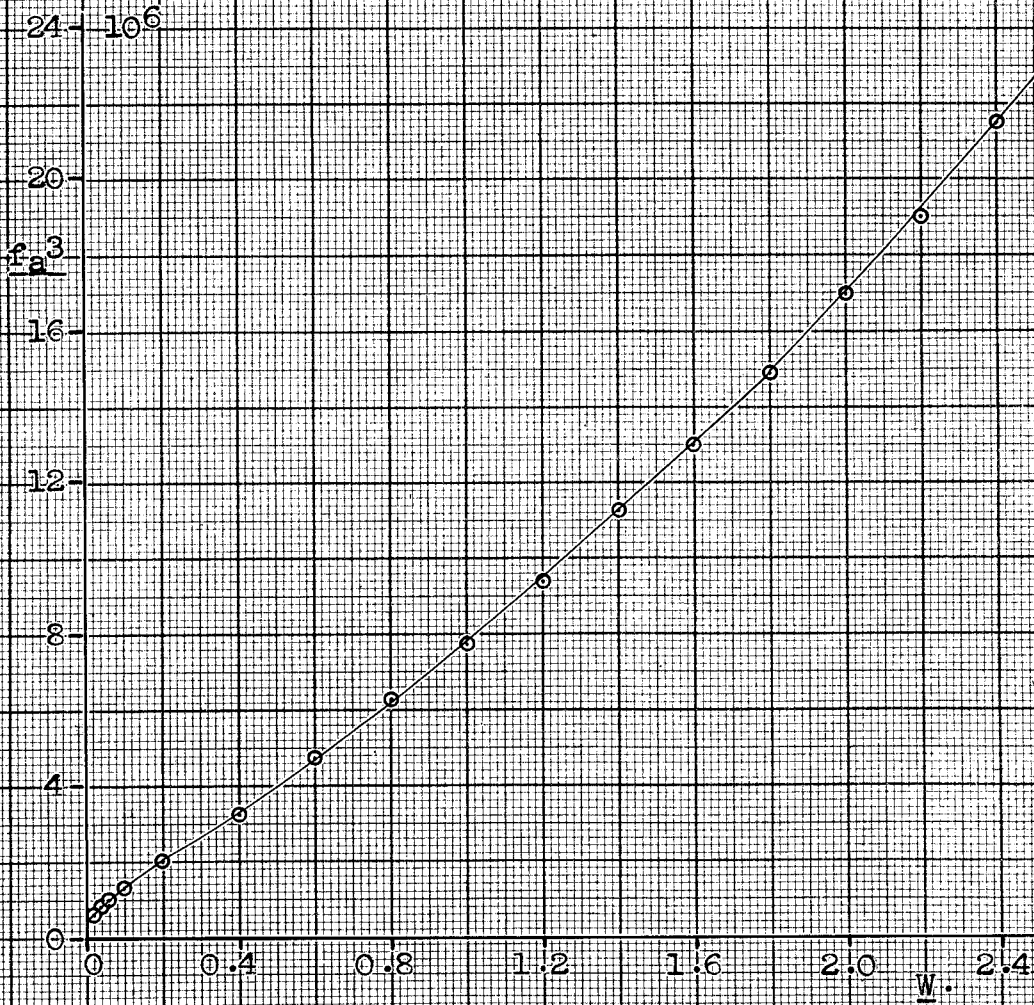
f_R .	$3q'$	$\frac{f_R dq'}{df_R}$	g_R .	g_a .	$g_R - g_a$.	f_R/g_R	g_R/f_R
100	0.03	0.54	0.74	0.76	- 3%	135	0.0074
120	0.66	0.79	1.45	1.54	- 6%	83	0.0121
140	1.14	1.39	2.53	2.48	2%	55	0.0181
160	1.77	1.78	3.55	3.58	- 1%	45.1	0.0222
180	2.46	2.20	4.66	4.71	- 1%	38.7	0.0259
200	3.24	2.70	5.94	5.96	0%	33.7	0.0297
220	4.08	3.15	7.23	7.26	0%	30.4	0.0329
240	4.95	3.48	8.43	8.63	- 2%	28.5	0.0351
260	5.82	3.85	9.67	9.78	- 1%	26.9	0.0372
280	6.75	4.23	10.98	11.14	- 1%	25.3	0.0392
300	7.65	4.65	12.30			24.4	0.0410
320	8.58	5.09	13.67			23.4	0.0427

4. Comparison of the results.

(a) Direct comparison.

The direct comparison is effected by comparing the values of g_a and g_R given in Table XXIII. These results show that the individual values of g_a and g_R agree (to within the limits of the error involved in their determination) over the whole of the range of shearing stresses used.

Graph XVII - f_a^3 v. W .



(b) Indirect comparison.

The method of Chapter IV, 2. is used. f_a is

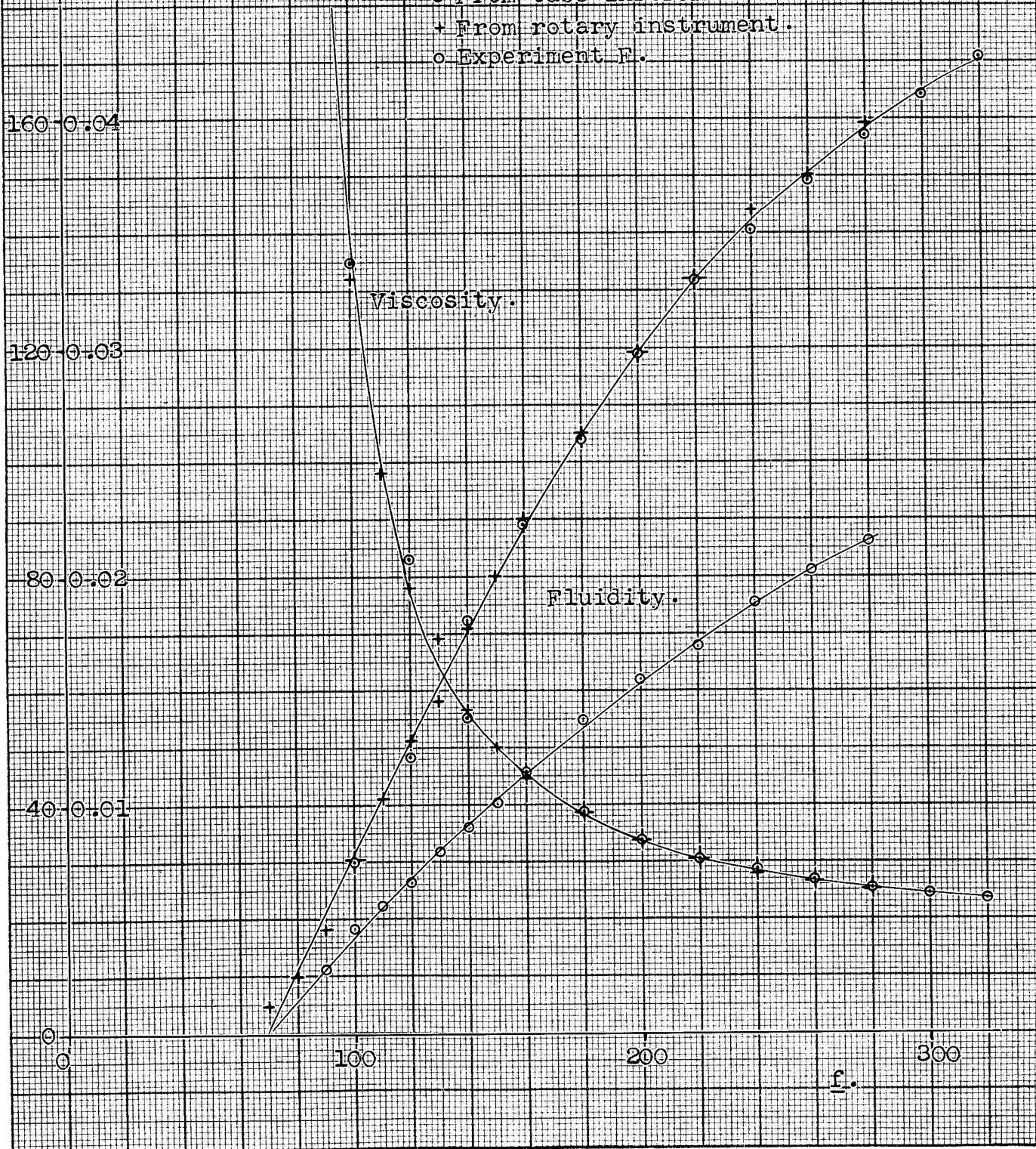
Table XXIV - q' - f values obtained from W - f_a curve.

<u>W.</u>	<u>f_a.</u>	<u>f_a^3.</u>	<u>$D(I)$.</u>	<u>I.</u>	<u>q'cal</u>	<u>q'exp</u>
0.02	84	$0.59 \cdot 10^6$				
0.04	94	0.83				
0.06	100	1.00				
0.10	109	1.29	$0.084 \cdot 10^6$	$0.084 \cdot 10^6$	0.13	0.14
0.2	126	2.00	0.164	0.248	0.25	0.26
0.4	148	3.24	0.524	0.772	0.48	0.47
0.6	168	4.74	0.798	1.57	0.66	0.68
0.8	184	6.23	1.097	2.67	0.86	0.87
1.0	198	7.76	1.399	4.07	1.04	1.05
1.2	211	9.39	1.715	5.78	1.24	1.23
1.4	224	11.24	2.063	7.84	1.39	1.41
1.6	235	12.98	2.422	10.27	1.58	1.59
1.8	246	14.89	2.787	13.05	1.75	1.75
2.0	257	16.97	3.186	16.24	1.91	1.91
2.2	267	19.03	3.600	19.84	2.08	2.07
2.4	278	21.48	4.051	23.89	2.22	2.23
2.6	288	23.89	4.536	28.43	2.38	2.39

determined from Graphs XIII and XIV for a series of

Graph XVIII - Viscosity and fluidity: Experiment D.

- From tube instrument
- + From rotary instrument.
- Experiment F.



values of W , and f_a^3 evaluated and plotted against W on Graph XVII. This graph shows that, above $W = 0.1$, the integration in equation 4.8 can be performed (as in previous examples) by considering the area under the curve between successive values of W to be a trapezium: below this value the area is determined by counting squares on the graph paper. The results are shown in Table XXIV, where $D(I)$ denotes the area under the curve between the successive values of W , and I the sum of $D(I)$ up to the appropriate value of W . The value of q' thus calculated, q'_{cal} , is compared with the value of q' , q'_{exp} , obtained from the curve on Graph XVI: the values of q'_{cal} are also plotted on this graph. The measure of agreement between the two sets of values of q' shows that the comparison has been effected to within the limits of the error involved in the measurement of W , q' , and f .

C H A P T E R X I I

CONCLUSION TO PART I.

1. Accuracy of the results.

It was shown in Chapter VIII that the two instruments had been calibrated to an accuracy better than 1%. Thus for the tube instrument, q' and the relation between h and f_R are uncertain by less than 1%: since h varied between about 2 cm. and 7 cm., and could be measured to 0.02 cm., h and therefore f_R are known to within about 1%. Equilibrium at the pressure measuring hole could be recognized within a pressure variation of less than 0.02 cm. For the rotary instrument the relation between motor speed and W , and that between deflection and f_a , are uncertain by less than 1%. The motor speed could be read to about 1% on the tachometer and given to less than 2% by the voltmeter: the scale was read to the nearest $\frac{1}{2}$ degree, and, as the deflections varied between 25 and 90 degrees, the inaccuracy in the deflection is less than 2%. Thus individual values of W and f_a may be in

error by 2%, but as a large number of readings were taken, the effect of drawing a smooth curve through the plotted points reduces this error. It is therefore considered that the $q'-f_R$, and $W-f_a$ curves can be drawn with an accuracy of the order of $\pm 1\%$ over the greater part of their range.

It was found that the error introduced in drawing tangents to the experimental curves might be as great as $\pm 2\%$. A further error is introduced here since the gradient of the curves drawn can vary by more than this amount at their extremes (10% at each end in the case of the tube instrument, but less in the case of the rotary instrument as there are more plotted points). Thus the individual values of g obtained may be in error by 2%. If estimations of the gradient are made at a large number of shearing stresses, it is considered that the g_R and g_a curves can be obtained from the experimental curves with a loss in accuracy of the order of 1%.

Uncertainty in the temperature will, as has been shown, introduce an error of 7% per degree change in temperature. Measurement of the temperature of the sample in each instrument at the conclusion of each experiment showed that it was within 0.1°C . of the

nominal temperature, 25.0°C . Thus the error arising was about $\frac{1}{2}\%$.

In making the direct comparison, therefore, the difference expected between g_R and g_a may be as great as 4% for most of the range of shearing stresses, and greater than this at the extremes. In making the indirect comparison, it is considered that the errors involved are those of curve drawing (excluding gradient estimation) and temperature, and that the comparison can be made to the order of $\pm 1\%$.

The results of the experiments described in previous chapters bear out these conclusions.

2. The effects of the assumptions made.

The fact that the comparison of the flow functions has been effected to within the experimental error shows that the steps taken to justify the assumptions set out in Chapters II and III are correct. It may be assumed therefore that there was no slip at the boundary walls; that the proper flow conditions had been established; and that the measuring techniques employed were correct.

Some results were taken for the tube instrument,

with and without the constriction, using the same sample in both cases. These results were:-

<u>Speed No.</u>	1	1½	2	2½	3	3½	4	4½	5
f _R with:-	150	194	215	242	266	290	312	334	357
f _R without:-	131	177	196	218	239	256	276	294	305
% difference:-	14	9	9	11	11	12	12	13	16

Although increasing readings were taken, these results serve to indicate the magnitude of the effect of the constriction. They show that, at a given rate of flow, a greater pressure difference exists in the presence of the constriction, supporting the argument that the sample is driven down the tube partly by a direct (solid) thrust in the absence of the constriction. The average percentage difference is about 12, which is much greater than the difference between increasing and decreasing readings (see Experiment A). The results of Experiment B have shown the magnitude of the difference between increasing and decreasing readings for the rotary instrument.

Thus if the various assumptions are ignored, considerable errors are introduced.

It can be concluded, therefore, that the theory and methods used in the comparison are correct, and

that the flow functions of the materials used have in fact been determined, as they have been shown to be independent of the method of determination. In other words, the absolute viscosity of fluids exhibiting anomalous flow properties has been measured in the case where the fluids are instantaneously thixotropic.

3. Introduction to Part II.

The principal aim of this thesis has been the establishment of the methods of measurement. Part II is concerned with some properties of the samples which have been found incidentally to the main enquiry. The properties of a sample are given as the graphical relation between rate of shear and shearing stress, i.e., the flow function, which includes the dynamic yield value and the limiting viscosity at high rates of shear. These properties will be dependent on the nature and proportions of the two components, solid and liquid, and on the temperature of the sample.

Results pertaining to the flow function and yield values have been presented in Part I. In the instruments described there, it was not possible to reach high shearing stresses, and thus the limiting

viscosity could not be approached. A further instrument of the concentric cylinder type was therefore constructed with a narrow annulus between inner and outer cylinders: this instrument will be described briefly. It was used for the sample of Experiment D.

The effect of temperature change on the sample of Experiment D was also investigated and some results will be presented in Part II.

An empirical equation is suggested to represent the absolute viscosity as a function of shearing stress, and this equation is used to illustrate the results obtained in Experiment B.

PART II

C H A P T E R X I I I

A HIGH RATE OF SHEAR ROTARY INSTRUMENT.

1. The instrument.

In order to determine the limiting viscosity of the sample used in Experiment D, an instrument of the concentric cylinder type was constructed which had a narrow gap between inner and outer cylinders. From the viscosity - shearing stress curves given in Part I it can be seen that for shearing stresses greater than those obtained there, the change in viscosity over a narrow gap will be small. Thus the viscosity at high rates of shear can be obtained by treating the fluid as a Newtonian fluid.

The outer cylinder of this instrument is similar to that of the rotary instrument described in Chapter VI: it has an internal diameter of 9.6 cm., and a depth of 13.6 cm. It is mounted vertically on an axle carried by ball bearings set in a base-plate. The inner cylinder is constrained to move about the axis of the outer: its diameter is about 0.1 cm. less

than the outer, and it is mounted so that its lower plane face is 1 cm. above the plane face of the outer cylinder, and its upper plane face is above the upper rim of the outer cylinder. The base-plate supports, on three pillars, a rigid top-plate. The inner cylinder is mounted, by means of a hollow axle, in a small ball-race set in this top-plate, and is arranged to rest lightly and centrally on a single ball-bearing set in the lower face of the outer cylinder.

The hollow axle enables leads to be taken from a thermojunction soldered to the inside of the (thin) wall of the inner cylinder. The axle carries a short arm which is connected to the mid-point of a spiral spring stretched horizontally between two posts on the top-plate. The couple on the inner cylinder is measured by the deflection of the cylinder against the restoring force of this spring: deflections in either direction can be measured. The deflection is measured with the usual lamp, mirror (mounted on the axle) and scale. The outer cylinder is driven through a worm drive reduction gear by the variable speed motor used for the rotary instrument. The speed of the motor spindle is measured by means of the tachometer. The instrument could be mounted inside the same constant

temperature enclosure as was used for the tube instrument. The motor is mounted outside the enclosure, with its spindle passing through the wall.

If the instrument is considered to behave as a concentric cylinder viscometer for the fluid between the curved surfaces, and as a parallel disc viscometer for the fluid between the lower plane faces, it can be shown that the contribution to the couple on the inner cylinder due to the parallel disc part is negligible. Thus the viscosity is proportional to the ratio of the deflection to the speed. The instrument is calibrated by using a Newtonian oil of known viscosity. The deflection, x , is taken as the distance moved in cm. by the spot of light on the scale set at 100 cm. from the axis of the instrument, and the speed as the speed of the motor spindle in r.p.m.; the constant relating the viscosity in poises to the ratio of deflection to speed is calculated accordingly.

The speeds used were not great enough to cause appreciable heating ($0.2^{\circ}\text{C}.$) of the samples during an experiment, but it is considered that the rate of shear was sufficiently high for the limiting viscosity to be approached.

2. Use and calibration of the instrument.

For the purpose of filling, the top-plate and inner cylinder can be removed in one piece from the rest of the instrument by removing three nuts which hold the top-plate to the supporting pillars. The oil, or sample, is then poured into the outer cylinder until it reaches a certain depth: when the inner cylinder is replaced there is then sufficient sample to fill the annulus, and enough surplus to remove any air bubbles caused by the filling operation. The instrument is then placed in the constant temperature enclosure.

Using the calibration oil at 25.0°C . (see Chapter VIII, 3(a).), the results given in Table XXV were obtained: S is the speed of the motor in revolutions per minute, and x is the corresponding scale reading. These results are plotted on Graph XIX.

The gradients, m , of the lines through the four sets of points and the intercepts, x_0 , on the x -axis are given in each case. The differences in the values of x_0 are due to friction in the mounting, which was found to give a 0.3 cm. deflection at all speeds when the instrument was empty.

Graph XIX - Calibration of high rate of shear instrument.

o Increasing readings.
+ Decreasing readings.

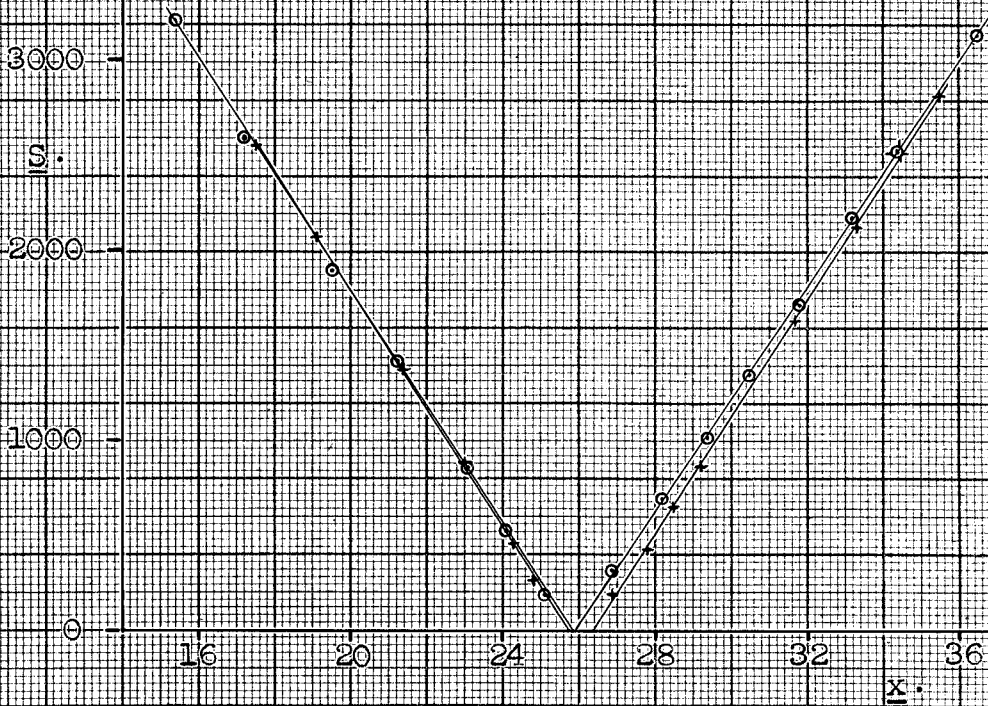


Table XXV - S and x for calibration oil.

<u>Forward:-</u>				<u>Reverse:-</u>			
<u>Increasing</u>		<u>Decreasing</u>		<u>Increasing</u>		<u>Decreasing</u>	
<u>S.</u>	<u>x.</u>	<u>S.</u>	<u>x.</u>	<u>S.</u>	<u>x.</u>	<u>S.</u>	<u>x.</u>
310	26.9	2820	35.5	180	25.1	2560	17.5
690	28.2	2520	34.5	520	24.1	2080	19.1
1010	29.4	2130	33.3	850	23.1	1380	21.4
1350	30.5	1630	31.7	1420	21.2	880	23.0
1720	31.8	860	29.2	1900	19.5	460	24.3
2180	33.2	650	28.5	2600	17.2	260	24.8
2530	34.4	420	27.8	3220	15.4		
3140	36.5	180	26.9				
$m = 3.38 \cdot 10^{-3}$		$m = 3.23 \cdot 10^{-3}$		$m = 3.25 \cdot 10^{-3}$		$m = 3.18 \cdot 10^{-3}$	
$x_0 = 25.9$		$x_0 = 26.4$		$x_0 = 25.8$		$x_0 = 25.7$	

These values give a mean value of $m = 3.26 \pm 0.08 \cdot 10^{-3}$.

The viscosity of the oil is 4.12 poises. Hence the calibration gives:-

$$\underline{\text{Viscosity}} = \underline{(1.27 \pm 0.03)10^3 \frac{x}{S} \text{ poises.}}$$

The relation between the deflection and the shearing stress at the inner cylinder was also determined. A known couple was applied to the inner

cylinder by means of weights connected to its periphery by parallel threads passing over pulleys. Scale readings, x , were taken for a range of values of these masses, M , for increasing and decreasing values and for deflections in either direction. The mean value of x/M obtained was:-

$$x/M = (2.50 \pm 0.02) 10^{-2} \text{ cm/gram.}$$

The diameter of the inner cylinder, $2c$, is 9.50 cm., hence the couple exerted by a mass of M grams on each thread is $9.32 10^3 M$ dyne cm. The depth of the inner cylinder immersed is 12.6 cm., hence the shearing stress which would exert a couple corresponding to a mass of M grams is $5.22 M$ dynes per cm^2 . From the value of x/M , the shearing stress at the inner cylinder (ignoring end corrections), f_c , can be found. The results obtained were:-

$$f_c = 209 x \text{ dynes per cm}^2.$$

$$C = 1.79 10^3 f_c,$$

$$= 3.74 10^5 x \text{ dyne cm.}$$

The gear reduction between motor and outer cylinder is 72:1, hence W , the angular velocity of the outer cylinder, is given by:-

$$W = 1.454 10^{-3} \text{ S radians per sec.}$$

From the calibration equation and the above results it

can be shown that:-

$$\eta = 8.84 \cdot 10^{-3} (f/W),$$

but $\eta = f_c/g_c,$

hence $g_c = 113 W \text{ sec}^{-1}.$

g_c is the rate of shear at the inner cylinder, and is approximately equal to cW/e , where e is the width of the annulus. These results give $e = 0.042 \text{ cm.}$, a value which is in agreement with that found by direct measurement.

3. Approximate end corrections.

Approximate end corrections can be found, as outlined in 1., by assuming that the flow between the lower plane faces of the cylinders is the idealized flow between two discs of the radius of the inner cylinder. The couple on the plane faces will be represented by C' , and the total couple by C .

For a Newtonian fluid,

$$C' = \frac{1}{2} \pi \eta c^4 (W/d) = 0.86 \cdot 10^3 \eta W$$

where d is the separation of the plane faces (0.93 cm. for this instrument). The total couple C , from the calibration equation, is:-

$$C = 202 \cdot 10^3 \eta W$$

hence C' contributes less than $\frac{1}{2}\%$ to the total couple and can therefore be ignored in comparison with that due to the cylindrical part of the instrument.

For the anomalous fluid of Experiment D, the flow properties can be represented approximately by the expression:-

$$g = 0.061(f - 100)$$

for the range of shearing stresses encountered between the plane faces (0 - 400 dynes per cm^2). Using this relation, the values of C' are calculated for a number of values of S and compared with the value of C given by $C = 3.74 \cdot 10^5 x$. The values of x have been determined from the S - x graph for an experiment to be described in Chapter XIV, 3., in which the sample of Experiment D was used. The results are:-

<u>S.</u>	<u>x.</u>	<u>W.</u>	<u>C.</u>	<u>C'.</u>	<u>C'/C.</u>
2000	11.7	2.91	$433 \cdot 10^4$	$6.3 \cdot 10^4$	1.5 %
1500	9.1	2.18	340	5.3	1.6 %
1000	6.5	1.45	244	4.3	1.8 %
500	4.0	0.73	150	3.3	2.2 %

These results show that if S is kept above about 1000 r.p.m., the effect of the flow between the plane faces can be disregarded since it falls within the

limits of error of the calibration.

C H A P T E R X I V

THE VARIATION OF THE FLOW FUNCTION WITH TEMPERATURE.

1. Introduction.

At the conclusion of Experiment D (Part I), the filled rotary instrument was allowed to fall to room temperature overnight. The experiment was repeated with this instrument at the new temperature. This is Experiment E. The room temperature was then lowered and the experiment repeated. This is Experiment F.

The high rate of shear instrument was also used at all three temperatures. It was filled at the same time as the other two instruments, and readings on it were taken immediately after those on the rotary instrument. The temperature of its inner cylinder was compared with that of the oil bath of the rotary instrument by means of a calibrated thermojunction.

Since the purpose of these experiments was to investigate the variation of the flow function with temperature in order to calculate the errors to be

expected in the comparison experiments for small temperature changes, the temperatures were not thermostatically controlled in Experiments E and F. It is certain that the temperature in Experiment F was $16.3 \pm 0.1^{\circ}\text{C}.$, but there was some uncertainty in the temperature for Experiment E, which was about $19^{\circ}\text{C}.$ For this reason the results of this experiment will not be given here, but it may be stated that they bear out the conclusions arrived at for the other two experiments.

With the sample used sedimentation is slight over a period of a few days, but as the sample had been standing for some weeks prior to these experiments it was found possible to remove sufficient of the medium from the top of the sample for the purpose of measuring its viscosity in a standard Ostwald Viscometer. The viscosity was determined at a number of temperatures with an accuracy of better than 1%: these results are given in Table XXVI. It was found that the logarithm of the viscosity was linear with respect to the temperature and in the range investigated could be represented by:-

$$\log_{10} \eta = 1.031 - 0.0316 T$$

where T is the temperature in $^{\circ}\text{C}.$, and η is in poises.

Table XXVI - Viscosity of medium.

<u>Temp. °C.</u>	<u>Viscosity.</u>	<u>Log₁₀η.</u>	<u>(Log₁₀η)_c.</u>
17.0	3.12	0.494	0.494
21.3	2.28	0.358	0.358
22.3	2.12	0.326	0.326
25.0	1.75	0.243	0.241
26.0	1.62	0.209	0.209

In the above table $(\text{Log}_{10}\eta)_c$ is the value of $\text{Log}_{10}\eta$ calculated from the above relation.

Using these results the viscosity of the sample can be compared with the viscosity of the medium.

2. Experiment F.

The values of W and f_a obtained within the range of Experiment D are given in Table XXVII. Within this range there was found to be no effect from the static yield value: the values given are for successively decreasing readings. These values are plotted on Graphs XIII and XIV together with the results of Experiment D. The values of g_a , the fluidity, and the

Table XXVII - Results from the rotary instrument.

<u>Fast setting:-</u>				<u>Slow setting:-</u>	
<u>W.</u>	<u>f_a.</u>	<u>W.</u>	<u>f_a.</u>	<u>W.</u>	<u>f_a.</u>
1.38	289	0.495	194	0.092	119
1.26	279	0.456	187	0.076	114
1.14	267	0.400	181	0.059	108
1.04	257	0.344	171	0.044	104
0.93	245	0.300	165	0.038	101
0.82	234	0.228	150	0.027	97
0.76	226	0.184	144	0.015	89
0.70	218	0.143	134	0.009	86
0.62	210	0.101	123		
0.56	202				

viscosity are calculated in the usual way, and are given in Table XXVIII.

The values of g_a are plotted on Graph XV. From this graph it would appear that, for a given shearing stress, the values of g_a at the two temperatures are in a constant ratio. If this is true, then the dynamic yield value should be independent of temperature: that this is so is indicated by the plot of fluidity against shearing stress for the two temperatures on

Table XXVIII - Values of g_a , ϕ , and η .

<u>f_a.</u>	<u>Fluidity.</u>	<u>g_a.</u>	<u>Viscosity.</u>
From Graph XIV: -			
90	0.0028	0.25	336
100	0.0046	0.46	217
110	0.0056	0.62	179
120	0.0066	0.79	152
130	0.0079	1.03	126
140	0.0090	1.26	111
150	0.0101	1.52	99
160	0.0114	1.82	88
From Graph XIII: -			
160	0.0118	1.89	85
180	0.0137	2.46	73
200	0.0155	3.10	64
220	0.0169	3.72	59
240	0.0188	4.51	53
260	0.0202	5.25	49
280	0.0214	5.99	47

Graph XVIII. Extrapolation of the two curves to the axis of f give values of f_d which are equal, within the limit of error of their determination. It is

concluded therefore that the dynamic yield value is independent of temperature in the range 16°C. to 25°C.

The constancy of the ratio between the values of g_a at the two temperatures is indicated in Table XXIX.

Table XXIX - Ratio of $g_a(D)$ to $g_a(F)$.

<u>f_a.</u>	<u>$g_a(D)$ 25.0°C.</u>	<u>$g_a(F)$ 16.3°C.</u>	<u>Ratio.</u>	<u>% diff.</u>
90	0.41	0.25	1.64	-14
100	0.76	0.46	1.65	-14
110	1.12	0.62	1.81	- 4
120	1.54	0.79	1.95	+ 3
130	1.87	1.03	1.82	- 4
140	2.48	1.26	1.97	+ 4
150	3.00	1.52	1.97	+ 4
160	3.58	1.85	1.94	+ 3
180	4.71	2.46	1.91	+ 1
200	5.96	3.10	1.92	+ 2
220	7.26	3.72	1.95	+ 3
240	8.63	4.51	1.91	+ 1
260	9.78	5.25	1.86	- 2
280	11.14	5.99	1.86	- 2

Viscosity

of medium: - 1.74 poise. 3.28 poise. 1.89

In Table XXIX the column headed % diff. gives the percentage difference between the ratio of the viscosities of the medium and the ratio of the values of g_a at the two temperatures. From these values it can be seen that, when the temperature is varied, the value of g_a at a given shearing stress is inversely proportional to the viscosity of the medium. In other words, the viscosity of the sample at a given shearing stress is proportional to the viscosity of the medium for variation of temperature. The viscosity of the sample includes the limiting viscosity: the variation of the limiting viscosity with temperature will be considered in the next section.

3. Limiting viscosity.

The limiting viscosity was determined in the high rate of shear instrument at the temperatures of the above experiments. The deflection, x , was determined for a number of values of the motor speed, S , and the viscosity found from the gradient of a straight line drawn through the plotted points, using the calibration given in Chapter XIII, 3. The results are given in Table XXX, and plotted on Graph XX. It was shown

Graph XX - Limiting viscosity: Experiments D and F.

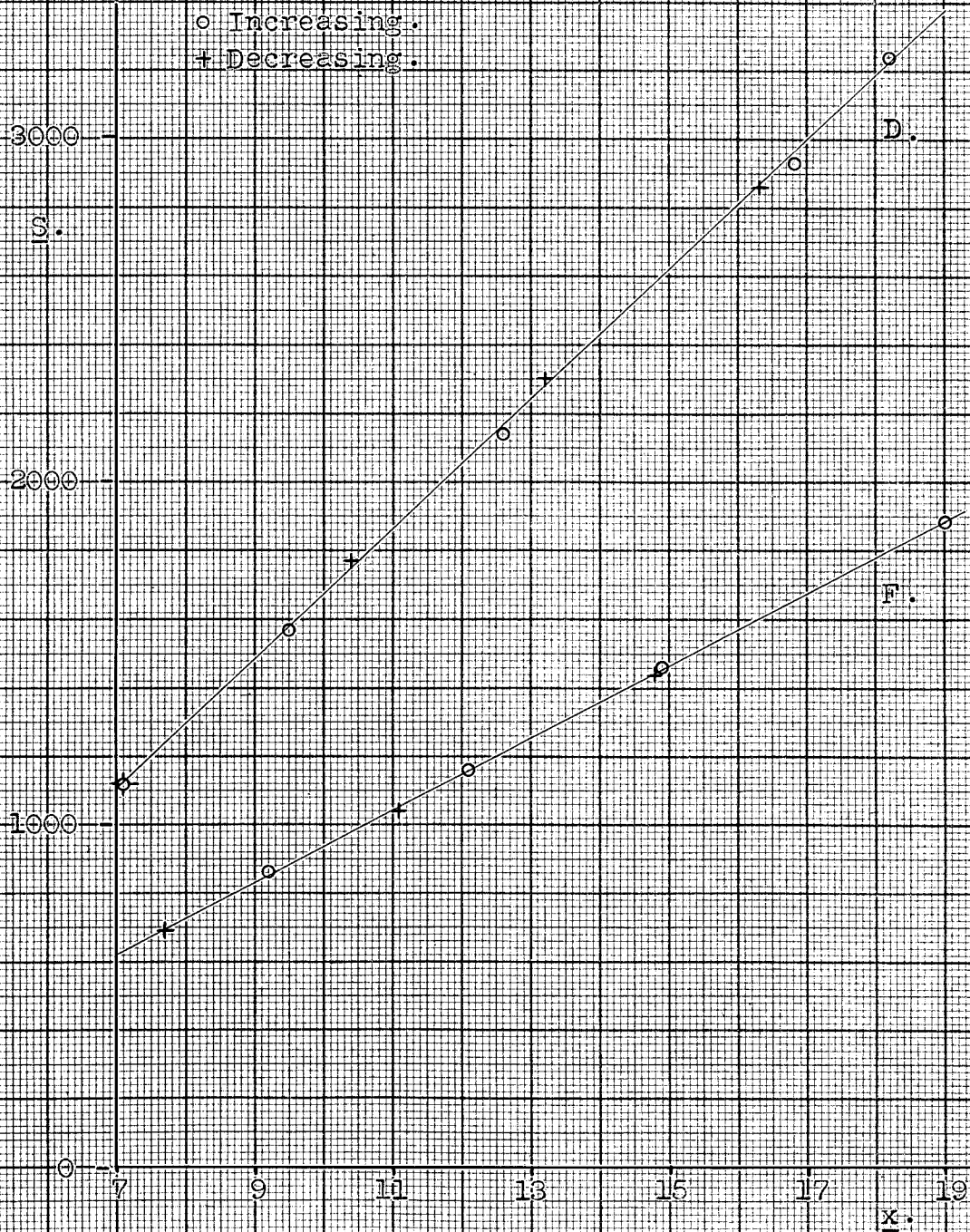


Table XXX - Values of S and x.

	<u>Experiment D.</u>		<u>Experiment F.</u>	
	<u>S.</u>	<u>x.</u>	<u>S.</u>	<u>x.</u>
Increasing readings:-	1120	7.1		
	1570	9.5	860	9.2
	2140	12.6	1160	12.1
	2930	16.8	1460	14.9
	3240	18.2	1880	19.0
Decreasing readings:-	2860	16.3	1440	14.8
	2300	13.2	1040	11.1
	1770	10.4	690	7.7
	1120	7.1		
Temperature:-	24.4°C.		16.3°C.	
Limiting viscosity:-	6.7 ± 0.15		12.1 ± 0.3 poises.	
Viscosity of medium:-	1.82		3.28 poises.	
Ratio of limiting viscosity to viscosity of medium:-	3.68 ± 0.08		3.69 ± 0.09	

in Chapter XIII, 3., that in the case of Experiment D the error due to the fluid between the plane faces was less than 2% for values of S greater than 1000 r.p.m.,

which corresponds to a deflection of about 7 cm.: in Experiment F only those deflections above 7 cm. are taken.

The results in Table XXX show that the limiting viscosity is proportional to the viscosity of the medium, within the limits of experimental error.

4. Conclusion.

Results which have been obtained from Experiments B and C, and D and F, for the variation with temperature of the flow functions of instantaneously thixotropic fluids, lead to the following conclusions:-

- (i) the dynamic yield value is not influenced by temperature changes, and
 - (ii) the viscosity of the fluid at any shearing stress is proportional to the viscosity of the medium,
- for the range of temperature used.

CHAPTER XV

AN EMPIRICAL EQUATION.

1. Introduction.

An empirical equation has been sought which will represent the flow properties of the samples used in these experiments, in order that the behaviour of the instruments may be predicted.

The shape of the viscosity - shearing stress curve suggests immediately that this relationship might be represented by a rectangular hyperbola with asymptotes given by the yield value and the limiting viscosity. This relation is:-

$$(\eta - \eta_0)(f - f_d) = A \quad \dots 15.1$$

where η_0 is the limiting viscosity, f_d is the dynamic yield value, and A is a constant for the fluid at a given temperature. It may be noted that since η/η_m at a given shearing stress, η_0/η_m , and f_d are independent of temperature, where η_m is the viscosity of the medium, equation 15.1 can be written:-

$$(\eta - \eta_0)(f - f_d) = B\eta_m \quad \dots 15.2$$

where B is a constant for the fluid, and is independent of temperature.

2. The empirical equation applied to Experiment B.

In order to evaluate the three constants in equation 15.1, the following procedure is adopted. The viscosity, η , is taken to be the mean value of η_a (Table XVI) and η_R (Table XVIII) for each shearing stress f , and $1/(\eta - \eta_0)$ is plotted against f for a number of values of η_0 . The value of η_0 for which the points most closely fit to a straight line is taken, and from the intercept of this line on the axis of f , f_d is obtained: an approximate value of η_0 is sufficient to give an accurate value of f_d . Using this value of f_d , $1/(f - f_d)$ is then plotted against η , and the best straight line drawn through these points. The intercept of this line on the axis of η gives η_0 , and the gradient of the line gives A.

With η in poises, and f in dynes per cm^2 . (as is the case throughout), the values of f and $1/(\eta - \eta_0)$ are given in Table XXXI for a number of values of η_0 ,

Graph XXI - $1/(\eta - \eta_0)$ v. f .

0.14 -

$\frac{1}{\eta - \eta_0}$

0.12 -

0.10 -

0.08 -

0.06 -

0.04 -

0.02 -

0

60

100

150

200

250

300

f

Experiment B.

$\eta_0 = 10$

$\eta_0 = 9$

$\eta_0 = 8$

Experiment D.

Experiment F.

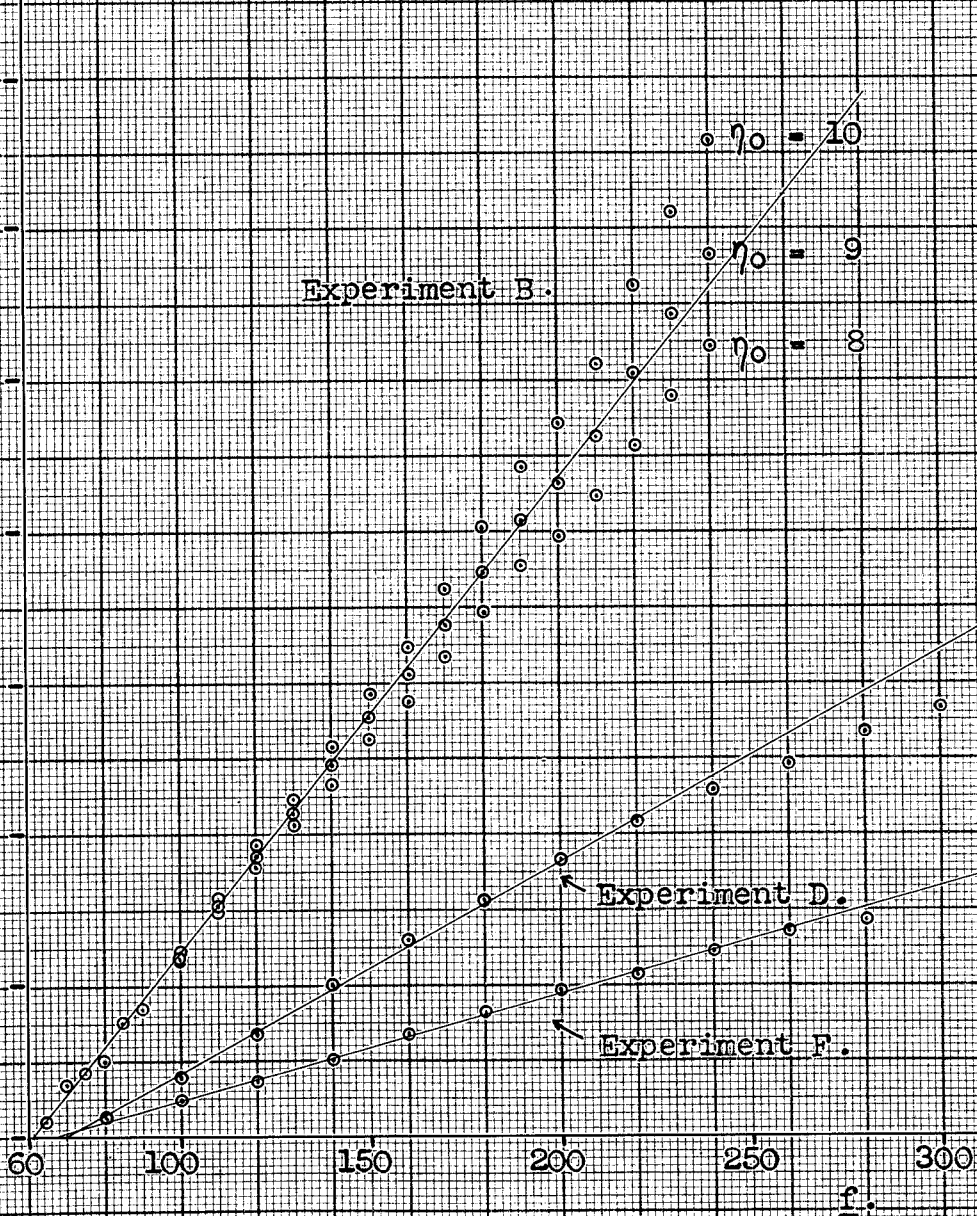


Table XXXI - Determination of f_d .

<u>f.</u>	<u>η.</u>	<u>$1/(\eta - \eta_0)$.</u>		
		<u>$\eta_0 = 8$.</u>	<u>$\eta_0 = 9$.</u>	<u>$\eta_0 = 10$.</u>
65	500	0.0020	0.0020	0.0020
70	152	0.0069	0.0070	0.0070
75	125	0.0085	0.0086	0.0087
80	108	0.0100	0.0101	0.0102
85	75	0.0149	0.0151	0.0154
90	68	0.0167	0.0170	0.0172
100	51	0.0233	0.0238	0.0244
110	41.6	0.0298	0.0307	0.0316
120	36.0	0.0357	0.0370	0.0385
130	32.3	0.0411	0.0429	0.0448
140	29.4	0.0467	0.0490	0.0515
150	27.1	0.0524	0.0552	0.0585
160	25.4	0.0575	0.0610	0.0649
170	23.8	0.0633	0.0676	0.0725
180	22.4	0.0694	0.0746	0.0806
190	21.3	0.0752	0.0813	0.0885
200	20.6	0.0794	0.0862	0.0943
210	19.8	0.0847	0.0926	0.1020
220	18.9	0.0917	0.1010	0.1124
230	18.2	0.0980	0.1087	0.1220
240	17.6	0.1042	0.1163	0.1316

Graph XXII - η v. $1/(f - f_a)$.

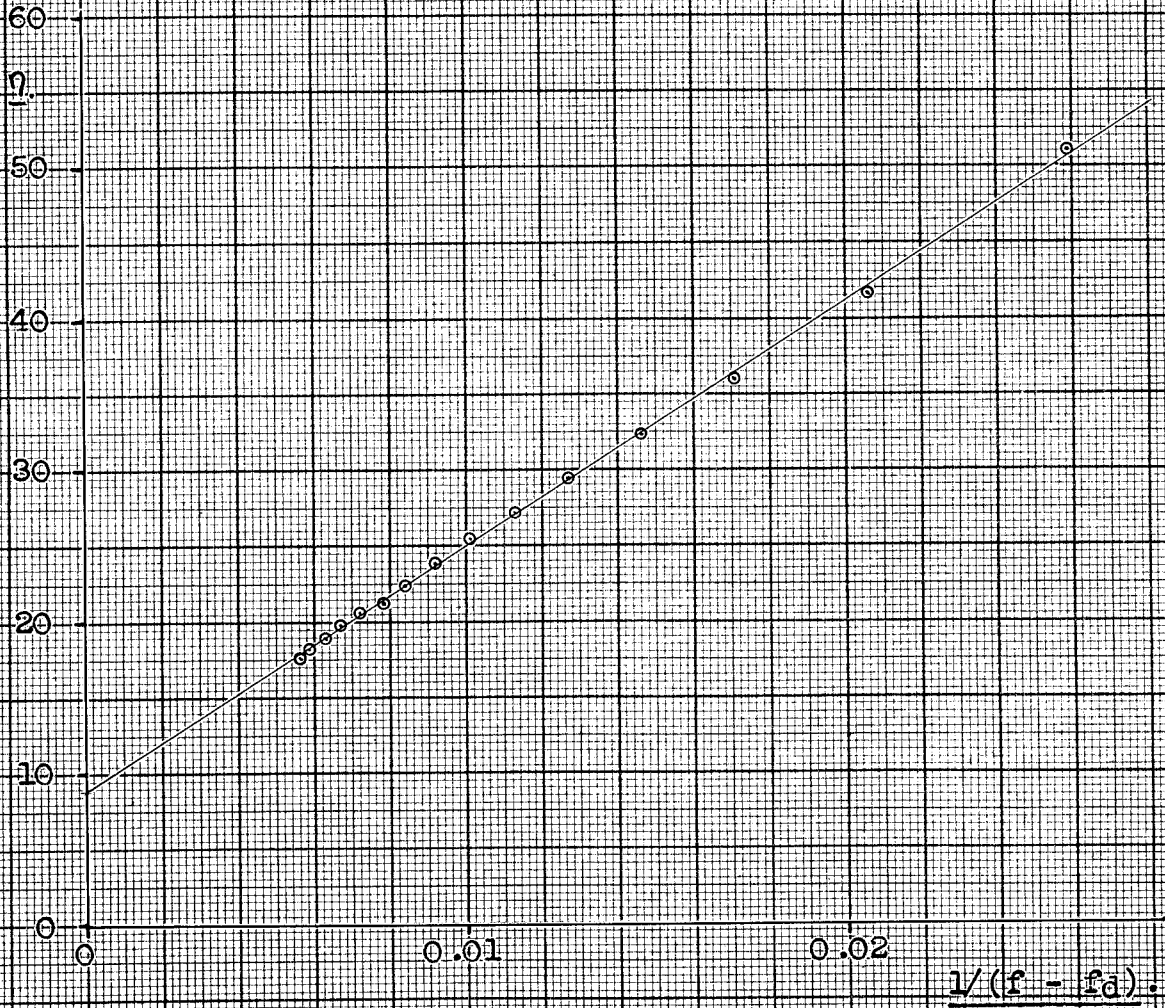


Table XXXII - Determination of η_0 , A.

<u>f.</u>	<u>1/(f - 61.4).</u>	<u>η.</u>	<u>η_c.</u>	<u>% diff., η, η_c.</u>
65		500	457	- 9
70		152	196	+25
75		125	127	+ 2
80		108	96	-12
85		75	77	+ 3
90		68	65	- 4
100	0.0259	51	51	0
110	0.0206	41.6	41.9	+ 1
120	0.0171	36.0	36.3	+ 1
130	0.0146	32.3	32.3	0
140	0.0127	29.4	29.3	0
150	0.0113	27.1	27.0	0
160	0.0101	25.4	25.1	- 1
170	0.0092	23.8	23.6	0
180	0.0084	22.4	22.4	0
190	0.0078	21.3	21.3	0
200	0.0072	20.6	20.4	- 1
210	0.0067	19.8	19.6	- 1
220	0.0063	18.9	18.9	0
230	0.0059	18.2	18.3	0
240	0.0056	17.6	17.8	+ 1

and are plotted on Graph XXI. The points for $\eta_0 = 9$ give a better straight line than the points for $\eta_0 = 8$ or 10: the best straight line through the points for $\eta_0 = 9$ below $f = 200$ gives $f_d = 61.4$. Using this value of f_d , $1/(f - f_d)$ is calculated and given in Table XXXII, and plotted against η on Graph XXII for the values of f above $f = 100$. From this graph it is found that $\eta_0 = 8.8$ and $A = 1610$. The empirical equation becomes, in this instance:-

$$(\eta - 8.8)(f - 61.4) = 1610$$

$$\text{or } ((\eta/8.8) - 1)((f/61.4) - 1) = 2.98$$

to give a dimensionless constant on the right hand side.

Table XXXII also shows a comparison between the values of the viscosity calculated from the above relation, η_c , and those found by experiment. It can be seen that the above equation represents the flow properties of the sample, within the limits of experimental error, over the whole range of shearing stress in which the viscosity was measured.

3. The equation applied to the rotary instrument.

Having established the validity of the empirical equation for giving the viscosity of the sample of Experiment B as a function of shearing stress, within the range of the rotary instrument, it is then possible to derive a relation between W and f_a which should give results in agreement with experiment.

Three cases have to be considered: increasing values, i.e., where the shearing stress at the solid-fluid boundary is f_s ; decreasing values, where the stress at the boundary is f_d ; and the transition region, where the boundary remains at the position it occupied for the maximum shearing stress at the inner cylinder, $f_a(\max)$. The relations obtained are:-

for increasing values,

$$W_s = \frac{1}{2\eta_0} \left\{ (f_a - f_s) - A' \log_e \frac{f_a + A' - f_d}{f_s + A' - f_d} \right\}$$

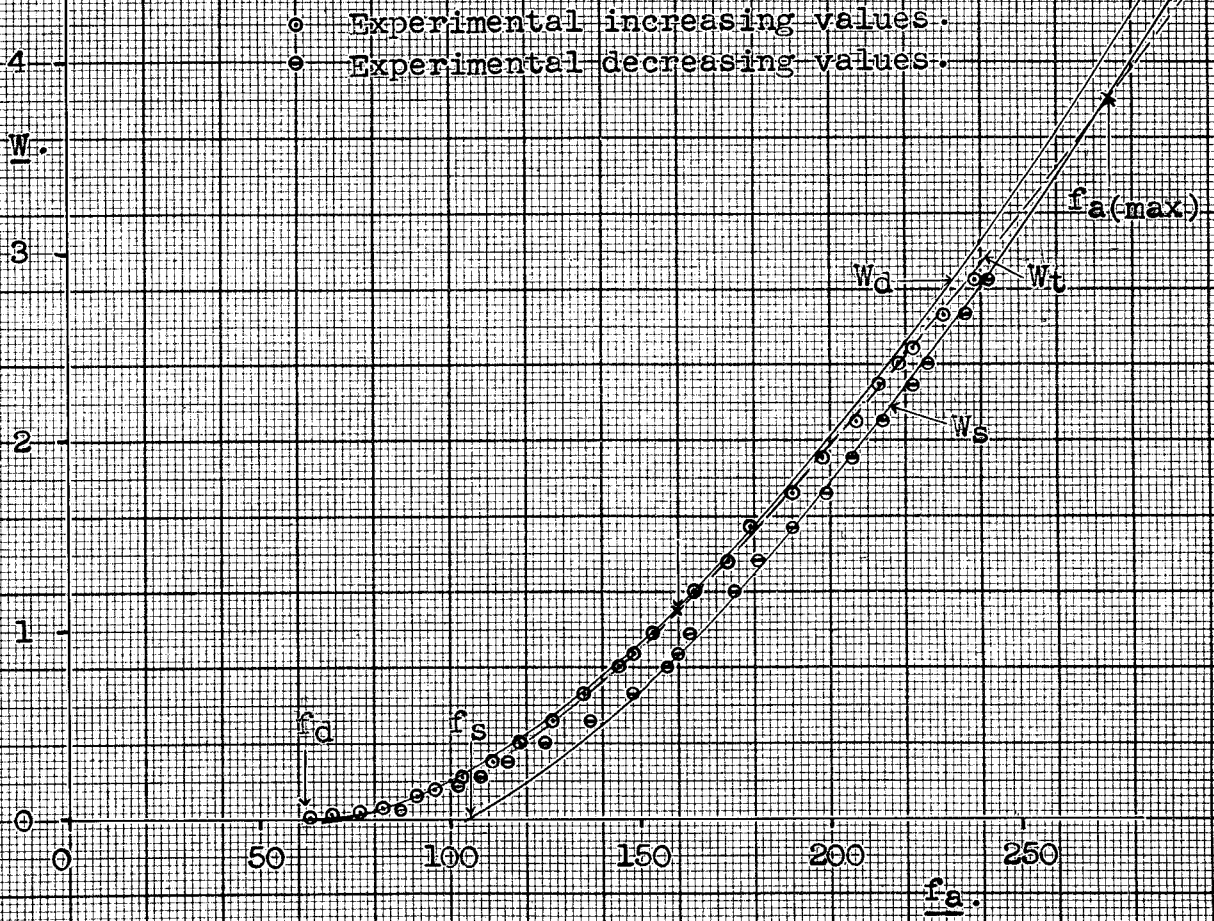
for decreasing values,

$$W_d = \frac{1}{2\eta_0} \left\{ (f_a - f_d) - A' \log_e \frac{f_a + A' - f_d}{A'} \right\}$$

for transition values,

$$W_t = \frac{1}{2\eta_0} \left\{ f_a(1 - k) - A' \log_e \frac{f_a + A' - f_d}{kf_a + A' - f_d} \right\}.$$

Graph XXIII - Empirical equation: rotary instrument.



In the above equations, $A' = A/\eta_0$, and $k = f_s/f_{a(\max)}$.

Values of W_s , W_d , and W_t have been calculated from these equations using the data of Experiment B. These values, suffix (c), are given in Table XXXIII, where

Table XXXIII - Values of W_s , W_d , and W_t .

<u>f_a</u>	<u>$W_s(c)$</u>	<u>$W_s(e)$</u>	<u>$W_d(c)$</u>	<u>$W_d(e)$</u>	<u>$W_t(c)$</u>	<u>$W_t(e)$</u>
70	--	--	0.01	0.02	--	--
80	--	--	0.05	0.05	--	--
90	--	--	0.12	0.11	--	--
100	--	--	0.20	0.19	--	--
105	0.00	0.20	0.25	0.24	--	--
120	0.19	0.34	0.44	0.43	--	--
140	0.50	0.56	0.75	0.73	--	--
160	0.86	0.88	1.11	1.12	1.11	1.12
180	1.29	1.30	1.54	1.53	1.53	1.53
200	1.76	1.76	2.01	1.96	1.99	1.96
220	2.26	2.25	2.51	2.42	2.46	2.42
240	2.80	2.78	3.05	2.90	2.93	2.90
260	3.38	--	3.63	--	3.44	--
280	3.98	--	4.23	--	3.95	--

they are compared with the experimental values, suffix (e).

The values of the constants taken are:-

$$f_d = 61.4; \quad f_s = 105; \quad f_a(\max) = 274 \text{ dynes per cm}^2.$$

$$A' = 183 \text{ dynes per cm}^2.; \quad \eta_0 = 8.8 \text{ poises}; \quad k = 0.341.$$

Taking $f_a(\max) = 274$ gives the shearing stress at which the discontinuity in the whole decreasing $W-f_a$ curve occurs as $f_a = 160$. The curves obtained from the above equations are shown on Graph XXIII, where some of the experimental points from Table XV are also plotted. The experimental curves were given on Graph VIII.

4. The equation applied to the tube instrument.

A relation can also be obtained between q' and f_R using the empirical equation to give the rate of shear as a function of shearing stress. The relation obtained is:-

$$q' = \frac{f_d(f'-1)}{12\eta_0 f'^3} \left\{ 3f'^3 - (4a-3)f'^2 + (6a^2-10a+3)f' \right. \\ \left. - (12a^3-30a^2+22a-3) + \frac{f_d a(a-1)^3}{(f'-1)} \log_e \left\{ 1 + \frac{f'-1}{a} \right\} \right\}$$

where $a = A/f_d\eta_0$, and $f' = f_R/f_d$.

Using the values of the constants given in the previous section, values of q' have been calculated for

a number of values of f' , and, in Table XXXIV, these are compared with the experimental values: they can be seen to agree with the experimental values over the whole range, as indeed they should since the empirical equation predicts the viscosity over the whole range of shearing stresses used for this particular sample.

Table XXXIV - Values of q' from empirical equation.

<u>f'</u>	<u>f_R</u>	<u>q' calculated</u>	<u>q' experimental</u>	<u>% difference</u>
1.5	92	0.19	0.19	0
2.0	123	0.56	0.58	+ 4
2.5	153	1.06	1.06	0
3.0	184	1.62	1.60	- 1
3.5	215	2.24	2.23	0
4.0	246	2.88	2.91	+ 1

5. The empirical equation applied to Experiment D.

In the case of Experiment D the limiting viscosity is known. Since $\eta_0 = 3.7 \eta_m$ from Table XXX, Chapter XIV, 3., then for 25.0°C ., $\eta_0 = 6.4$ poises. Graph XXI shows the values of $1/(\eta - \eta_0)$ given in Table XXXV plotted against f . From this graph it can be seen

that the empirical equation does not represent the flow properties of the fluid over the whole of the range of shearing stresses. It appears that the value of η_0 given by experiment is too small to give good agreement

Table XXXV - Values of $1/(\eta - \eta_0)$ for Expts. D and F.

<u>f.</u>	<u>$\eta(D)$.</u>	<u>$\eta(F)$.</u>	<u>$1/(\eta(D) - 6.4)$.</u>	<u>$1/(\eta(F) - 12)$.</u>
100	133	217	0.0079	0.0049
120	80	152	0.0135	0.0071
140	56	111	0.0200	0.0101
160	44.8	88	0.0260	0.0132
180	38.5	73	0.0311	0.0164
200	33.7	64	0.0366	0.0192
220	30.4	59	0.0417	0.0213
240	28.2	53	0.0459	0.0244
260	26.8	49	0.0490	0.0270
280	25.2	47	0.0532	0.0286

between the experimental results and the empirical equation. For example the value of $\eta_0 = 8.8$ poises given for the results of Experiment B is greater than the expected limiting viscosity: for Experiment D, a value of $\eta_0 = 10$ poises gives a greater region of agreement with the empirical formula than the measured

value of 6.4 poises.

6. The empirical equation and change of temperature.

In the case of Experiment F, $\eta_0 = 12.1$ poises. Table XXXV also gives the values of $1/(\eta - \eta_0)$ for this experiment, taking $\eta_0 = 12$: these values are also plotted on Graph XXI. From the best straight line through the points below, and including, $f = 240$ for each experiment, the values of f_d and A can be found. They are given, together with the value of $B = A/\eta_m$, in the following table:-

<u>Expt.</u>	<u>Temp.</u>	<u>η_0.</u>	<u>f_d.</u>	<u>A.</u>	<u>η_m.</u>	<u>B.</u>
D	25.0°C.	6.4	69	3620	1.74	2080
F	16.3°C.	12	67	7040	3.28	2140

These results show that f_d and B are sensibly constant between 16°C. and 25°C., and, taking mean values, equation 15.2 can be written, in this instance:-

$$\left\{ \frac{\eta}{\eta_m} - 3.7 \right\} \left\{ \frac{f}{68} - 1 \right\} = 31.0$$

7. Conclusion.

It can be concluded that the empirical equation proposed gives a reasonable value for the viscosity at low shearing stresses, but that it does not give a reliable result for the limiting viscosity. It serves as an accurate method of determining the dynamic yield value and has predicted the experimental results for the tube and rotary instruments in Experiment B, and could be used for predicting the results of Experiment D at low rates of shear. It cannot be used, however, for examining the behaviour of instruments at high rates of shear, for example it cannot be used for an analysis of the high rate of shear instrument.

A P P E N D I X I

THE PRODUCTION OF THE SAMPLES.

The necessary characteristics of the samples are that they should be instantaneously thixotropic, isotropic, and reasonably stable. Instantaneous thixotropy appears to arise from the presence of strong inter-particle forces in dispersions of solid particles in liquid media; isotropy can be obtained by using approximately spherical particles, of which an even distribution throughout the medium is produced by using a sufficiently great concentration; and stability by using non-reactive materials.

Titanium dioxide particles and liquid paraffin were therefore used as the two components, but such dispersions had disadvantages. At sufficiently high concentrations, the yield value was too great for successful operation in the rotary instrument; the sample tended to 'stand away' from the inner cylinder. At concentrations low enough for successful operation in this instrument, sedimentation and flocculation were apparent. It was found that a concentration of solid

particles of about 10% by volume would be satisfactory if the yield value could be reduced to about 100 dynes/cm².

The yield value can be reduced by reducing the number of inter-particle attractions by the addition of a wetting agent in small quantities (in this case 0.7% of oleic acid). Its effect was found to be gradual and difficult to predict, so that this method was abandoned. A 10% sample treated in this way and kept for some months was found to have a negligible yield value and to have become normally thixotropic to some extent. Samples of smaller concentrations were made by adding extra liquid paraffin, the medium of this dispersion. These samples were used for the measurements on the change of limiting viscosity with concentration given in Appendix III.

The samples used in the experiments of Part I were made by adding quantities of an aged dispersion of titanium dioxide particles in linseed oil to a dispersion of titanium dioxide in liquid paraffin. This addition reduced the yield value fairly quickly to a value sensibly constant, so that samples of the required yield value could be readily made. The linseed oil sample consisted of 33% by volume of

particles (90% titanium dioxide and 10% barium sulphate) dispersed in linseed oil of specific gravity 0.92 and viscosity 0.47 poises at 25°C. The liquid paraffin samples were made from anatase titanium dioxide particles, of mean size 0.5 to 1.0 microns, dispersed in liquid paraffin of specific gravity 0.89 and viscosity 2.02 poises at 25°C. The liquid paraffin samples were made in the ball-mill described in Appendix II. The volume of the solid component was determined from its mass, taking the specific gravity of titanium dioxide to be 3.84.

The sample used in Experiments A and B was made by adding about one part of the linseed oil dispersion to seven parts of a newly prepared 7.5% by volume liquid paraffin dispersion. During three months of storage, chemical changes took place in this sample owing to the presence of the linseed oil. About 10% of the medium having been removed (and its viscosity measured), the remainder was remilled and the resulting sample was found to have similar characteristics to those of the sample as used in Experiments A and B, but a different flow function. It remained instantaneously thixotropic. This new sample was used for Experiments D and F.

A P P E N D I X I I

THE BALL-MILL.

The purpose of the mill is to disperse the particle component of the sample in the medium, or liquid component. These particles have strong forces between them, and the act of milling is the separation of the individual particles in order to allow the medium to penetrate between them, so that the particles are evenly distributed and their forces act through the medium.

If a quantity of the medium is mixed with a quantity of the particles, in the first instance the mixture will consist of aggregates of particles separated by the medium. In order to break up these aggregates into smaller and smaller units, until the particle itself becomes the unit, sufficient shearing force must be applied at every point within the liquid and particle mixture. It is considered that this shearing force is too great to be applied through the medium, hence the milling surfaces must supply this force directly to the aggregates; the surfaces must

therefore be distributed throughout the sample and must be capable of being brought into contact as the particles may have a diameter as small as 0.5 microns. This contact can only be achieved by using convex surfaces of small radius.

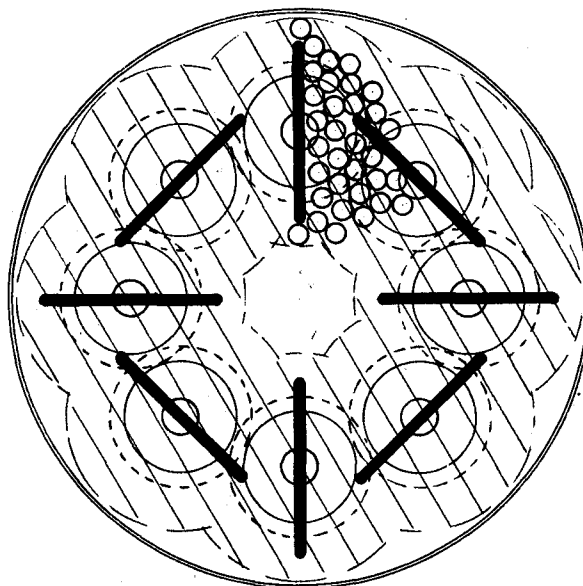
The required large number of convex surfaces in contact and sufficient shearing force throughout the sample are obtained by adding ball bearings to the constituent materials, and stirring. In order to obtain as much relative movement of the balls as possible, the shape of any part of the mixture must be continually changing in order that shearing forces are operative throughout; rotation or translation of large parts of the mixture reduces the efficiency of the mill. The volume of the balls must be about the same as that of the sample so that as much as possible of the material is being milled.

To meet these requirements, a mill was constructed in which eight steel blades rotated in a container of diameter 6", such that the minimum clearance between blades, and between blade and container, was slightly greater than the diameter of a ball ($7/32$ "). The axes on which the blades are mounted are set symmetrically round a circle as shown in Fig XVII; a

gear wheel on each axle engages with a similar wheel on each neighbouring axle, so that, when rotating, the blades continually change the shape of the mixture between them. The shaded area represents that part of

Fig XVII.

Plan: $\frac{1}{2}$ scale.



the mixture which is within the diameter of one ball from the sweep of the blades: this region fulfils the above requirements. The central unshaded region can be filled in by a steel cylinder.

In practice the materials for the fluid are put in the container with a quantity of the balls. The blades are rotated at about 130 r.p.m. by means of a $\frac{1}{4}$ h.p. motor. Further balls are added as the materials are mixed until they are evenly distributed through the whole depth of the mixture (about 4"). The mill is run for about half an hour and then stopped: a rise in temperature of about 10°C. occurs in this time. The blades are then removed from the container and the mixture stirred by hand in order to mix in a layer of balls which have remained stationary over the surface of the container: the mill is then run for further periods of about half an hour as above, until it is considered that the sample is well milled. No criterion of complete dispersion is available, but milling in this way for six hours produced samples which were satisfactory for the experiments in which they were used.

A P P E N D I X III

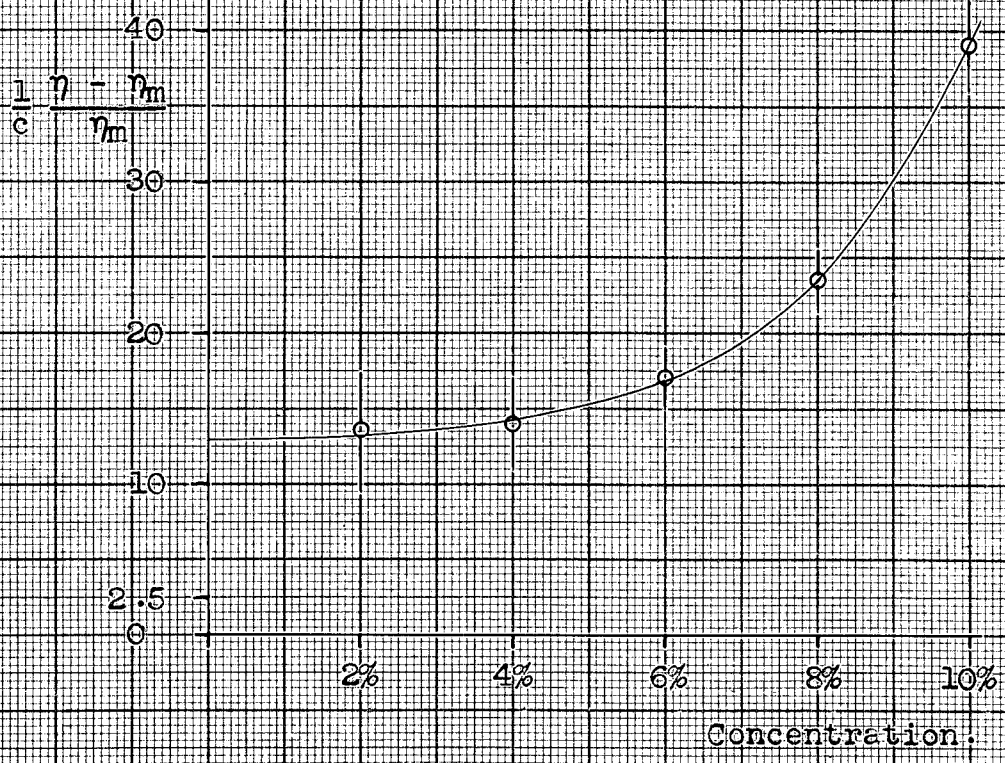
CHANGE OF LIMITING VISCOSITY WITH CONCENTRATION.

The high rate of shear instrument described in Chapter XIII, 1. was used to measure the limiting viscosity of the dispersions with added oleic acid described in Appendix I. The 10% sample was diluted with liquid paraffin to give samples of 2, 4, 6, 8 and 10% volume concentrations of particles. Details of the measurements, which were carried out at 25°C., will not be given: the results are given in Table XXXVI, where the viscosity in poises is calculated from the known viscosity of the medium, $\eta_m = 2.02$ poises.

Table XXXVI - Limiting viscosities.

<u>Concentration</u>	<u>(x/S).10³</u>	<u>Viscosity (mean values)</u>	<u>$\frac{1}{c} \frac{\eta - \eta_m}{\eta_m}$</u>
medium	1.50 \pm 0.06	2.02	
0.02	1.90 \pm 0.04	2.56	13.5 \pm 4
0.04	2.34 \pm 0.05	3.15	14 \pm 3
0.06	3.06 \pm 0.05	4.12	17 \pm 2
0.08	4.32 \pm 0.08	5.82	23.5 \pm 2
0.10	7.30 \pm 0.20	9.83	39 \pm 3

Graph XXIV - $(\eta - \eta_m)/cm_m$ v. c .



Einstein's equation:-

$$\eta = \eta_m(1 + kc) \quad \dots 1.$$

gives the viscosity η of a suspension of rigid, spherical, non-interacting particles at volume concentration c in a normal fluid of viscosity η_m , for small concentrations. In order to determine experimentally the value of the constant k , it is necessary to extrapolate the value of $(\eta - \eta_m)/c\eta_m$ obtained from the results in the above table to $c = 0$: this treatment gives a value of 13 ± 3 for k . The theoretical value obtained by Einstein is 2.5.

It may be assumed that under the conditions existing when the fluid approaches its limiting viscosity, it behaves as a normal fluid and the inter-particle forces are negligible: the particles used were approximately spherical. However, it is not certain whether the flow in the neighbourhood of the particles is laminar, or whether the volume of the particles is the effective volume for hydrodynamical considerations. The discrepancy between the experimental and theoretical values of k may be due to these causes.

If a fluid of concentration c approaches its

limiting viscosity, η , and to it is added a small quantity of particles to increase the concentration by δc , then, by equation 1, the limiting viscosity will be increased by an amount $\delta\eta$ given by:-

$$\eta + \delta\eta = \eta(1 + k\delta c)$$

As $\delta c \rightarrow 0$, this becomes:-

$$\frac{1}{\eta} \frac{d\eta}{dc} = k$$

which on integration, since $\eta = \eta_m$ when $c = 0$, becomes:

$$\eta = \eta_m e^{kc} \quad \dots 2.$$

an equation originally proposed by Arrhenius.

Using equation 2, the values of k obtained from the results in Table XXXVI are:-

<u>c.</u>	2%	4%	6%	8%	10%
<u>k.</u>	12 \pm 3	11 \pm 2	12 \pm 1	13 \pm 1	16 \pm 1

These values show that equation 2 holds for concentrations less than 10% with a value of k approximately equal to 12, which is in agreement with the results of the first method.

